The Dissertation Committee for Joseph Eugene Chipuk Jr. Certifies that this is the approved version of the following dissertation:

Development of Transmission Mode Desorption Electrospray Ionization (TM-DESI)

Committee:

Jennifer S. Brodbelt, Supervisor

Keith J. Stevenson

Katherine A. Willets

Lauren J. Webb

Michelle A. Lane >

Development of Transmission Mode Desorption Electrospray Ionization (TM-DESI)

by

Joseph Eugene Chipuk Jr., B.S., M.A.

Dissertation

Presented to the Faculty of the Graduate School of

The University of Texas at Austin

in Partial Fulfillment

of the Requirements

for the Degree of

Doctor of Philosophy

The University of Texas at Austin

December, 2009

Dedication

For Ed; promise kept.

Acknowledgements

While numerous colleagues, friends and family members have made this work possible, I am most grateful to Sara, my wife, for her never-ending patience, comforting support and encouragement to persevere and achieve. Furthermore, my development as a scientist would not have been possible without my advisor, Dr. Jennifer Brodbelt. Her willingness to accept non-traditional schedules and be open to creative thoughts allowed me to transform an idea to reality.

Funding from the Robert A. Welch Foundation (F1155), the National Institutes of Health (RO1 GM65956) and the National Science Foundation (CHE-0315337) is gratefully acknowledged.

Development of Transmission Mode Desorption Electrospray Ionization (TM-DESI)

Publication No._____

Joseph Eugene Chipuk Jr., Ph.D.

The University of Texas at Austin, 2009

Supervisor: Jennifer S. Brodbelt

A new era of high-throughput mass spectrometry emerged with the nearly simultaneous introduction of two ambient ionization techniques: desorption electrospray ionization (DESI) and direct analysis in real time (DART). The ability to integrate near instantaneous sample analysis with the specificity of mass spectrometry opened up a broad range of applications. While some of these involve the direct analysis of bulk materials, many others require the collection and deposition of samples onto suitable substrates.

This dissertation details the development of a new mode of operation for DESI. Instead of depositing a sample onto a continuous surface, the sample is either collected by or deposited onto a mesh substrate. Analytes either adsorb to the mesh strands or become suspended within the confines of the mesh in macroscale droplets. The samples are then analyzed by scrolling the mesh orthogonally into the path of an electrospray plume positioned coaxial to the inlet capillary of the mass spectrometer, thereby resulting in the transmission of the ionizing plume directly through the material.

The transmission mode results in desorption and ionization typical of DESI, but with the added benefits of a simpler experimental geometry and the convenient analysis of both dry (i.e., following evaporation of the deposition solvent) and wet (i.e., solvated) samples. The simplification of the experimental arrangement increases method robustness and reproducibility, while the inclusion of a mesh substrate introduces new possibilities for sample collection and introduction, due to the intricate chemistry between the mesh material, analytes, and deposition/electrospray solvent system.

However, the most important benefit lies in the development of surface-enhanced TM-DESI, whereby mesh substrates are derivatized to specifically capture and concentrate targeted analytes directly from solution. Following removal of matrix interferences by sample rinsing and subsequent cleavage of a photolabile linker, the mesh is analyzed directly by TM-DESI-MS. The technique has the potential to overcome interferences that have typically required chromatographic separations using LC-MS or have been insurmountable using ambient ionization methods. The impact of the surface-enhanced method could be tremendous as it may ultimately unite the competing metrics of analytical speed and specificity for ambient ionization mass spectrometry.

Table of Contents

Chapter 1: Introduction

The discovery of two ionization methods, matrix assisted laser desorption ionization (MALDI)[1,2] and electrospray ionization (ESI)[3], in the late 1980's dramatically changed the scope and potential applications of mass spectrometry. These landmark innovations created the new frontier of biological mass spectrometry by enabling the transfer of larger biomolecules, including proteins and oligonucleotides, into the gas phase. The impact on the field of mass spectrometry was tremendous, simultaneously creating a host of new applications and reinforcing the importance of ionization research.

The mid 2000's spawned another flurry of discovery in ionization methods for mass spectrometry with the invention of two new ambient ionization techniques, desorption electrospray ionization (DESI) [4] and direct analysis in real time (DART) [5]. These new techniques began a new era of mass spectrometry, one in which samples were analyzed in a high throughput manner in their native environment with little or no sample preparation. The scope of applications remained broad as researchers soon showed that small molecules such as pharmaceuticals and environmental contaminants as well as larger biomolecules such as peptides and proteins could be rapidly analyzed in the open environment and directly from a sample surface. This dissertation was motivated by the significant potential of these new ambient ionization methods and the possibility that their continued exploration could redefine the field of mass spectrometry, both in the laboratory and as part of a new wave of field portable mass spectrometers.

As a fundamental component to any mass spectrometer, the ionization source converts the neutral molecules present in a sample into ions that can be subsequently focused and transferred to a mass analyzer. Ionization can be accomplished in a variety of ways including: 1) the removal or addition of an electron to create a radical cation or

anion; 2) abstraction or adduction of a proton to create an even electron anion or cation; 3) abstraction of a hydride to create an even electron anion, and; 4) adduction of a suitable cation or anion (e.g., sodium, potassium, ammonium, chlorine) to form a positively or negatively charged ion-molecule complex.

Mass spectrometry is inherently a gas-phase analysis technique. Thus, when the samples of interest are in the condensed state, the combination of a sample introduction and ionization method must also transfer liquid or solid samples to the gas phase. In some cases, such as in gas chromatography-mass spectrometry (GC-MS) analysis of liquid samples, the sample introduction and ionization are decoupled, meaning ionization is performed remotely from sample volatilization. In other cases, such as in electrospray ionization, the conversion to the gas phase and ionization are essentially simultaneous in space and time. As long as the mass range, mass accuracy, and resolving power of the analyzer are sufficient, the array of samples and analytes that can be investigated using a particular mass spectrometer is primarily attributed to the efficiency of sample introduction and ionization.

1.1 THE NEW ERA OF IONIZATION METHODS: APCI, ESI, AND MALDI

Compounds that are both volatile and resistant to pyrolytic degradation are readily analyzed by GC-MS. However, while GC-MS analyses are widespread, it is estimated that only twenty percent of known chemicals meet both these criteria.[6] Therefore, mass spectrometric analysis of an overwhelming majority of compounds requires an alternate means of sample introduction and ionization. Techniques such as matrix assisted laser desorption ionization (MALDI)[1,2] electrospray ionization (ESI),[3,7-9] atmospheric pressure chemical ionization (APCI),[10-12] and atmospheric pressure photoionization (APPI)[13,14] were developed specifically to address this need. Together, these ionization methods have

dramatically extended the range of compounds that can be studied using mass spectrometry. Analysis of non-volatile and thermally labile small molecules, high molecular weight synthetic polymers, and biomolecules such as peptides, oligonucleotides, oligosaccharides, proteins and DNA are now commonplace in the field. Furthermore, ESI and MALDI also facilitate the analysis of these species from aqueous biological matrices such as urine, plasma, and saliva, matrices that are otherwise difficult to address directly using GC-MS.

Atmospheric pressure chemical ionization (APCI) and atmospheric pressure photoionization (APPI) are closely related and rely on vaporization of a liquid sample using a combination of heat and a nebulizing gas to create an aerosol. The aerosolized vapor is then subjected to either a corona discharge (APCI) or vacuum UV photons (APPI) to create reagent ions from the solvent or suitable dopant molecules.[10-14] These reagent ions exist in tremendous excess compared to the analytes within the vaporized cloud. Therefore, collisions between the gas-phase ions and vaporized neutrals are highly favored and the resulting ion-molecule reactions create positive ions via proton transfer, hydride abstraction, or cation adduction and negative ions via proton abstraction or anion adduction.[10-12] In some cases molecular ions (i.e., radical cations created by the loss of a single electron) are also observed in APCI and APPI via the direct ionization of the gas-phase analyte.[12,13]

Mass spectral analysis of solid samples is often accomplished via matrix assisted laser desorption ionization (MALDI) carried out inside the vacuum of a mass spectrometer[1,2] or at atmospheric pressure (AP-MALDI) [15]. In both cases a sample is dissolved in solution and subsequently co-crystallized with an acidic, low molecular weight matrix that absorbs strongly in the UV or IR region.[16] The sample thus takes the form of a solid solution where the matrix molecules are interspersed between the analyte.

When the sample is exposed to the UV or IR laser pulse, the laser energy is absorbed by the chromogenic matrix causing rapid vibrational excitation and localized disintegration of the solid solution.[16] This process releases clusters of molecules into the gas phase where transfer of protons or other salt cations from the matrix to the analytes stabilizes the structures and creates singly charged positive ions.[1,2,16]

While APCI, APPI, and MALDI are all useful ionization techniques, the research discussed in this dissertation focuses more closely on electrospray ionization (ESI), and its application to the direct analysis of both liquid and solid samples. A summary of the electrospray ionization process is depicted in Figure 1.1.

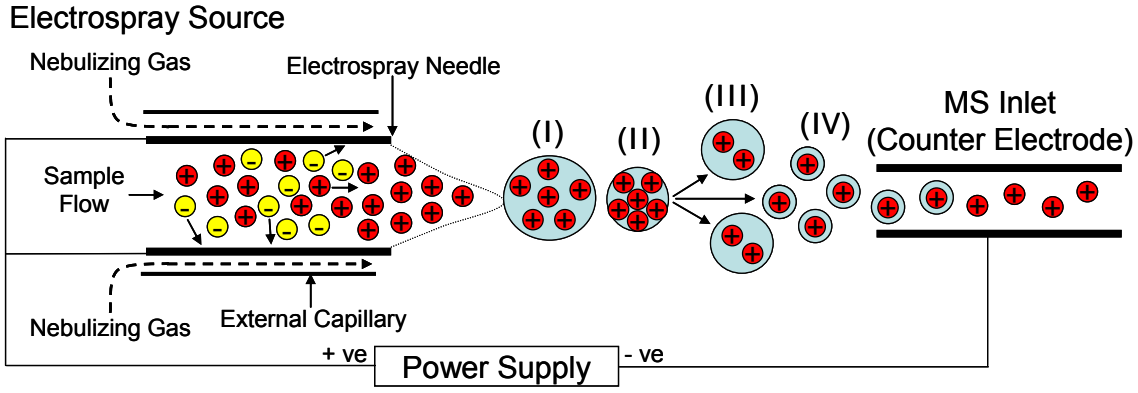

Figure 1.1: Schematic view of electrospray ionization (ESI). Phase I depicts repulsion of the ions from the Taylor cone. Phase II follows from desolvation of the Phase I droplet and results in highly charged droplets at the Rayleigh charge limit. Phase III and Phase IV encompass droplet fission and further desolvation which transform the analytes to free gas-phase ions.

Electrospray ionization is characterized by the application of a positive or negative potential of several kilovolts to a small diameter conductive electrospray needle. The applied potential is distributed to the solution where solution phase ions with the same polarity as the applied potential are forced away from the needle walls while ions of the opposite polarity are attracted it. The repelled ions extend beyond the tip of the

needle forming a Taylor cone where they eventually overcome the surface tension of the solvent and transfer from the solution phase to the vapor phase as a fine mist of multiply charged droplets.[3,7-9]

The electric field created by the electrospray needle and its counter electrode (i.e., the mass spectrometer inlet), the directional flow of the nebulizing gas, and the pressure differential created by the high vacuum of the mass spectrometer cause migration of the charged droplets toward the inlet. Within the droplet, analytes organize based on their polarity, with highly polar species tending toward the core of the droplet and less polar species migrating to the highly charged droplet surface.[7,8] As the solvent evaporates, the droplets become smaller while the charge on the droplet remains constant, thereby resulting in an increase of charge density until the droplet eventually approaches the Rayleigh charge limit.[7,8] In practice the fundamental ionization process is often assisted by a nebulizing gas, a curtain gas, and/or a heated capillary inlet to the mass spectrometer, each of which assist in the droplet desolvation and the creation of free gas-phase ions.[7-9]

Two competing mechanisms have been proposed for the remainder of the ionization process. The first mechanism suggests that the initial droplet undergoes coulombic fission whereby it divides into progeny droplets that eventually lose all of the remaining solvent to create free gas-phase ions.[17] This mechanism is termed the charge residue model since the charge never leaves the droplet, but instead remains on the droplet until the droplet becomes a single desolvated ion. The second mechanism suggests that free gas-phase ions are created by the evaporation of ions from the surface of the droplet.[18] In this case the evaporation is influenced by the desolvation process and the buildup of columbic repulsion, but the droplet does not undergo charge-induced fission until much later in the process. To date neither mechanism has been completely

proven or disproven, but strong evidence suggests that the charge residue model is applicable to larger molecules while smaller molecules may ionize by an ion evaporation mechanism.[7-9]

In many cases electrospray ionization is a solution phase ionization process.[7-9] Dissociated salts and highly acidic and basic species produce ions in solution that are subsequently transferred to the gas phase via the aerosolization and desolvation process. In addition, ionization may also take place within the aerosolized droplets as highly reactive free protons generated from acidic species and free metal cations form adducts with highly basic analytes and free halogens form adducts with highly electronegative species.[7,8] The result is a distribution of ions that depends on the polarity of the applied potential, the components of the solution and ultimately the constituents of each aerosolized droplet. Positive ions are formed by the application of a positive potential to the electrospray needle and the adduction of a proton or suitable cation (e.g., Na, K), while negative ions are formed by the application of a negative potential to the electrospray needle and deprotonation of the analyte or adduction of a suitable anion (e.g., Cl). Therefore, due to the fundamentals of the ionization mechanism, ESI is primarily amenable to polar or moderately polar molecules that are non-volatile or only moderately volatile.

1.2 Ambient Ionization Mass Spectrometry

The development of atmospheric pressure ionization techniques (i.e., ESI, APCI, APPI, and MALDI) extended the types of samples that could be analyzed by mass spectrometry. However, the aforementioned techniques all require significant sample preparation and time, especially when they are coupled to a chromatographic step. These limitations have driven the recent development of ambient ionization techniques that seek

to analyze liquid and solid samples in a high throughput manner in their native condition, or with limited sample preparation. The area is of tremendous interest in mass spectrometry, and numerous techniques have been developed since the introduction of desorption electrospray ionization (DESI) in 2004. While the various techniques differ in their execution, they all provide a means to desorb or extract analytes from the condensed phase and form gas-phase ions from the desorbed neutrals.[19,20] In some cases, desorption and ionization are performed by a single method, while in others desorption and ionization are decoupled and distinctly separated in space and time.[19,20]

One convenient method for organizing ambient ionization techniques is to group them by the atmospheric pressure ionization methods they most closely resemble. To date, techniques which produce mass spectra indicative of ESI, APCI, or APPI have been developed, but none have been shown to consistently produce MALDI-like mass spectra. Further delineation of the ambient ionization techniques can be achieved by considering the method used for analyte desorption (e.g., momentum transfer, laser activation, thermal desorption, analyte extraction, acoustic desorption). This aspect of the technique often dictates the suitable sample types and sample introduction method for the analysis.

1.3 Ambient Ionization Techniques Related to APCI

APCI related techniques such as direct analysis in real time (DART)[5], atmospheric surface analysis probe (ASAP)[21], desorption atmospheric pressure chemical ionization (DAPCI)[22,23], flowing atmospheric pressure afterglow (FAPA)[24,25], and low temperature plasma (LTP) probe ionization[26] all produce ions using ion-molecule reactions consistent with those utilized by traditional APCI. The mass spectra may contain protonated species, molecular ions, deprotonated ions, adducted species, and in some cases fragment ions associated with low energy fragmentation and reaction within

the ion-molecule complex. Figure 1.2 depicts a schematic of DART ionization. The experimental arrangement for DAPCI, ASAP, FAPA, and LTP is similar.

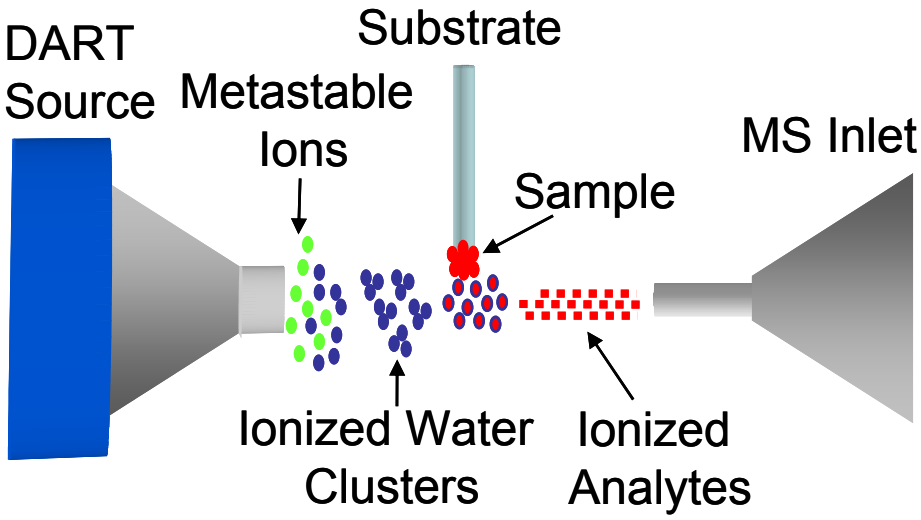

Figure 1.2: Schematic view of direct analysis in real time (DART). The experimental arrangement for DAPCI, ASAP, FAPA and LTP ionization is similar.

The aforementioned techniques are primarily differentiated by the voltage and current used to form the initial ionizing plasma.[19,20,25] In the case of DAPCI and ASAP, the formation of a corona discharge using a highly curved electrode (typically a needle) held at ~4kV in a helium or nitrogen rich atmosphere creates a current of ~5 μA between two electrodes.[21,22,25] A series of ionization reactions occur within the local environment of the discharge to generate ionized species (e.g., ionized water clusters, ionized oxygen) that subsequently react with neutral molecules located on a nearby surface. In the case of DAPCI, the desorption phenomena is driven primarily by the momentum of the ionizing gas stream whereas in ASAP the process is facilitated by heating a secondary nitrogen stream. The low energy associated with the corona discharge enables DAPCI and ASAP to be relatively "soft" ionization techniques that produce less fragmentation than other more energetic techniques. However, the relatively low flux of reagent ions created by

the ion source also limits the sensitivity and introduces complications with competitive ionization between neutral analytes.[25]

The ionization reactions in DART are similar to those utilized in DAPCI and ASAP, however in this case a more energetic glow discharge is used.[5,25] In DART, the voltage is held near 3 kV, but the configuration of the ion source allows for currents of up to 5 mA to be maintained. These currents allow for the generation of metastable helium atoms which in turn efficiently react with atmospheric species such as water and oxygen to produce abundant reagent ions.[5] The desorption process in DART is a combination of thermal forces and particle momentum derived from the interaction of the surface with a heated gas stream of temperatures of up to 300 °C.[5,25] By comparison, the FAPA ionization method is even more energetic than DAPCI, ASAP, or DART.[19,25] In this case the discharge is characterized as a true glow to arc and maintained at currents approaching 25 mA. The discharge itself is also much hotter, resulting in slightly different ionization pathways and efficient desorption without the use of additional heating.[24,25]

The pursuit of ambient ionization methods related to APCI continues to be an active research area.[19,20] While there are some clear distinctions between the methods in this classification, the commonality that a plasma type source is used to generate precursor ions that subsequently react to form a chemical ionization reagent remains consistent. Further research in APCI related ambient ionization may result in the development of an ionization source that is capable of spanning the various energy regimes, thereby creating a tunable method that can be optimized to suit an even broader range of applications.

1.4 AMBIENT IONIZATION TECHNIQUES RELATED TO ESI

Ambient ionization methods related to ESI such as desorption electrospray ionization (DESI),[4,22] electrospray laser desorption ionization (ELDI),[26,27] matrix assisted laser desorption electrospray ionization (MALDESI),[28,29] and extractive electrospray ionization (EESI)[30] all produce mass spectra similar to those observed using ESI, where ions are typically protonated, deprotonated, or adducted and contain a single or multiple charges. Table 1.1 lists the techniques that most closely resemble ESI along with the method used for analyte desorption and the year the technique was introduced. Again, while analyte desorption and transfer to the gas phase differs among the methods, they all fundamentally rely on electrospray ionization mechanisms and consequently produce mass spectra that are comparable to those obtained using conventional ESI.

Table 1.1: ESI Related Ambient Ionization Techniques

Acronym	Name	Desorption	Year	Ref.
DESI	Desorption Electrospray Ionization	Momentum	2004	4
DeSSI	Desorption Sonic Spray Ionization	Momentum	2006	33
ND-EESI	Neutral Desorption Extractive Electrospray Ionization	Momentum	2007	34
ELDI	Electrospray Laser Desorption Ionization	Laser	2005	26
MALDESI	Matrix Assisted Laser Desorption Electrospray Ionization	Laser	2006	28
LAESI	Laser Ablation Electrospray Ionization	Laser	2007	36
liq-MALDESI	Liquid Matrix Assisted Laser Desorption Electrospray Ionization	Laser	2008	35
SSP	Surface Sampling Probe	Extraction	2004	38
FD-ESI	Fused Droplet Electrospray Ionization	Extraction	2005	37
EESI	Extractive Electrospray Ionization	Extraction	2006	30
LIAD-ESI	Laser Induced Acoustic Desorption Electrospray Ionization	Acoustic	2009	43
RADIO	Radio Acoustic Desorption Ionization	Acoustic	2009	44

1.4.1 Comparison of Momentum Based Techniques

Ambient ionization techniques such as DESI, desorption sonic spray ionization (DeSSI),[33] and neutral desorption extractive electrospray ionization (ND-EESI)[34] rely on particle momentum to desorb analytes from a sample surface. The experimental arrangement for each of these techniques is similar in that a sample, whether it is a bulk solid or a residue left after sample deposition and solvent evaporation, is exposed to an incoming stream of particles produced at a defined incident angle and distance away from the sample. In DESI, charged electrospray droplets provide the necessary particle momentum, whereas in DeSSI the stream is produced by a sonic spray that is similar to an electrospray, but with a much smaller charge density. Figure 1.3 provides a schematic representation of DESI and DeSSI analysis.

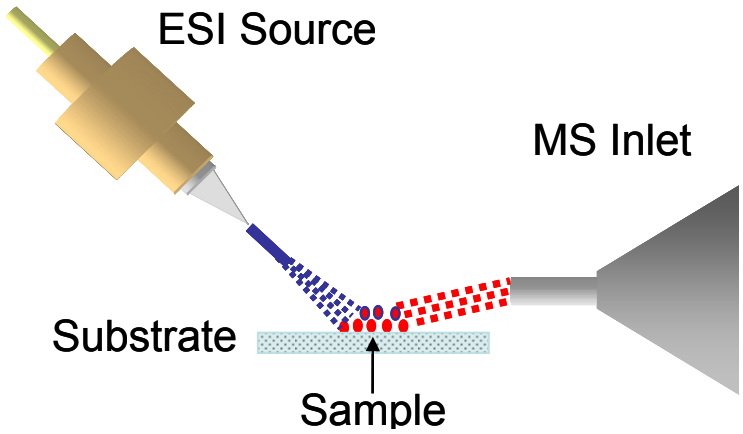

Figure 1.3: Schematic view of desorption electrospray ionization (DESI) and desorption sonic spray ionization (DeSSI).

In ND-EESI, the necessary particle momentum is provided by a high pressure nitrogen gas flow that effectively dislodges analytes from the surface and entrains them in a gaseous stream for subsequent ionization by a secondary electrospray plume. Unlike

DESI and DeSSI, ND-EESI utilizes decoupled desorption and ionization modes. This approach tends to decrease the dependency of the technique on the sample substrate but simultaneously necessitates accounting for the efficiency of transporting neutral molecules to the ionization zone. Figure 1.4. illustrates a basic ND-EESI experiment.

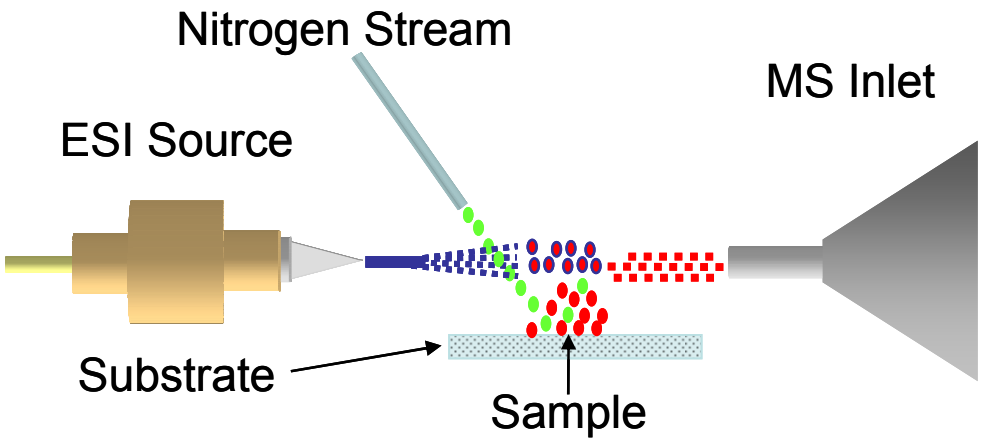

Figure 1.4: Schematic view of neutral desorption extractive electrospray ionization (ND-EESI).

Of the ESI-related ambient ionization techniques, the momentum based desorption methods have had the widest range of applications. The list of applications includes forensics,[19,40,45-47] explosives detection,[48-50,73] chemical warfare agent detection,[45,50-53] pharmaceutical analysis,[47,54-57,60,61] natural product analysis,[40,62] polymer analysis,[63,64] metabolomics,[40,65-67] proteomics,[40] glycomics,[70] and imaging.[22,71,72] This is in part because they were amongst the first to be developed, but also because they can be applied to a variety of surfaces, and do not require additional instrumentation. ND-EESI is a relatively new ambient ionization method, however the technique has tremendous potential since the nitrogen gas stream provides a non-destructive method of dislodging particles from fragile surfaces. (e.g., human tissues)

1.4.2 Comparison of Laser Desorption-Techniques

Whereas momentum based techniques rely on the kinetic energy provided by incoming particles to dislodge analytes from the surface, laser desorption techniques such as ELDI, MALDESI, liquid-MALDESI,[35] and laser ablation electrospray ionization (LAESI)[36] rely on the energy from an incoming laser pulse to lift neutrals from the surface. The desorbed neutrals are subsequently ionized either by entrainment into an orthogonal electrospray (ELDI, MALDESI, LAESI) or by undergoing electrospray like droplet fission directly from a desorbed liquid sample (liq-MALDESI). As was the case in MALDI, desorption and ionization are decoupled in time, but in this case the ionization is also decoupled in space and attributed to the interaction of the ablated plume with a secondary electrospray droplet, not with an ionized sample matrix. Figure 1.5 presents a schematic view of an ELDI process; the experimental arrangement for MALDESI and LAESI is similar, but in the case of MALDESI a matrix is co-crystallized with the sample and in LAESI a mid infrared laser is used instead of the UV laser typically employed in ELDI and MALDESI.

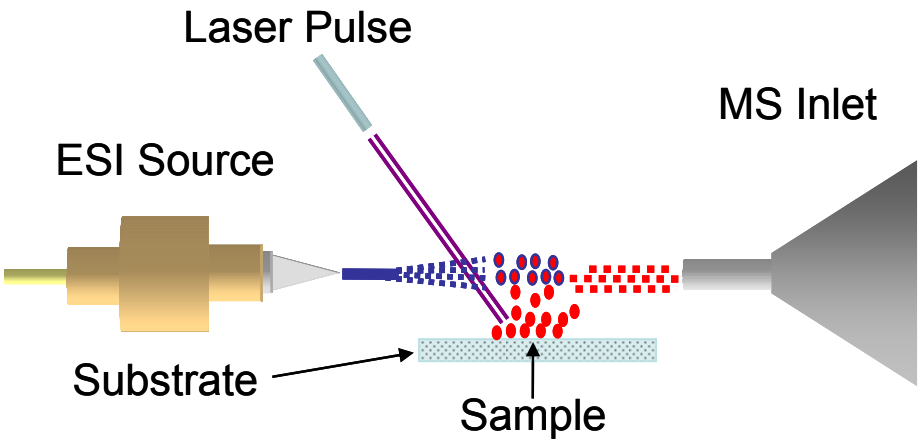

Figure 1.5: Schematic view of electrospray laser desorption ionization (ELDI). MALDESI and LAESI have a similar experimental setup.

As in MALDI, the laser desorption methods are very effective at removing materials from the surface. Once in the gas-phase, the polar molecules can be selectively ionized by ESI type mechanisms. Thus, the aforementioned techniques (ELDI, MALDESI, and LAESI) seek to combine the best characteristics of the two techniques that redefined biological mass spectrometry (ESI and MALDI) and it is not surprising that they have been primarily applied to the analysis of peptides and proteins. Whereas the desorption based methods can be applied to multiple types of surfaces and are relatively non-destructive, the laser based methods are destructive to the sample and typically require deposition of the sample onto well characterized substrates. Therefore, it is likely that these methods will not be extended to *in situ* analyses, but instead remain focused on addressing biological mass spectrometry applications such as proteomics and glycomics.

1.4.3 Comparison of Extraction Based Techniques

Extractive desorption techniques such as EESI, fused droplet electrospray ionization (FD-ESI)[37], and surface sampling probe (SSP) rely on the polarity of a solvent to extract analytes from either a surface (SSP)[38] or an aerosol (EESI, FD-ESI). In the case of the surface sampling probe, a liquid junction between a non-polar surface and the sampling probe is created. This junction effectively extracts analytes into a liquid layer above the surface that is subsequently directed to an electrospray emitter. In EESI and FD-ESI a charged electrospray plume is used to intersect an aerosolized sample. Analytes of interest are transferred to the ionizing plume due to their preference for the ionizing solvent versus the neutral spray solvent. In the case of EESI, there is a charge transfer between the extractive electrospray and the extracted analytes. In FD-ESI, the droplets from the electrospray fuse with neutral analyte droplets before subsequently

undergoing ESI like fission processes. Figure 1.6 depicts an overhead view of a typical EESI experiment.

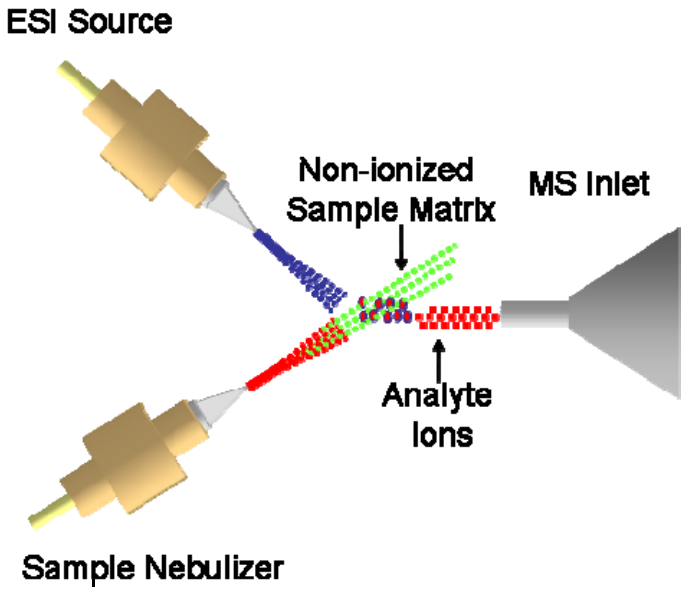

Figure 1.6: Schematic view of extractive electrospray laser ionization (EESI). FD-ESI has a similar experimental arrangement.

The extraction based techniques have extended the scope of ambient ionization mass spectrometry. In the case of SSP, the technique essentially acts as a method to interface a nano-electrospray source directly to the sample surface, effectively interfacing a small scale solvent extraction directly to electrospray ionization. While the method is not striking, it has been shown to be a very robust and reproducible means of analyzing particular substrates. Likewise, EESI and FD-ESI have opened up new avenues for ambient ionization by focusing on the analysis of liquid samples. In this case the major benefit is in the selective extraction of target analytes from difficult matrix interferences. The techniques are relatively new, but applications describing the analysis of complex perfumes,[74] milk,[75] and breath vapors[76] illustrate the direction of continued research.

1.5 CHARACTERISTICS OF DESORPTION ELECTROSPRAY IONIZATION (DESI)

In DESI, ions are produced by directing charged solvent droplets from an electrospray source toward a sample that is either a bulk material in its native state (e.g., pharmaceutical tablet) or one that has been deposited from solution onto a sampling substrate.[4] Analytes present at the surface are solvated by the electrospray to form an initial solvent layer; desorbed by the momentum of secondary droplet impact; and ultimately ionized by typical electrospray mechanisms.[19,20] The resulting gas-phase ions are then transferred to the mass spectrometer inlet by the influence of the applied potential and the pressure differential between atmospheric pressure and the low-pressure region of the mass analyzer.

DESI has enjoyed tremendous success since its introduction in 2004. However, like any other newly developed analytical technique there are issues requiring further attention. For DESI these challenges stem primarily from the geometry of the experimental arrangement and the physical characteristics of typical sample substrates. In the case of the experimental geometry, conventional DESI is dependent on as many as seven geometric variables as the electrospray tip, sample, and mass spectrometer inlet effectively form a scalene, obtuse triangle composed of independent angles, and distances.[39] Moreover, DESI analyses have been reported to be somewhat sensitive to the experimental geometry and optimization of the various parameters for each type of analyte requires a fair degree of experience.[40] Thus, it has been suggested that the complexity of the ionization technique may impact reproducibility and method robustness, ultimately impeding its transition from the research environment to the industry laboratory.[41]

Successful sample deposition for DESI analyses involves balancing drying time and sample spreading. If low volatility solvents such as water are used, the drying time

often becomes the rate limiting step of the analyses. If a more volatile solvent such as methanol is used, the evaporation time may be reduced; however the low surface tension of the solvent makes uniform sample deposition more challenging. These effects often produce "sweet spots" as the rate of solvent evaporation results in uneven sample distribution.[40] In addition, sample analyses that utilize smooth substrates are typically prone to erosion effects, thereby requiring alternative deposition onto porous or rough surfaces that retain the adsorbed analyte during the formation of the initial solvation layer.[42] It is therefore unsurprising that the impact of the sample substrate continues to be an area of interest in DESI related research.

TM-DESI was designed to overcome the aforementioned challenges regarding complexity and sample deposition. The concept (Figure 1.7) was proposed as a new mode of sample introduction, whereby samples were deposited onto substrates that were transparent to the ionizing electrospray. Thus, the new technique aimed to convert the triangular experimental arrangement of conventional DESI to a linear one in which the electrospray was no longer positioned off-axis to the mass spectrometer but instead held coaxial to it. Furthermore, the choice of a grid-like substrate was intended to reduce sample spreading by allowing the surface tension of the deposition solvent to effectively suspend the sample between the mesh strands.

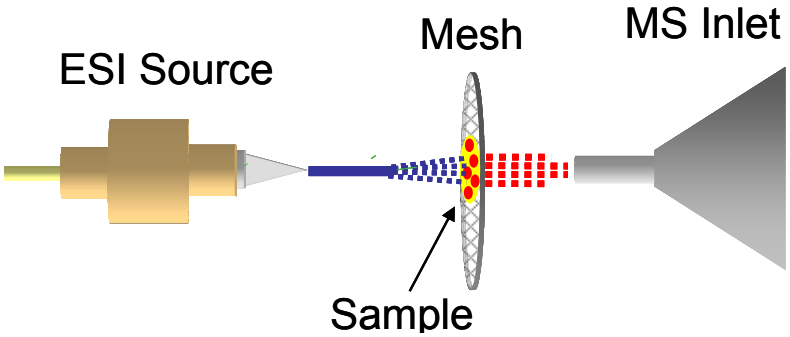

Figure 1.7: Schematic view of Transmission Mode Desorption Electrospray Ionization (TM-DESI).

1.6 Chapter Overview

The remaining chapters of this dissertation detail the development, optimization and application of TM-DESI and introduce an additional variant, surface-enhanced TM-DESI. Chapter two discusses the experimental techniques employed throughout the body of the work, with special attention given to the various types of materials and hardware developed and utilized throughout the subsequent chapters. Chapter three provides a summary of the development and optimization of TM-DESI and discusses the processes used during the initial characterization of the technique. The experiments discussed in Chapter 4 focus more closely on the influence of the mesh substrate on the performance of TM-DESI. These experiments provide an important foundation for more complicated studies in subsequent chapters and future developments. In Chapter five the attention shifts primarily to example applications of TM-DESI, however, various means of sample preparation and their impact on method performance are also highlighted. Chapter six discusses the development of surface-enhanced TM-DESI, a significant variant intended to increase the method specificity and in doing so, dramatically improve analytical performance relative to other ambient ionization techniques. Finally, Chapter seven takes a critical look at the body of work discussed in the previous chapters, draws several overarching conclusions, and makes recommendations for future studies.

1.7 References

(1) Karas, M.; Bachmann, D.; Hillenkamp, F. *Anal. Chem*. **1985,** 57, 2935–2939.

(2) Tanaka, K.; Waki, H.; Ido, Y.; Akita, S.; Yoshida, Y.; Yoshida, T. *Rapid Commun Mass Spectrom.* **1988**, 2 (20), 151–153.

(3) Yamashita, M.; Fenn, J. *J. Phys. Chem*., **1984**, 88 (20), 4451-4459.

(4) Takats, Z.; Wiseman, J.M.; Gologan, B.; Cooks, R.G. *Science.* **2004**, 306, 471-473.

(5) Cody, R.B.; Laramee, J.A.; Durst, H.D. *Anal. Chem*. **2005**, 77, 2297-2302.

(6) Instrumental Methods of Analysis, Willard, H.H.; Merritt, L.L.; Dean, J.A.; Settle, F.A. Wadsworth: Belmont, CA, 1988.

(7) Electrospray Ionization Mass Spectrometry: Fundamentals, Instrumentation, and Applications, Cole, R. B., Ed.; Wiley: New York, 1997.

(8) Applied Electrospray Mass Spectrometry, Gross, M.; Pramanik, B. N.; Ganguly, A.K. Marcel Dekker: New York, 2002.

(9) Cech, N. B.; Enke, C. G. *Mass Spectrom. Rev*. **2001**, 20, 362–387.

(10) Covey, T.R.; Lee, E.D.; Bruins, A.P.; Henion, J.D. *Anal. Chem*. **1986**, 58, 1451A-1461A.

(11) Thomson, B.A. *J. Am. Soc. Mass Spectrom*. **1998**, 9(3), 187-193.

(12) Chemical Ionization Mass Spectrometry, Harrsion, A.G. CRC Press: Boca Raton, FL, 1992.

(13) Robb, D.B.; Covey, T.R.; Bruins, A.P. *Anal. Chem*. **2000**, 72(15), 3653-3659.

(14) Kauppila, T.J.; Kotiaho, T.; Kostiainen, R.; Bruins, A.P. *J Am Soc Mass Spectrom.* **2004**, 15, 203-211

(15) Laiko, V.V.; Baldwin, M.A., Burlingame, A.L. *Anal. Chem*. **2000**, 72(4), 652-657.

(16) Zenobi, R.; Knochenmuss, R. *Mass Spectrom. Rev*. **1998**, 17, 337-366.

(17) Dole, M.; Mack, L. L.; Hines, R. L.; Mobley, R. C.; Ferguson, L. D.; Alice, M. B.*J. Chem. Phys.* **1968**, *49*, 2240-2249.

(18) Iribarne, J. V.; Thomson, B. A. *J. Chem. Phys*. **1976**, 64, 2287-2294.

(19) Venter, A.; Nefliu, M.; Cooks, R. G. *Trends Anal. Chem.* **2008,** *27,* 284–290.

(20) Chen, H.; Gamez, G.;Zenobia, R. *J Am Soc Mass Spectrom* **2009**, 20, 1947–1963.

(21) McEwen, C. N.; McKay, R. G.; Larsen, B. S. *Anal. Chem.* **2005,** *77,* 7826–7831.

(22) Cooks, R. G.; Ouyang, Z.; Takats, Z.; Wiseman, J. M. *Science* **2006,** *311,* 1566–1569.

(23) Williams, J. P.; Patel, V. J.; Holland, R.; Scrivens, J. H. *Rapid Commun. Mass Spectrom.* **2006,** *20,* 1447–1456.

(23) Andrade, F. J.; Shelley, J. T.; Wetzel, W. C.; Webb, M. R.; Gamez, G.; Ray, S. J.; Hieftje, G. M. *Anal. Chem.* **2008,** *80*, 2646–2653.

(24) Shelley, J. T.; Wiley, J. S.; Chan, G. C. Y.; Schilling, G. D.; Ray, S. J.;Hieftje, G. M. *J. Am. Soc. Mass Spectrom.* **2009,** *20*, 837–844.

(25) Harper, J. D.; Charipar, N. A.; Mulligan, C. C.; Zhang, X. R.; Cooks, R. G.; Ouyang, Z. *Anal. Chem.* **2008,** *80*, 9097–9104.

(26) Shiea, J.; Huang, M. Z.; Hsu, H. J.; Lee, C. Y.; Yuan, C. H.; Beech, I.; Sunner, J. *Rapid Commun.Mass Spectrom.* **2005,** *19*, 3701–3704.

(27) Peng, I. X.; Loo, R. R. O.; Shiea, J.; Loo, J. A. *Anal. Chem.* **2008,** *80*, 6995–7003.

(28) Sampson, J.S.; Hawkridge, A.M.; Muddiman, D.C. *J Am Soc Mass Spectrom* **2006**, 17, 1712–1716.

(29) Sampson, J.S.; Hawkridge, A.M.; Muddiman, D.C *Rapid Commun. Mass Spectrom*. **2007**; 21: 1150–1154.

(30) Chen, H.; Venter, A.; Cooks, R.G. *Chem. Commun*. **2006**, 2042–2044.

(31) Cheng, S. C.; Cheng, T. L.; Chang, H. C.; Shiea, J. *Anal. Chem.* **2009,** *81*, 868–874.

(32) Dixon, R. B.; Sampson, J. S.; Muddiman, D. C. *J. Am. Soc. Mass Spectrom.* **2009,** *20*, 597–600.

(33) Haddad, R.; Sparrapan, R.; Eberlin, M. N. *Rapid Commun. Mass Spectrom.* **2006,** *20*, 2901–2905.

(34) Chingin, K.; Chen, H.; Gamez, G.; Zhu, L.; Zenobi, R. *Anal. Chem.* **2009,** *81*, 123–129.

(35) Sampson, J.S.; Hawkridge, A.M.; Muddiman, D.C. *Anal. Chem*. **2008**, 80 (17), 6773-6778.

(36) Nemes, P.; Vertes, A. *Anal. Chem*. **2007**, 79, 8098-8106.

(37) Shieh,I-F,; Lee,C-Y.; Shiea, J, *J. Proteome Research* **2005**, 4, 606-612.

(38) Ford, M.j.; Van Berkel, G.J. *Rapid Commun. Mass Spectrom*. **2004**, 18,1303–1309.

(39) Nefliu, M.; Smith, J. N.; Venter, A.; Cooks, R. G. *J. Am. Soc.Mass Spectrom*. **2008**, 19, 420–427.

(40) Takats, Z.; Wiseman, J. M.; Cooks, R. G. *J. Mass Spectrom*. **2005**, 40, 1261–1275.

(41) Green, F.M.; Stokes, P.; Hopley, C.; Seah, M.P.; Gilmore, I.S.; O'Connor, G. *Anal. Chem*. **2009**, 81, 2286–2293.

(42) Pasilis, S. P.; Kertesz, V.; Van Berkel, G. J. *Anal. Chem*. **2007**, 79, 5956–5962.

(43) Cheng, S. C.; Cheng, T. L.; Chang, H. C.; Shiea, J. *Anal. Chem.* **2009**, 81, 868–874.

(44) Dixon, R. B.; Sampson, J. S.; Muddiman, D. C. *J. Am. Soc. Mass Spectrom*. 2009, 20, 597–600.

(45) D'Agostino, P. A.; Hancock, J. R.; Chenier, C. L.; Lepage, J. *J. Chromatogr. A* **2006,** *1110,* 86–94.

(46) Ifa, D. R.; Wiseman, J. M.; Qingyu, S.; Cooks, R. G. *Int. J. Mass Spectrom.* **2007,** *259,* 8–15.

(47) Nyadong, L.; Green, M. D.; De Jesus, V. R.; Newton, P. N.; Fernandez,F. M.. *Anal. Chem.* **2007,** *79,* 2150–2157.

(48) Cotte-Rodriguez, I.; Takats, Z.; Talaty, N.; Chen, H.; Cooks, R. G.. *Anal. Chem.* **2005,** *77,* 6755–6764.

(49) Takats, Z.; Cotte-Rodriguez, I.; Talaty, N.; Chen, H.; Cooks, R. G. *Chem. Comm.* **2005**, 1950–1952.

(50) Justes, D. R.; Talaty, N.; Cotte-Rodriguez, I.; Cooks, R. G. *Chem. Commun*. **2007**, 2142–2144.

(51) Cotte-Rodriguez, I.; Cooks, R. G. *Chem. Commun.* **2006**, 2968–2970.

(52) D'Agostino, P. A.; Chenier, C. L.; Hancock, J. R.; Lepage, J. *Rapid Commun. Mass Spectrom.* **2007,** *21,* 543–549.

(53) Song, Y.; Cooks, R. G. *J.Mass Spectrom.* **2007,** *42,* 1086–1092.

(54) Chen, H.; Talaty, N.; Takats, Z.; Cooks, R. G. *Anal. Chem.* **2005,** *77,* 6915–6927.

(55) Van Berkel, G. J.; Ford, M. J.; Deibel, M. A. *Anal. Chem.* **2005,** *77,* 1207–1215.

(56) Weston, D. J.; Bateman, R.; Wilson, I. D.; Wood, T. R.; Creaser, C. S. *Anal. Chem.* **2005,** *77,* 7752–7580.

(57) Williams, J. P.; Scrivens, J. H. *Rapid Commun. Mass Spectrom.* **2005,** *19,* 3643–3650.

(58) Hu, Q.; Talaty, N.; Noll, R. J.; Cooks, R. G. *Rapid Commun. Mass Spectrom.* **2006,** *20,* 3403–3408.

(59) Williams, J. P.; Patel, V. J.; Holland, R.; Scrivens, J. H. *Rapid Commun. Mass Spectrom.* **2006,** *20,* 1447–1456.

(60) Ricci, C.; Nyadong, L.; Fernandez, F. M.; Newton, P. N.; Kazarian, S. G. *Anal. Bioanal. Chem.* **2007,** *387,* 551–559.

(61) Ifa, D. R.; Manicke, N. E.; Rusine, A. L.; Cooks, R. G. *Rapid Commun. Mass Spectrom.* **2008,** *22,* 503–510.

(62) Talaty, N.; Takats, Z.; Cooks, R. G. *Analyst* **2005,** *130,* 1624–1633.

(63) Jackson, A. T.; Williams, J. P.; Scrivens, J. H. *Rapid Commun. Mass Spectrom.* **2006,** *20,* 2717–2727.

(64) Williams, J. P.; Hilton, G. R.; Thalassinos, K.; Jackson, A. T.; Scrivens, J. H. *Rapid Commun. Mass Spectrom*. **2007,** 21, 1693–1704.

(65) Chen, H.; Zhengzheng, P.; Talaty, N.; Raftery, D.; Cooks, R. G. *Rapid Commun. Mass Spectrom.* **2006,** *20,* 1577–1584.

(66) Kauppila, T. J.; Wiseman, J. M.; Ketola, R. A.; Kotiaho, T.; Cooks, R. G.;Kostiainen, R. *Rapid Commun. Mass Spectrom*. **2006,** 20, 387–392.

(67) Pan, Z.; Gu, H.; Talaty, N.; Chen, H.; Shanaiah, N.; Hainline, B. E.; Cooks, R. G.; Raftery, D. *Anal. Bioanal. Chem.* **2007,** *387,* 539–549.

(68) Bereman, M. S.; Nyadong, L.; Fernandez, F. M.; Muddiman, D. C. *Rapid Commun. Mass Spectrom.* **2006,** *20,* 3409–3411.

(69) Shin, Y.-S.; Drolet, B.; Mayer, R.; Dolence, K.; Basile, F. *Anal. Chem.* **2007,** *79,* 3514–3518.

(70) Bereman, M. S.; Williams, T. I.; Muddiman, D. C. *Anal. Chem.* **2007,** *79,* 8812–8815.

(71) Ifa, D.R.; Wiseman, J.M.; Qingyu, S.; Cooks, R.G. *Int. J. Mass Spectrom*. **2007**, 259, 5-15.

(72) Wiseman, J.M.; Ifa, D.R.; Venter, A.; Cooks, R.G. *Nat. Protocols* **2008**, 3, 517-524.

(73) Chen, H.; Hu, B.; Hu, Y.; Huan,Y. Zhou, Z.; Qiaoc, X. *J Am Soc Mass Spectrom* **2009**, 20, 719–722.

(74) Chingin, K.; Gamez, G.; Chen, H. W.; Zhu, L.; Zenobi, R. *Rapid Commun. Mass Spectrom*. **2008**, 22, 2009–2014

(75) Chen, H. W.; Venter, A.; Cooks, R. G. *Chem. Commun*. **2006,** 2042-2044.

(76) Chen, H. W.; Wortmann, A.; Zhang, W. H.; Zenobi, R. *Angew. Chem. Int. Ed*. **2007**, 46, 580–583.

.

Chapter 2: Experimental Methods

Chapter 1 of this dissertation incorporated a review of the electrospray ionization process along with an introduction to desorption electrospray ionization and its adaptation to a transmission mode (TM-DESI). This chapter provides a summary of the materials, hardware and procedures used in the development, optimization and application of TM-DESI using both unmodified and enhanced substrates. It is important to note that while the mass spectrometry experiments discussed in this dissertation were all performed using a linear ion trap mass spectrometer, TM-DESI is equally applicable to other mass spectrometers equipped with an atmospheric interface (e.g., triple stage quadrupoles, quadrupole ion traps, time of flight mass spectrometers). Therefore, this chapter focuses on the general points regarding the ionization technique and the mass spectrometric analysis. Further details of the mass spectrometric conditions used in the specific experiments are left to subsequent chapters.

2.1 Mesh Materials and Sample Holders

2.1.1 Mesh Materials

A total of 21 different mesh substrates manufactured from five different polymeric materials; polypropylene, polyetheretherketone (PEEK), ethylene tetrafluoroethylene, nylon-6,6, and polyethylene terephthalate along with several types of stainless steel mesh sheets were purchased from Small Parts, Inc. (Miramar, FL). For studies discussed in Chapter 3 through Chapter 5 mesh sheets were cut into 5 mm x 10 mm rectangular pieces and rinsed with a mixture of water, methanol, and acetone and allowed to dry before use. Blank measurements were taken prior to sample preparation to ensure that the mesh pieces were free of analyte or any detectable chemical interference.

2.1.2 Sample Holders

In Chapter 3 samples were introduced using a holder constructed of two rectangular pieces of high density polyethylene (HDPE) that allowed the mesh to protrude from one end. In Chapter 4 the sample holder was modified and constructed of two rectangular support pieces (1.2 cm x 15 cm): one HDPE 2.3 mm thick and one oriented polyester 0.3 mm thick. A 7 mm diameter hole was drilled through both support pieces and the sample mesh was held between the two layers. In Chapter 6, the design of the sample holder was modified to accommodate materials specifically designed for surface-enhanced TM-DESI analysis. In this case, a transmissive sample stage for TM-DESI analyses with a 2 cm square cutout was constructed of 2.3 mm thick HDPE and mounted orthogonally to an Omni Spray ion source (Prosolia, Indianapolis IN). Mesh samples were affixed to a 3.5 cm x 6.5 cm slide constructed of 0.77 mm thick oriented polyester with an 8 mm square cutout to accommodate transmission through the mesh sample, slide and transmissive sample stage. All of these sample holders were utilized in Chapter 5. The design of the TM-DESI sample holder continues to be improved with the newest version including a professionally machined mounting plate that incorporates two-piece PEEK sample slides with square and circle masking plates to provide a more consistent sampling area. These components were designed in conjunction with Prosolia Inc. (Indianapolis, IN) as part of a prototype TM-DESI adaptation kit and manufactured by Prosolia Inc.

2.2 Surface Enhanced Mesh Preparation

Mesh materials were marked, cut into 1cm x 1cm squares and thoroughly cleaned with methanol to remove any residual ink. The materials were then sonicated in an aqueous solution of Synthrapol (1%) to remove any surface contaminants. Following a thorough rinse with DI H_2O, the cleaning procedure was completed by sonicating the

materials in an acetonitrile and water solution (50:50 v:v) for five additional minutes. Cleaned materials were stored for future use in HPLC grade H_2O.

Acid-catalyzed hydrolysis of polyamide (nylon-6,6) materials to expose carboxyl groups was performed using a 3M solution of HCl. The 125 μm strands of the polyamide mesh materials used in Chapter 6 were found to hydrolyze sufficiently after 2 hours of exposure at a temperature of 40 °C but more completely after 24 hours of exposure at 25 °C or 40 °C. Following hydrolysis, mesh materials were rinsed with HPLC grade H_2O to remove any residual acid, blown dry with compressed air, and stored dry in sealed glass or PTFE containers.

Derivatization of the hydrolyzed mesh materials with neutravidin (a deglycosylated form of avidin) was performed using a two step procedure for carbodiimide mediated coupling of the surface carboxyl groups to primary amines of the protein. In the first step the free carboxyl groups of the hydrolyzed polyamide mesh materials were converted to reactive NHS esters by placing them in a room temperature solution of EDC (108mM) and sulfo-NHS (77mM) in MES coupling buffer (pH = 5) for 15 min. After rinsing the mesh materials in phosphate buffered saline (pH = 7.4), neutravidin (either in FITC derivatized or native form) was coupled to the mesh by immersing the mesh materials (20 per batch) for 24 hours in a 3.3 μM solution of the protein in PBS (pH = 7.4). Following protein derivatization, the mesh materials were rinsed free of excess protein with PBS and immersed in a 100 μM solution of $VICAT_{SH}$. The biotin group of the reagent bound to the free binding sites of the neutravidin while the iodoacetaminyl capture agent remained exposed and therefore capable of reacting specifically with free sulfhydryl analytes.

2.3 SAMPLE PREPARATION

Five different methods were used for sample preparation. For analyses of bulk mosquito nets, the sample was held in place by affixing it to a 26 mm by 76 mm x 3 mm PEEK backing plate with an 8 mm by 38 mm slot cut into it to facilitate transmission of the electrospray through both the sample and the backing plate. For analyses requiring direct deposition of individual spots, a 5 μL syringe (SGE, Austin, TX) was used to deposit between 1μL and 3μL of solution directly onto a sample mesh. For analyses requiring deposition of gross amounts of sample followed by sample masking, an Eppendorf pipetter was used to deliver 25 μL of sample solution in a stream several mesh cells wide across the entire length of the mesh surface. A sample mask was then placed over the mesh to create a series of subsamples from one deposition. For analyses requiring mesh immersion, mesh materials immersed directly in the sample for 1s before being affixed to the sample holder. Finally, for analyses requiring the direct sampling of surfaces, mesh materials were initially pressed against an adhesive film (Tritech, Southport, NC) that transferred some of the adhesive to the mesh. The modified mesh materials were then used to collect samples directly from the laboratory bench top. Specific studies discussed in Chapter 3 were carried out to assess the impact of the sample deposition solvent and the drying time (i.e., wet vs. dry analysis).

Sample preparation for surface-enhanced analysis involved adjusting the pH of the sample to greater than 9.5 using NH_4OH; immersing the sample mesh in the solution for 5 minutes; removing the mesh from the sample; and rinsing it with HPLC grade water and methanol. The mesh was then placed under a UV lamp for approximately 10 minutes to facilitate photocleavage of the o-nitrobenzyl linkage connecting the captured analyte to the mesh surface. Following photocleavage, the mesh was introduced directly to the TM-DESI source for analysis.

2.4 IONIZATION AND MASS ANALYSIS

A Prosolia Omni Spray™ ion source was mounted to a Thermo Fisher Scientific LTQ XL mass spectrometer (Thermo Fisher Scientific Inc., Waltham, MA) and modified to allow an angle of zero degrees between the electrospray tip and capillary inlet to the mass spectrometer. Mass spectra were acquired by scrolling the sample mesh (either manually or via a computer controlled stepping motor) perpendicularly into the electrospray plume between the spray tip and the capillary inlet, thereby allowing transmission of the ionizing spray through the mesh. Specific studies discussed in Chapter 3 were carried out to determine the optimum position of the sample mesh and electrospray tip relative to the capillary inlet to the mass spectrometer.

Mass spectra were acquired using the Xcalibur 2.0 software program in either positive or negative mode, depending on the ionization affinity of the sample, with the ion accumulation time set between 5 ms and 10 ms and signal averaging set for 3 or 4 microscans. The temperature of the heated capillary was held at 200 ^{o}C for all sample analysis. Nitrogen was used as the DESI nebulizing gas. A syringe pump (Harvard Apparatus, Holliston, MA) was used to deliver water; methanol; acetonitrile; a 50:50 (v:v) mixture of water and methanol; a 49:49:1 (v:v:v) mixture of water, methanol, and formic acid, or a 5:1 (v:v) mixture of acetonitrile and chloroform as the electrospray solvent. Specific studies discussed in Chapter 3 were carried out to determine the appropriate range of nitrogen pressures, electrospray solvent flow rates, and electrospray voltages.

2.5 LINEAR ION TRAP MASS SPECTROMETER

The linear ion trap mass spectrometer (LIT)[1] is a two dimensional (2-D) variation on the three dimensional (3-D) ion trap originally reported by Nobel Laureate Wolfgang Paul in 1953.[2] Like many mass spectrometers it incorporates the basic elements of an ion

introduction source; ion optics for focusing and transport; a mass analyzer; and a detection system. A schematic of the LIT used in this work is shown if Figure 2.1.

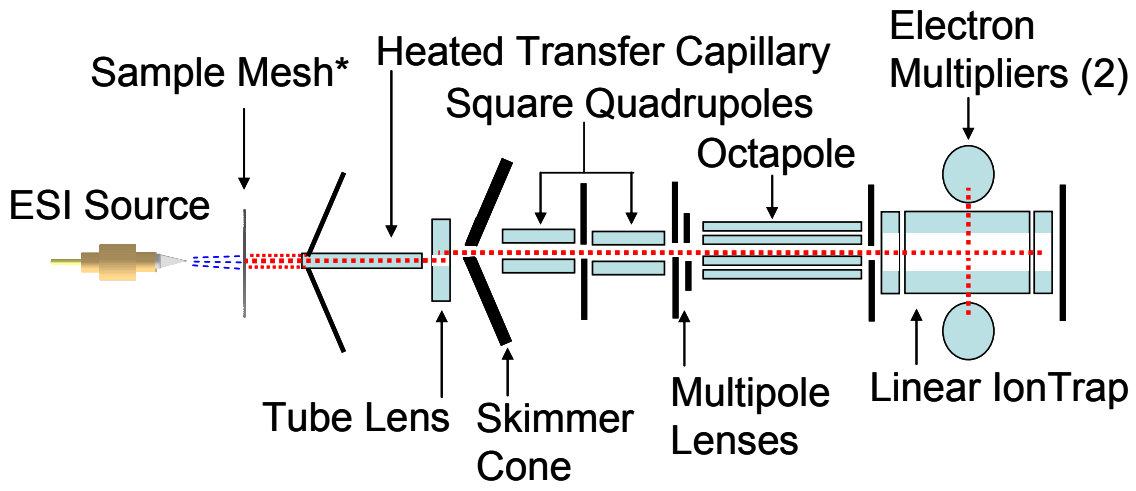

Figure 2.1: A schematic view of the two dimensional ion trap used in this dissertation (i.e., Thermo LTQ XL) coupled to a TM-DESI source.

In this configuration ions are created in the open atmosphere and transferred under the influence of an applied voltage and the pressure differential between atmospheric pressure and the lower pressure region of the LIT to the sample inlet (i.e., the heated transfer capillary in Figure 2.1). The heated capillary acts as ion desolvation region and transfers the ions to a tube lens whose exit is off axis from a skimmer cone. The tube lens and skimmer cone act to remove additional unwanted neutral molecules and steer ions into the quadrupole, multipole, and octapole region. Ultimately, this ion optics system is tuned to transfer a beam of ions through the conductance limits at the entry to the linear ion trap.

The linear ion trap uses a set of quadrupolar rods to confine ions radially and a static potential on the two end electrodes to confine the ions axially.[3] The three electrode configuration can be used to trap ions in a well along their axis.[4] Ions are then sorted

using mass selective instability and resonance ejection techniques. Ultimately, the trapped ions are scanned out of the trap and ejected between the rods of the center section of the ion trap to two electron multiplier located on either side of it. Since resonance ejection will destabilize the ions in either a positive or negative direction, the two multipliers are used to detect ions ejected in either manner. Along with an increased ion volume, and faster scan times, the ability to detect more of the ejected ions is an advantage of the two dimensional trap over its three dimensional counterpart.[1,3]

2.6 Fluorescence Microscopy and Fluorimetry

Microscopy of mesh materials was performed using either the 2.5X or 4X objective of an Olympus BX2 epifluorescent microscope equipped with a 12 bit CCD camera (DVC Co., Austin, TX) and high-pressure mercury bulb excitation source. Excitation occurred at 480 nm and emission was monitored at 535 nm. Photomicrographs were captured via DVC software with adjustable gain, offset, and exposure time. While various microscopy settings were used for different experiments based on the sensitivity of the microscope, all settings were consistent among the samples being compared.

Fluorimetry experiments were conducted using a Perkin Elmer Victor 3 fluorimeter equipped to read samples presented in 24 well plates. Aqueous samples (1 mL) were deposited in plate wells and the fluorescence was counted for 1 second. Excitation and emission were modulated using filters of 480+/-5 nm and 535+/-5 nm. Analysis of mesh samples was performed by placing the mesh material flat on the bottom of the well and reading the fluorescence from the top side of the plate.

2. References

(1) Schwartz, J.C.; Senko, M.W.; Syka, J.E.P; J Am Soc Mass Spectrom. 2002, 13 659-669.

(2) Paul, W.; Steinwedel, H. Zeitschrift fur Naturforschung 1953, 8(7), 448-450.

(3) Douglas, D.J.; Frank, A.J.; Mao, D. Mass Spec. Rev. 2005, 24(1), 1-29.

(4) March, R.E. *Int. J. Mass Spectrom*. **2000**, 200, 285-312.

Chapter 3: Development and Optimization of Transmission Mode Desorption Electrospray Ionization

3.0 Chapter Overview

A new mode of operation for desorption electrospray ionization (DESI) analysis of liquids or solid residues from evaporated solvents is presented. Unlike traditional DESI, the electrospray is not deflected off of a surface but instead is transmitted through a sampling mesh at a 0° angle between the electrospray tip, sample mesh, and capillary inlet of a mass spectrometer. In this configuration, deposited samples can be analyzed rapidly without rigorous optimization of spray distances or angles and without the preparation time associated with solvent evaporation. The new transmission mode desorption electrospray ionization (TM-DESI) technique is not applicable to bulk materials, but instead is a method designed to simplify the sample preparation process for liquid samples and sample extracts. The technique can reduce analysis time to seconds while consuming only microliters of sample. The results presented in this chapter summarize the optimization of the technique and highlight key figures of merit for several model compounds.

3.1 Introduction

Desorption electrospray ionization (DESI)[1-40], direct analysis in real time (DART)[41], desorption atmospheric pressure chemical ionization (DAPCI)[12,22,42], electrospray assisted laser desorption ionization (ELDI)[43], atmospheric solids analysis probe (ASAP)[44], and flowing afterglow atmospheric pressure glow discharge ionization (FA-APGD)[45,46] are among the recently developed ambient ionization techniques that have revolutionized mass spectrometric analysis by facilitating direct and rapid analysis of both bulk materials (e.g., tissues, pharmaceuticals) and samples deposited from a solution onto a sampling surface. In the case of DESI, ions are produced by directing charged solvent droplets from an electrospray source toward a sample. Analytes on the

surface are ionized and desorbed by the incoming plume prior to mass analysis. DESI is one of the more universal techniques since it can be used to analyze larger biomolecules and exploit reactive chemistry via alteration of the solvent and solvent additives.[5] DESI requires optimization of an array of experimental variables including DESI spray solvent composition, desorption angle and distances, sampling angle and distances.[5] Optimization is especially critical as the chemical identity of the target analytes varies.[5]

In some cases samples analyzed by DESI are ionized directly in their native environment (e.g., imaging, pharmaceutical analysis) without any pre-treatment. However, in many others the sample is extracted or otherwise prepared in a suitable solvent and ultimately deposited onto a surface (e.g., glass slide, paper, metal, plastic, TLC plate). This sample preparation process often requires the complete evaporation of the solvent prior to analysis since the typical incident angle of the electrospray nebulizing plume tends to rapidly erode liquids and dissolved solids from the surface before they are ionized. When the solvent is highly volatile (e.g., methanol), the evaporation time may be minimal; however the low surface tension of the solvent makes reproducible sample deposition more challenging. In cases where the solvent is less volatile (e.g., water), the slow evaporation time of the solvent may reduce sample throughput.

Historically, a major factor in the successful application of DESI has been the tuning of the geometry of the experiment. The numerous degrees of freedom associated with a freely adjustable sample stage and spray tip relative to a fixed capillary inlet allow incredible flexibility, but in doing so add inherent complexity. Key adjustable parameters including incident and collection angles, sample height and spray heights, and plume impact to inlet distance are typically optimized, but often differ among sample types. Recent efforts have been aimed at simplifying the DESI experiment by fixing the geometric arrangement of the sample surface, spray tip and capillary inlet.[34] In these

studies the dependence on angles and distances is minimized by enclosing the sampling surface in a small chamber and spraying the surface with both the spray tip and capillary held near 90 degrees to it. The ion cloud is created within the sample chamber and transferred into the mass spectrometer due to the pressure differential of the vacuum. In other work, solid phase microextraction (SPME) fibers used to extract either vapors from the headspace of samples or analytes from solution have been inserted into an electrospray plume for DESI analysis.[24,39] In these instances the surface area was sufficiently small relative to the electrospray plume and ionization of adsorbed surface analytes occurred as the plume traveled around the fiber.

The present investigation reports an alternate method for simplifying the geometry dependence of DESI experiments that require sample deposition. In this method the sample is not deposited onto a continuous solid surface but rather onto a sampling mesh. Instead of deflecting the electrospray plume off of the surface and into the mass spectrometer, the incident spray angle is reduced to zero degrees and the spray is transmitted through the sample. This "transmission-mode" DESI technique allows for rapid analysis of both deposited residues and solutions without rigorous optimization of spray distances or angles and without the preparation time associated with solvent evaporation. Figure 3.1 presents a schematic view of TM-DESI and illustrates the simplification provided by the implementation of a transmissive substrate.

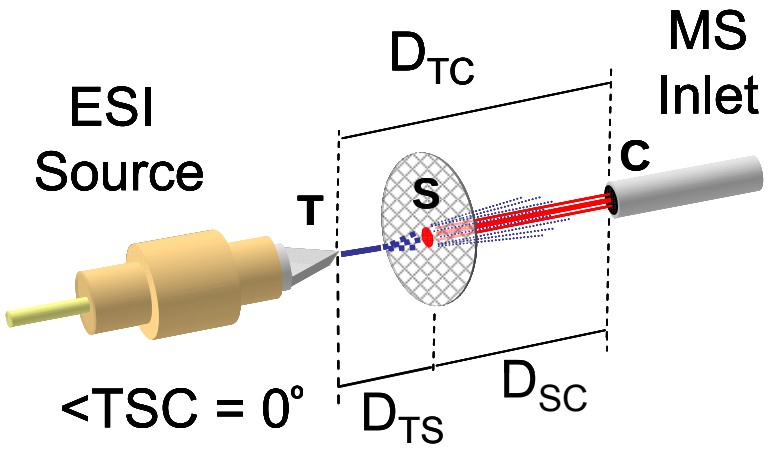

Figure 3.1: Transmission mode desorption electrospray ionization (TM-DESI) geometry. Sample (S) is deposited on a mesh substrate and analyzed by passing an electrospray through it. The angle between the electrospray tip (T), sample (S), and capillary inlet (C) to the mass spectrometer is set to 0 degrees. D_{TC} is the distance from the electrospray tip to the capillary, D_{TS} is the distance from the electrospray tip to the sample, and D_{SC} is the distance from the sample to the capillary.

3.2 EXPERIMENTAL

3.2.1 Materials

Nicotine, bradykinin, and rhodamine 6G were purchased from Sigma Aldrich. (St. Louis, MO). All standards were used without further purification and prepared in high purity solvent (e.g., water, methanol, hexane or acetonitrile) obtained from Fisher Scientific (Hampton, NH). Red and blue permanent markers (Fine Sharpie, Sanford Corporation, Oak Brook, IL) were also used as sources of the easily ionized dyes rhodamine 6G and Basic Blue 7.

Five different sheets of mesh material with similar characteristics (Table 3.1) were purchased from Small Parts Inc. (Miramar, FL) and cut into 5 mm x 10 mm rectangular pieces. Mesh pieces were rinsed with a mixture of water, methanol, and

acetone and allowed to dry before use. Blank measurements were taken prior to sample preparation to ensure that the mesh pieces were free of analyte or any detectable chemical interference.

Table 3.1: Sample Mesh Characteristics

Mesh Material	Open Space (µm)	Strand Diameter (µm)	Transmittance (%)
PEEK	300	200	36.0
Nylon (6,6)	350	240	35.0
Polyester	350	250	34.0
Polypropylene	297	215	33.5
Stainless Steel	381	250	36.0

3.2.2 Mass Spectrometry

An Omni Spray™ ion source (Prosolia, Inc., Indianapolis, IN) was mounted to a Thermo Fisher Scientific LTQ XL mass spectrometer (Thermo Fisher Scientific Inc., Waltham, MA) and modified to allow an angle of zero degrees between the electrospray tip and capillary inlet to the mass spectrometer. Samples were affixed to the sample slide arm of the Omni Spray™ ion source using a sample holder constructed of two rectangular pieces of high density polyethylene (HDPE) that held the sample screen on one end. Mass spectra were acquired by scrolling the sample mesh perpendicularly into the electrospray plume between the spray tip and the capillary inlet, thereby allowing transmission of the ionizing spray through the mesh. Specific studies were carried out to determine the optimum position of the sample mesh and electrospray tip relative to the capillary inlet to the mass spectrometer.

Mass spectra were acquired in either positive or negative mode, depending on the ionization affinity of the sample, with the ion accumulation time set to 10 ms and signal averaging set for 4 microscans. The temperature of the heated capillary was held at 200 ^{o}C for all sample analysis. Nitrogen was used as the DESI nebulizing gas. A syringe pump (Harvard Apparatus, Holliston, MA) was used to deliver water; methanol; acetonitrile; a 50:50 (v:v) mixture of water and methanol; or a 49:49:1 (v:v:v) mixture of water, methanol, and formic acid as the electrospray solvent. Specific studies were carried out to determine the appropriate range of nitrogen pressures, electrospray solvent flow rates, and electrospray voltages.

3.2.3 Fluorescence Microscopy

Microscopy was performed using either the 2.5X objective of an Olympus BX2 epifluorescent microscope equipped with a 12 bit CCD camera (DVC Co., Austin, TX) and high-pressure mercury bulb excitation source. Excitation occurred at 480 nm and emission was monitored at 535 nm. Photomicrographs were captured via DVC software with adjustable gain, offset, and exposure time.

3.2.4 Sample Preparation

Samples were prepared by spotting 1 μL of solution onto a sample mesh using a 5 μL syringe (SGE Austin, TX). Specific studies were carried out to assess the impact of the sample deposition solvent, the sample substrate and the drying time (i.e., wet vs. dry analysis).

3.3 Results and Discussion

Transmission mode desorption electrospray ionization depends on ten experimental variables that can be subdivided into three categories: those that define the

geometry of the experiment, those that characterize the electrospray, and those that govern the desorption/ionization chemistry at the sample surface.

3.3.1 Geometric Variables

With a fixed electrospray angle of zero degrees (Figure 3.1), the geometric variables of the experiment are reduced from seven[37] to two: the distance between the sample mesh and the capillary inlet to the mass spectrometer, D_{SC}, and the distance between the electrospray tip and the capillary inlet, D_{TC}. Defining these two distances necessarily dictates the position of the electrospray tip relative to the sample mesh.

Experiments using rhodamine 6G and Basic Blue 7 were conducted to determine the optimal range for the geometric variables D_{SC} and D_{TC}. With the solvent flow rate set to 10 μL/min and the nebulizing gas pressure set to 100psi, D_{SC} and D_{TC} were varied incrementally throughout their possible range (i.e., 5mm < D_{TC} < 21mm and 1mm < D_{SC} < 20mm) and an average peak area for the protonated species at each position was used to construct a contour plot of the response. (Figure 3.2)

Under these electrospray conditions, the largest responses were observed when the sample mesh was placed between 8 and 10 mm from the capillary inlet and the electrospray tip was held 2 to 3 mm from the mesh (i.e., D_{TC} between 10 and 12 mm) These findings correlate with what is already known about the optimal distance between an electrospray tip and a capillary inlet in a standard ESI experiment[47] and the distance between the ESI tip and a sample surface in a DESI experiment.[5] Furthermore, additional experiments conducted at lower flow rates (e.g., 3 μL/min) favored D_{SC} values of less than 8 mm; thereby indicating that a more compact geometry that is similar to traditional DESI may also be appropriate for TM-DESI analysis of dried residues. However, when extended to the analysis of wet samples, the response was lower at these shorter

distances, a result most likely due to the incomplete desolvation of the analyte ions. Finally, the experimental results also illustrate that the TM-DESI technique is only moderately sensitive to variations in these distances under given electrospray conditions and that slight differences in sample placement are unlikely to result in major fluctuations in signal intensities.

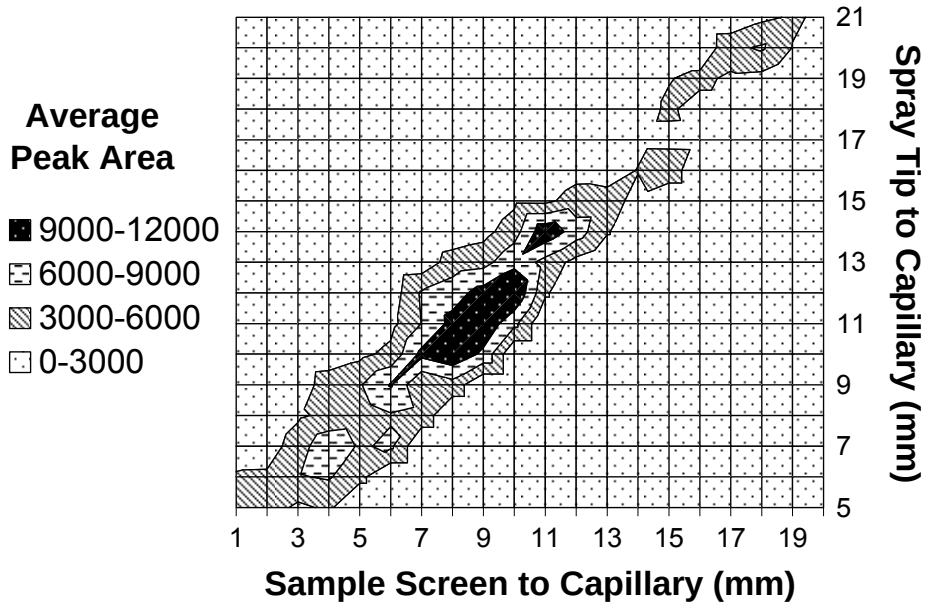

Figure 3.2: Average peak area of protonated Basic Blue 7 (m/z 478) across variations in the distance of the sample screen to capillary inlet (D_{SC}) and spray tip to capillary inlet (D_{TC}). The dark shaded region indicates the largest response

3.3.2 Electrospray Variables

Variables that characterize the electrospray in TM-DESI are identical to those in standard electrospray experiments, namely the electrospray voltage, the pressure or flow rate of the nebulizing gas, and the flow rate of the sample (i.e., the flow rate of the spray solvent). Experiments using rhodamine 6 G and Basic Blue 7 were conducted to determine the impact of varying these variables on the TM-DESI response. With the geometry set at D_{SC} equal to 8mm and D_{TC} equal to 10mm, the maximum average peak

area was observed when the solvent flow was 10 µL/min and the nitrogen pressure was 100 psi, although other pairings also produced strong responses. (Figure 3.3)

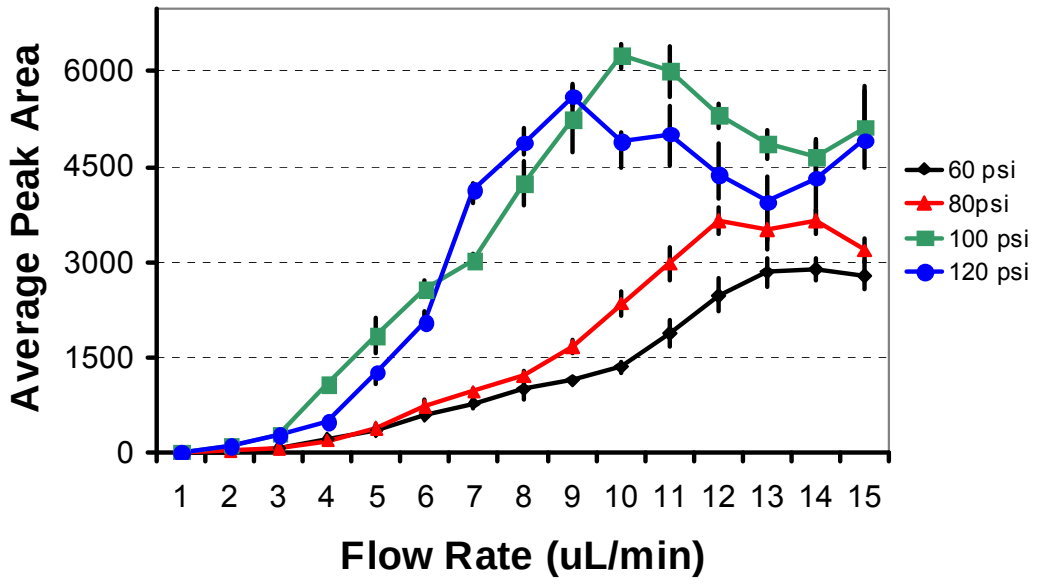

Figure 3.3: Response of protonated Basic Blue 7 (m/z 478) across variations in nebulizing gas pressure (psi of N_2) and flow rate of electrospray solvent (Methanol). Error bars are depicted as one standard deviation about the mean of 5 replicate measurements taken at each data point**.**

Variation of the electrospray voltage showed a maximum response at 4.0 kV, with a range of values greater than 3.0 kV providing adequate response. (Figure 3.4) While the results for nebulizing gas pressure and electrospray voltages are typical for both standard electrospray experiments and DESI analyses[5], the optimal flow rate of 10 µL/min concurred with several values reported for DESI,[7,17] but was higher than others performed with lower flow rates of only 2 - 5 µL/min.[5,12] As discussed in the previous section, this optimal flow rate is likely an artifact of the chosen geometry and would be reduced if the geometry were more compact.

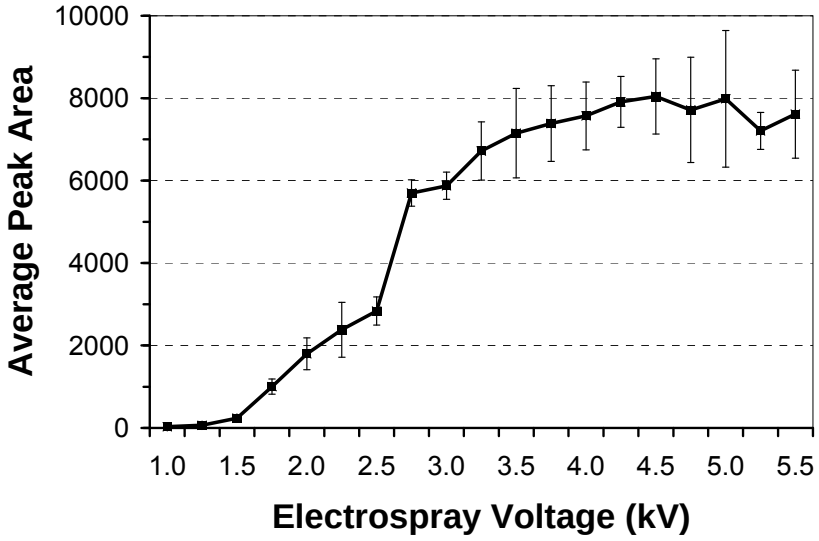

Figure 3.4: Response of protonated Basic Blue 7 (m/z 478) with variations in electrospray voltage. Error bars are depicted as one standard deviation about the mean of 5 replicate measurements taken at each data point.

3.3.3 Sample Spot Size and Shape in TM-DESI

Experiments were conducted to determine the influence of the electrospray solvent flow rate and experimental geometry on the TM-DESI sampling spot size and shape. Accordingly, a standard piece of printer paper was cut into 5 mm by 10 mm pieces and inserted into the sample holder in place of a sampling mesh. A solution of rhodamine 6G (100 pg/μL in MeOH) was electrosprayed for 30 s at various flow rates (2 μL/min to 10 μL/min) and distances (D_{TS} 2 mm to 8 mm) onto the paper substrate, resulting in depositions of 100 to 500 pg of rhodamine 6G. Fluorescence microscopy was used to determine the effective size and shape of the electrospray plume as it reached the substrate. Figure 3.5 shows an example where the electrospray flow rate was 5 μL/min and the distance from the spray tip to the sample was 2 mm. The bright area shown in the photomicrograph illustrates that the TM-DESI spot is dense, relatively symmetrical, and has a diameter of approximately 1 mm under these electrospray conditions. These

characteristics therefore result in an effective sampling area of approximately 0.8 mm^2. Higher flow rates and larger distances resulted in more irregular, diffuse spray patterns with sampling diameters about 2 to 3 mm. These results generally agree with recent reports for DESI imaging[48] but differ in that elliptical spray patterns are not observed at higher flow rates. Ultimately, a distance of 2 mm and an electrospray flow rate of 5 μL/min provide a balance between spot regularity and the flux of the ionizing solvent through the mesh.

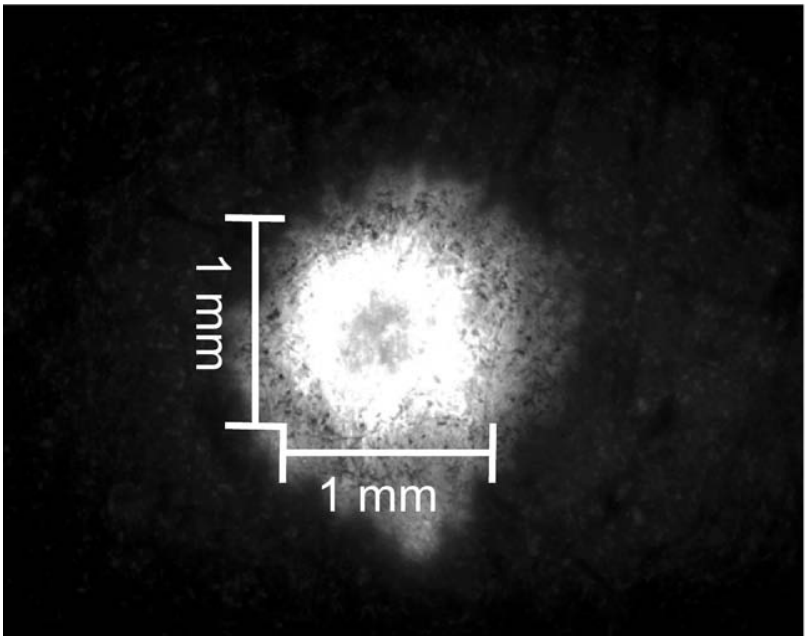

Figure 3.5: Fluorescence image of rhodamine 6G electrosprayed onto a paper substrate at a distance of 2 mm and an electrospray flow rate of 5 uL/min. Under these electrospray conditions the TM-DESI spot size remains essentially circular and has a diameter of approximately 1 mm.

3.3.4 Surface Desorption/Ionization Variables

Variables that influence the surface ionization in TM-DESI include the identity of the spray solvent, the identity of the sample deposition solvent, the composition and

physical characteristics of the substrate material, the identity of the target analyte, and the surface density of the target analyte deposited on the substrate. The chemistry of the desorption/ionization mechanism has been the subject of several reports [12,21,23,37]. TM-DESI depends on four variables that are in common with traditional DESI: the composition of the substrate material, the identity of the electrospray solvent, the identity of the target molecule, and the surface density of the target molecules on the substrate. Since TM-DESI can also be used for liquid samples, the identity of the sample deposition solvent is an additional variable that may directly influence the desorption and ionization in these analyses. While a complete investigation of surface parameters was outside the scope of this Chapter, exploratory studies were performed to investigate the potential influence of several of the principal variables.

3.3.5 Sample Substrate

Several attributes of the sample substrate, including the material of construction, the mesh stand size, and mesh open space (i.e., the mesh transmittance) govern how efficiently analytes are suspended on and removed from the surface. Five sample meshes of differing materials but with similar physical characteristics were investigated in this introductory investigation (Table 3.1). As an initial study, the effect of the substrate material on the lifetime of the TM-DESI signal was investigated for Rhodamine 6G, nicotine, and bradykinin at both low and high concentrations and for both wet (i.e., solvated) and dry analysis (i.e., analysis after evaporation of the deposition solvent).

As exemplified in Figure 3.6 for Rhodamine 6G, the substrate material had a noticeable impact on the response, especially at lower concentrations. In this case the polypropylene and PEEK meshes produced the largest responses while the polyester and stainless steel meshes produced much lower responses. It should be noted that no

additional potential was applied to the surfaces during analysis. Therefore, the relatively poor ionization efficiency for the stainless steel mesh may be caused by charge dispersion at the conductive surface. For all of the compounds studied, both wet and dry analysis of low concentration samples produced sharp initial peaks, as observed in Figure 3.6, followed by rapid signal decay. When the concentration was increased, a sharp initial peak was still observed, but decay proceeded at a much slower rate. In general, results obtained for nicotine and bradykinin were comparable to those for Rhodamine 6G and look very similar to what has been previously reported for other dyes by DESI .[25]

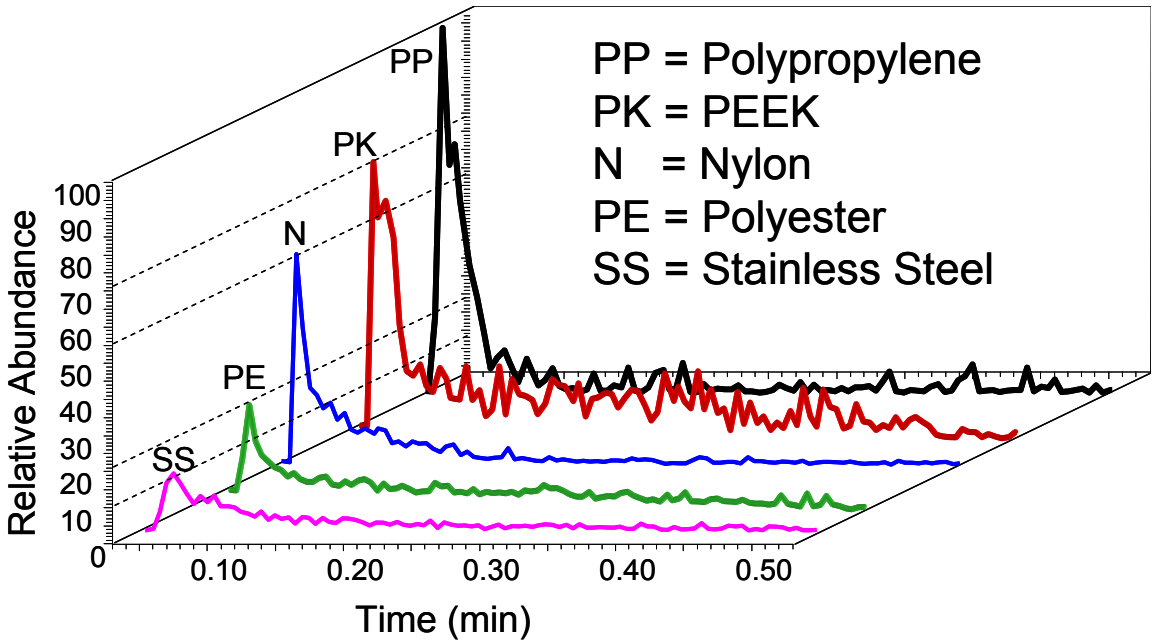

Figure 3.6: Relative TM-DESI signal of 10 pg of Rhodamine 6G from five different mesh materials with similar transmission characteristics (i.e., strand diameters of ~200-250 uM and open space of ~ 300-400 uM). Samples were spotted using 1 µL of methanol and allowed to dry prior to analysis.

Aside from the differences observed between the mesh materials, a difference was also noted between wet and dry analysis of samples at higher concentrations. In this case, the signal decay for dry analysis was much more gradual as analyte was continually

desorbed from the surface. In contrast, the wet analysis produced slightly larger but more rapidly decaying responses since the analyte was already solvated and thus easier to desorb from the surface. Overall, these results suggest that the identity of the surface substrate may influence the performance of TM-DESI. Therefore, additional studies that more comprehensively evaluate the performance of a larger variety of meshes were performed. These results are discussed in Chapter 4.

3.3.6 Electrospray Solvent

The importance of the electrospray solvent composition on DESI analysis has been reported numerous times.[5,12] These studies have suggested that the optimum solvent is analyte dependent and that the efficacy of a particular solvent is a function of its polarity and the solubility of the target analyte. Various common electrospray solvents including methanol, water, acetonitrile, and mixtures of these solvents have been utilized in DESI analyses. In the present study experiments were undertaken to study the effect of varying the electrospray solvent on the response of nicotine and bradykinin. In each case, 1 μL of solution (1 ng/μL of nicotine in methanol or 50 uM bradykinin in methanol) was deposited onto a nylon mesh and allowed to dry completely before analysis.

Table 3.2 summarizes the results for these experiments and confirms that electrospray solvent effects are also observed in the transmission mode. The largest response for nicotine was observed when methanol was used as the spray solvent while much lower responses were observed using water or acetonitrile. In contrast, the results for bradykinin show that the largest response was observed when water was the spray solvent and much lower responses were observed for either pure methanol or pure acetonitrile. Thus, the optimum spray solvent depended on the identity of the target analyte. These results again illustrate that the mechanism of desorption in the

transmission mode is likely similar to traditional DESI when the deposition solvent is allowed to evaporate completely before analysis.

Table 3.2: Relative Percent Responses of Dried Samples with Spray Solvent

Analyte	Methanol	Methanol/Water	Water	Acetonitrile
Nicotine	100.0	60.0	25.8	21.8
Bradykinin	10.7	82.2	100.0	4.2

3.3.7 Deposition Solvent

The electrospray angle in most DESI experiments is typically much greater than zero (i.e., 40° to 70°) which causes rapid erosion of liquids from uniform sample surfaces such as glass, plastics and metal. Thus, analysis of liquids in traditional DESI is most successful from rough substrates such as paper or TLC plates that absorb the solvent and hold the liquid analytes in place. The zero degree electrospray in TM-DESI lessens this erosion effect as the nebulizing gas, desolvated ions, and un-ionized droplets are directed through the surface at an angle perpendicular to it, thereby reducing the tendency for surface resolvation and spreading of the target analyte on the substrate. Therefore, analysis of liquids from smooth mesh surfaces is possible in TM-DESI and as a consequence, the deposition solvent plays a more prominent role in the surface chemistry of the analysis.

To investigate the impact of the deposition solvent, the experiments conducted to test the impact of the electrospray solvent were repeated using various deposition solvents. However, unlike the previous experiments, the samples were analyzed while they were suspended as liquid droplets in the mesh, not dried to a solid film. Table 3.3 summarizes the results obtained for nicotine using three electrospray solvents (i.e.,

methanol, acetonitrile, water) and four deposition solvents (i.e., methanol, acetonitrile, water, hexane). The most compelling results are the differences observed amongst a set of analyses that utilized the same electrospray solvent, but differing deposition solvents. For example, relative responses varied between 22.8% and 100% when the deposition solvent was varied and methanol was used as the electrospray solvent.

Table 3.3: Relative Percent Responses of Wet Nicotine Samples with Various Deposition and Electrospray Solvents

	Electrospray Solvent		
Deposition Solvent	Methanol	Acetonitrile	Water
Methanol	100.0	37.7	36.6
Acetonitrile	83.9	34.0	22.7
Water	22.8	10.2	11.5
Hexane	59.6	14.6	4.9

Table 3.4 summarizes the results obtained for bradykinin using four electrospray solvents (i.e., methanol, acetonitrile, water, methanol/water) and two deposition solvents (i.e., methanol and water). These results correlate well with those presented in Table 3.2 and also suggest that the efficiency of ionization may be controlled by either the electrospray solvent or the deposition solvent**.** More specifically, from Table 3.2 the largest responses for bradykinin (as a dried film) were observed when either water or a mixture of water and methanol was used as the electrospray solvent. Table 3.4 also shows that the largest responses for solvated bradykinin were observed when water was present, either as the deposition solvent in combination with a methanolic electrospray or as the electrospray solvent in combination with a methanolic deposition. Interestingly, the average responses for either the all-methanol or all-water systems were far lower.

Furthermore, the magnitude of the response observed when a mixture of methanol and water was used as the electrospray solvent was between that observed for the pure solvent systems.

Table 3.4: Relative Percent Responses of Wet Bradykinin Samples with Various Deposition and Electrospray Solvents

Deposition Solvent	Electrospray Solvent			
	Methanol	Methanol/Water	Water	Acetonitrile
Methanol	23.3	80.8	96.9	13.2
Water	100.0	64.5	42.0	44.6

These results clearly illustrate that the identity of the deposition solvent has an impact on the response in TM-DESI and that the mechanism in the solvated transmission mode analysis is dependent not only on the surface, analyte and ionizing solvent, but also on the solvent that suspends the target analyte on the mesh. Elucidation of the ionization mechanism must therefore consider not only the interaction of the electrospray solvent with the analyte, but also the interaction of the deposition solvent with the surface and electrospray solvent, the partitioning of the analyte between the deposition solvent and the surface, and the possible partitioning of the analyte between the two solvents.

One possible mechanism could assume that there is no adsorption of the target analyte to the surface and that the ionization results from a partitioning of the analyte between the two solvents. This mechanism would be similar to a liquid-liquid extraction where the miscibility of the two solvents and the corresponding solubility of the target analyte have a large influence on the eventual efficacy of the ionization. Results presented in Table 3.3 for the analysis of nicotine when hexane was used as the deposition solvent and water was used as the electrospray solvent support this argument.

Since the miscibility of these two solvents is minimal, the analyte would have less opportunity to partition into the electrospray solvent and therefore little tendency to be ionized.

Another possible mechanism could involve a "secondary" electrospray of a completely suspended analyte where a suspended analyte droplet is dislodged from the surface by the electrospray plume and then subsequently ionized by the desolvation of the analyte amidst the other electrospray solvent ions. Finally, like traditional DESI, the mechanism could involve a droplet pickup mechanism in which the analyte is picked up from the surface or from a thin layer of solvent surrounding the surface.[5,21,23] However, in this case the surface activity of the solute in the various deposition solvents would also be a factor as analytes that favored the surface over the solvent would more likely be available for "pickup" by the electrospray solvent. The data presented here are not sufficient to conclusively elucidate the mechanism of the solvated TM-DESI analysis, but they served as a guide for subsequent investigations in Chapter 4.

3.3.8 Figures of Merit

Table 3.5 summarizes the detection limit and precision results for nicotine and bradykinin by TM-DESI using a PEEK mesh and a deposition volume of 1 μL (methanol). For the nicotine analysis, methanol was used as the electrospray solvent, while a solution of water, methanol, and formic acid (50:50:1% by volume) was used for the analysis of bradykinin. Results of 10 replicate measurements at a concentration 10 times the limit of detection (LOD) were used to calculate the precision.

Table 3.5: Figures of Merit

Analyte	LOD (dry) pg	LOD wet pg/μL	%RSD (wet)
Nicotine	1.0	0.5	11.4
Bradykinin	0.3	0.3	9.6

Comparison of the results for wet and dry analysis does not suggest a clear benefit in sensitivity using either method. However, it is worth noting that TM-DESI analysis of wet samples consumes the sample more rapidly than dry analysis, since the release of the suspended solvent droplets is nearly instantaneous when the sample intersects the nebulizing plume. Therefore, samples deposited as 1 μL or less and analyzed wet have a spot size on the same order as the DESI spray. In contrast, TM-DESI of dry samples produces longer-lived signals because the desorption process must be initiated by resolvation of analytes that have dried on the mesh. In this case, the entire spot may not be sampled simultaneously. Therefore, the relative similarity in the sensitivity of the wet and dry analysis may be a balance between these factors. While the reported detection limits cannot necessarily be extended to all analyses, they do suggest that the transmission mode sensitivity is comparable with that of traditional DESI for small molecules like nicotine and peptides such as bradykinin.[5]

The precision results show approximately 10-12% RSD for the analysis of wet samples deposited as 1 μL in methanol. These results are promising for qualitative screening, but quantitative analyses may require even better precision. In addition to the quantitative precision, the qualitative repeatability of TM-DESI was tested by performing 50 replicate analyses of wet and dry samples of both bradykinin and nicotine at sample concentrations twice the limit of detection. For the nicotine samples, nicotine was

detected in all 50 samples, and for the bradykinin samples, 49 of 50 samples yielded positive results.

3.4 CONCLUSIONS

The results reported here demonstrate that TM-DESI is capable of producing high quality mass spectral data for both solid residues and liquid samples in very short periods of time. The zero degree electrospray angle transmits the ionizing plume through the sample surface and effectively reduces the number of geometric experimental variables to two, thus providing a useful simplification to the conventional DESI experiment. The bulk of the variability in the TM-DESI analysis remains defined by the five variables that describe the desorption process: the electrospray solvent, the deposition solvent, the substrate material, the target analyte and the partitioning of that analyte onto the substrate or into the deposition solvent. More extensive research beyond the simple surfaces and solvents discussed here is detailed in Chapter 4 and Chapter 6.

3.5 REFERENCES

(1) Takats, Z.; Wiseman, J.M.; Gologan, B.; Cooks, R.G. *Science.* **2004**, 306, 471-473.

(2) Chen, H.; Talaty, N.N.; Takats, Z.; Cooks, R.G. *Anal. Chem*. **2005**, 77, 6915-6927.

(3) Cotte-Rodriguez, I.; Takats, Z.; Talaty, N.; Chen, H.; Cooks, R.G. *Anal. Chem*. **2005**, 77, 6755-6764.

(4) Takats, Z.; Cotte-Rodriguez, I.; Talaty, N.; Chen, H.; Cooks, R.G.*Chem. Comm.* **2005**, 1950-1952.

(5) Takats, Z.; Wiseman, J.M.; Cooks, R.G. *J. Mass Spectrom*. **2005**, 40, 1261-1275.

(6) Talaty, N.; Takats, Z.; Cooks, R.G. *Analyst* **2005**, 130, 1624-1633.

(7) Van Berkel, G.J.; Ford, M.J.; Deibel, M.A. *Anal. Chem.* **2005**, 77, 1207-1215.

(8) Weston, D.J.; Bateman, R.; Wilson, I.D.; Wood, T.R.; Creaser, C.S. *Anal. Chem.* **2005**, 77, 7752-7580.

(9) Williams, J.P.; Scrivens, J.H. *Rapid Commun. Mass Spectrom*. **2005**, 19, 3643-3650.

(10) Bereman, M.S.; Nyadong, L.; Fernandez, F.M.; Muddiman, D.C. *Rapid Commun. Mass Spectrom.* **2006**, 20, 3409-3411.

(11) Chen, H.; Zhengzheng, P.; Talaty, N.; Raftery, D.; Cooks, R.G. *Rapid Commun. Mass Spectrom.* **2006**, 20, 1577-1584.

(12) Cooks, R.G.; Ouyang, Z.; Takats, Z.; Wiseman, J.M. Science 2006, 311, 1566-1569.

(13) Cotte-Rodriguez, I.; Cooks, R.G.. *Chem. Commun*. **2006,** 2968-2970.

(14) D'Agostino, P.A.; Hancock, J.R.; Chenier, C.L.; Lepage, J. *J. Chrom. A* **2006,**1110, 86-94.

(15) Hu, Q.; Talaty, N.; Noll, R.J.; Cooks, R.G. *Rapid Commun. Mass Spectrom.* **2006**, 20, 3403-3408.

(16) Jackson, A.T.; Williams, J.P.; Scrivens, J.H. *Rapid Commun. Mass Spectrom.* **2006**, 20, 2717-2727.

(17) Kauppila, T.J.; Talaty, N.; Salo, P.K.; Kotiaho, T.; Kostiainen, R.; Cooks, R.G. *Rapid Commun. Mass Spectrom.* **2006**, 20, 2143-2150.

(18) Kauppila, T.J.; Wiseman, J.M.; Ketola, R.A.; Kotiaho, T.; Cooks, R.G.; Kostiainen, R. *Rapid Commun. Mass Spectrom.* **2006**, 20, 387-392.

(19) Mulligan, C.C.; Talaty, N.; Cooks, R.G. *Chem. Commun*. **2006**, 1709-1711.

(20) Nefliu, M.; Venter, A.; Cooks, R.G. *Chem. Commun*. **2006**, 888–890.

(21) Venter, A.; Sojka, P.E.; Cooks, R.G. *Anal. Chem*. **2006**, 78, 8549-8555.

(22) Williams, J.P.; Patel, V.J.; Holland, R.; Scrivens, J.H.. *Rapid Commun. Mass Spectrom.* **2006**, 20, 1447-1456.

(23) Costa, A.B.; Cooks, R.G. *Chem. Commun*. **2007**, 3915-3917.

(24) D'Agostino, P.A.; Chenier, C.L.; Hancock, J.R.; Lepage, J. *Rapid Commun. Mass Spectrom.* **2007**, 21, 543-549.

(25) Ifa, D.R.; Gumaelius, L.M.; Eberlin, L.S.; Manicke, N.E.; Cooks, R.G. *Analyst*. **2007**, 132, 461-467.

(26) Ifa, D.R.; Wiseman, J.M.; Qingyu, S.; Cooks, R.G. *Int. J. Mass Spectrom*. **2007**, 259, 8-15.

(27) Justes, D.R.; Talaty, N.; Cotte-Rodriguez, I.; Cooks, R.G. *Chem. Commun.* **2007**, 2142-2144.

(28) Kauppila, T.J.; Talaty, N.; Kuuranne, T.; Kotiaho, T.; Kostiainen,R.; Cooks, R.G. *Analyst.* **2007**, 132, 868–875.

(29) Nyadong, L.; Green, M.D.; De Jesus, V.R.; Newton, P.N.; Fernandez, F.M. *Anal. Chem*. **2007**, 79, 2150-2157.

(30) Pan, Z.; Gu, H.; Talaty, N.; Chen, H.; Shanaiah, N.; Hainline, B.E.; Cooks, R.G.; Raftery, D. *Anal Bioanal Chem.* **2007,** 387, 539–549.

(31) Ricci, C.; Nyadong, L.; Fernandez, F.M.;Newton, P.N.; Kazarian, S.G. *Anal Bioanal Chem*. **2007**, 387, 551–559.

(32) Shin, Y-S.; Drolet, B.; Mayer, R.; Dolence, K.; Basile, F. *Anal. Chem.* **2007**, 79, 3514-3518.

(33) Song, Y.; Cooks, R.G. *J. Mass Spectrom*. **2007**, 42, 1086-1092.

(34) Venter, A.; Cooks, R.G. *Anal. Chem*. **2007**, 79, 6398-6403.

(35) Williams, J.P.; Hilton, G.R.; Thalassinos, K.; Jackson, A.T.; Scrivens, J.H. *Rapid Commun. Mass Spectrom.* **2007**, 21, 1693-1704.

(36) Jackson, A.U.; Talaty, N.; Cooks, R.G.; Van Berkel, G.J. *J. AM. Soc. Mass Spectrom.* **2007**, 18, 2218-2225.

(37) Nefliu, M.; Smith, J.N.; Venter, A.; Cooks, R.G. *J. AM. Soc. Mass Spectrom.* **2008**, 19, 420-427.

(38) Ifa, D.R.; Manicke, N.E.; Rusine, A.L.; Cooks, R.G. *Rapid Commun. Mass Spectrom*. **2008**, 22, 503–510.

(39) Huang, G.; Chen, H.; Zhang, X.; Cooks, R.G.; Ouyang, Z. *Anal. Chem*. **2007**, 79, 8327-8332.

(40) Bereman, M.S.; Williams, T.I.; Muddiman, D.C. *Anal. Chem*. **2007**, 79, 8812-8815

(41) Cody, R.B.; Laramee, J.A.; Durst, H.D. *Anal. Chem*. **2005**, 77, 2297-2302.

(42) Song, Y.; Cooks, R.G. *Rapid Comm. Mass Spectrom.* **2006**, 20, 3130-3138.

(43) Shiea J, Huang M, HSu H, Lee C, Yuan C, Beech I, Sunner J. *Rapid Commun. Mass Spectrom*. **2005**, 19, 3701-3704.

(44) McEwen, C. N.; McKay, R. G.; Larsen, B. S. *Anal. Chem*. **2005**, 77, 7826-7831.

(45) Andrade, F.J.; Shelley, J.T.; Wetzel, W.C.; Webb, M.R.; Gamez, G.; Ray, S.J.; Hieftje, G.M. *Anal. Chem*. **2008**, 80, 2646-2653.

(46) Andrade, F.J.; Shelley, J.T.; Wetzel, W.C.; Webb, M.R.; Gamez, G.; Ray, S.J.; Hieftje, G.M. *Anal. Chem*. **2008**, 80, 2646-2653.

(47) Page, J.S.; Kelly, R.T.; Tang, K.; Smith, R.D. *J. Am. Soc. Mass Spectrom*. **2007**, 18, 1582-1590.

(48) Wiseman, J. M.; Ifa, D. R.; Venter, A.; Cooks, R. G. *Nat. Protocols* **2008**, 3, 517–524.

Chapter 4: The Influence of Material and Mesh Characteristics on Transmission Mode Desorption Electrospray Ionization

4.0 Chapter Overview

Adaptation of desorption electrospray ionization to a transmission mode (TM-DESI) entails passing an electrospray plume through a sample that has been deposited onto or otherwise collected by a mesh substrate. In this chapter, a combination of mass spectrometry and fluorescence microscopy studies are used to illustrate the critical role material composition, mesh open space, and mesh fiber diameter play on the transmission, desorption, and ionization process. Substrates with open spaces less than 150 μm and accompanying minimal strand diameters produce less scattering of the plume and therefore favor transmission. Larger strand diameters typically encompass larger open spaces, but the increase in the surface area of the strand increases plume scattering as well as solvent and analyte spreading on the mesh. Polypropylene (PP), ethylene tetrafluoroethylene (ETFE), and polyetheretherketone (PEEK) materials afford much better desorption of polar analytes than similarly sized polyethylene terephthalate (PETE) or nylon-6,6 (PA66) substrates. Ultimately, the manner in which the electrospray plume interacts with the mesh as it is transmitted through the substrate is shown to be critical to performing and optimizing TM-DESI analyses. In addition, evidence is presented for analyte dependent variations in the desorption mechanisms of dry and solvated samples.

4.1 Introduction

Desorption electrospray ionization (DESI) is among the growing number of atmospheric pressure ionization techniques that are suitable for coupling to mass spectrometric analysis.[1-40] In DESI, ions are produced by directing charged solvent droplets from an electrospray source toward a sample that is either a bulk material in its native state (e.g., pharmaceutical tablet) or one that has been deposited from solution onto a sampling surface. Analytes present at the surface are desorbed and ionized by the incoming plume and subsequently transferred to the mass spectrometer inlet by the

influence of the applied potential and the pressure differential between atmospheric pressure and the low-pressure region of the mass analyzer.

Adaptations of DESI, including geometry independent DESI in gas tight enclosures[35] and transmission mode desorption electrospray ionization (TM-DESI) have been developed to reduce the geometry dependence of DESI experiments. In the transmission mode the sample is not deposited onto a continuous solid surface but rather onto a sampling mesh. In this adaptation, the incident spray angle and collection angle are fixed at 0° and the spray is transmitted through the sample. (See Figure 3.1) Along with the simplification of the experimental geometry, the transmission mode also allows convenient analysis of both dry (i.e., following evaporation of the deposition solvent) and wet (i.e., solvated) samples with similar performance characteristics to those achieved using traditional DESI.

Surface variables including the chemical composition, porosity, texture, and electrical conductivity of the substrate have been reported to affect DESI analyses.[24, 37–39] Dramatic reductions in response have been noted for high conductivity surfaces due to neutralization of the incoming ion plume at the surface.[2, 38] Variations in response due to the impact of the surface on crystallization of deposited samples have been reported,[2, 37] as well as increases in response for porous or rough surfaces due to a reduction in sample spreading,[2, 37] and increases in response due to chemical inertness and hydrophobicity of materials such as PTFE.[24, 38] DESI analyses have utilized a variety of surface materials, including glass, PMMA, PTFE, TLC plates, UTLC plates, porous silicon, nanoporous aluminum, paper, and stainless steel. However, in general the use of rough, non-conducting materials is now widely preferred.

The utilization of a mesh material as the sample substrate for TM-DESI analysis introduces a new set of experimental variables that have not been investigated by

traditional DESI. In TM-DESI, the mesh substrate is not only composed of a particular material, but also fashioned into a variety of different forms depending on the strand size used for the mesh and the open space between the various strands. Liquid samples spotted onto the sampling mesh fill one or more of the openings and the analyte may either adsorb onto the mesh or remain partitioned in the deposition solvent. Initial studies of rhodamine 6G, bradykinin, and nicotine by TM-DESI using mesh substrates composed of five different materials but with similar mesh characteristics were discussed in Chapter 3. Those results demonstrated tremendous differences in response depending on the mesh material. The present chapter expands on those results by including not only more materials but also substrates with widely varying mesh characteristics. Furthermore, more attention is given to the interaction of the electrospray plume with the mesh substrate, how the mesh characteristics impact the transmission of the electrospray, and how the material composition and mesh characteristics ultimately impact desorption and ionization mechanisms of liquid samples by TM-DESI.

4.2 EXPERIMENTAL

4.2.1 Materials

Rhodamine 6G and bradykinin were purchased from Sigma Aldrich (St. Louis, MO) and used without further purification. High purity methanol, water, and acetone were purchased from Fisher Scientific (Hampton, NH). Working standards of both rhodamine 6G and bradykinin were prepared at concentrations of 60 and 100 pg/μL in methanol. A total of 20 different mesh substrates manufactured from five different polymeric materials; polypropylene (PP), polyetheretherketone (PEEK), ethylene tetrafluoroethylene (ETFE), nylon-6,6 (PA66), and polyethylene terephthalate (PETE)

were purchased from Small Parts, Inc. (Miramar, FL). The monomeric structures for these materials are shown in Figure 4.1.

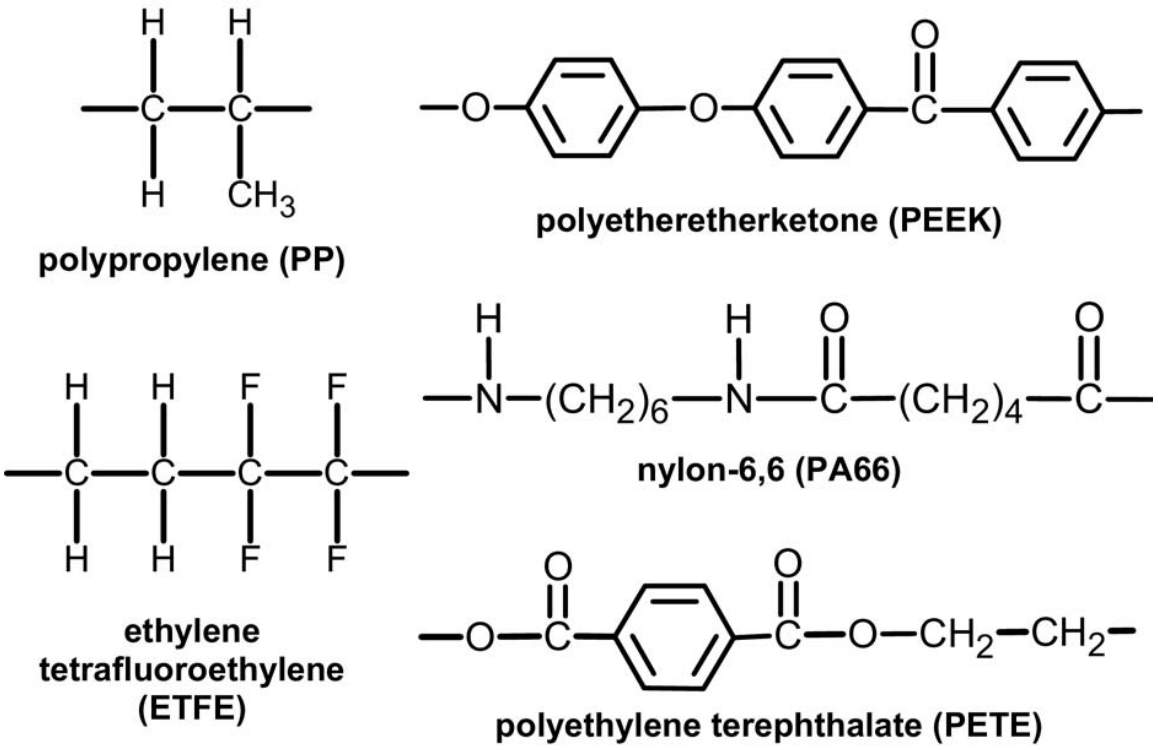

Figure 4.1: Monomers of the polymeric mesh materials used as TM-DESI substrates.

As indicated in Table 4.1, the different materials were fashioned into meshes with differing structural characteristics, namely the open space between the strands of the mesh and the diameter of the strands used to compose the mesh. Ultimately, these two variables were used to compute a theoretical percent transmittance (transmission %) of the mesh. (Figure 4.2)

Table 4.1: Sample Mesh Characteristics

Mesh Material	Open Space (µm)	Strand Diameter (µm)	Transmission (%)
Polypropylene(PP)	105	100	26.2
Polypropylene(PP)	129	100	30.9
Polypropylene(PP)	149	106	34.1
Polypropylene(PP)	250	200	30.9
Polypropylene(PP)	297	215	33.6
Polypropylene(PP)	500	300	39.1
Nylon (PA66)	110	51	46.7
Nylon (PA66)	130	50	52.2
Nylon (PA66)	150	92	38.4
Nylon (PA66)	250	180	33.8
Nylon (PA66)	310	151	45.2
Nylon (PA66)	500	315	37.6
Polyester (PETE)	105	42	51.0
Polyester (PETE)	132	54	50.4
Polyester (PETE)	150	96	37.2
Polyester (PETE)	250	152	38.7
Polyester (PETE)	300	143	45.9
Polyester (PETE)	500	220	48.2
ETFE	150	96	37.2
PEEK	300	200	36.0

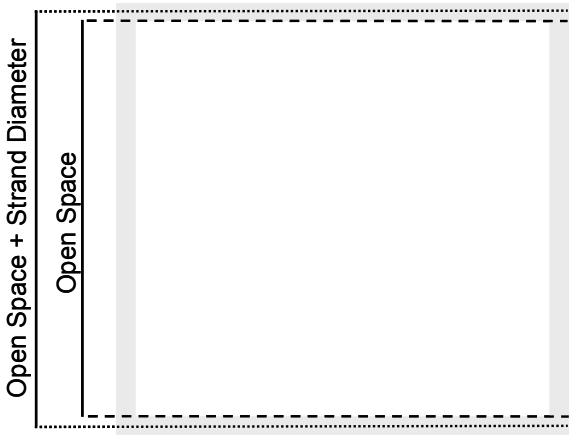

Figure 4.2: The percent transmittance was calculated as the square of the open space divided by the square of the sum of the open space and strand diameter.

Throughout this chapter, mesh materials are given an alphanumeric designation by their material composition and their open space. (e.g., PP 149 was the mesh composed of polypropylene fibers with an open space of 149 μm) Before analysis, each mesh substrate was rinsed with a mixture of high purity water, methanol, and acetone. After drying, the mesh sheets were cut into 5 mm x 10 mm rectangular pieces. Blank measurements were made on representative samples of each substrate to ensure that each was free of analyte or any detectable interference.

4.4.2 Mass Spectrometry

An Omni Spray ion source (Prosolia, Inc., Indianapolis, IN) was mounted to a Thermo Fisher Scientific LTQ XL mass spectrometer (Thermo Fisher Scientific Inc., Waltham, MA) and modified to allow a 0° angle between the electrospray tip and capillary inlet to the mass spectrometer. Samples were affixed to the sample slide arm of the Omni Spray ion source using a sample holder constructed of two rectangular support pieces (1.2 cm x 15 cm): one high density polyethylene (HDPE) 2.3 mm thick and one oriented polyester 0.3 mm thick. A 7 mm diameter hole was drilled through both support

pieces and the sample mesh was held between the two layers. Mass spectra were acquired by scrolling the sample holder perpendicularly into the electrospray plume between the spray tip and the capillary inlet, thereby allowing transmission of the ionizing spray through the mesh. All analyses were carried out with a TM-DESI geometry of D_{TS} equal to 2 mm and D_{TC} equal to 8 mm (see Figure 3.1).

Mass spectra were acquired using the Xcalibur 2.0 software program in the positive ion mode with the electrospray voltage set to 4.0 kV, the ion accumulation time set to 10 ms and signal averaging set for four microscans. Nitrogen at a pressure of 100 psi was used as the nebulizing gas. A syringe pump (Harvard Apparatus, Holliston, MA) was used to deliver either methanolic samples for ESI or methanol electrospray solvent for TM-DESI at a rate of 5 μL/min. Samples were prepared by spotting 1 μL of solution onto a sample mesh using a 5 μL syringe (SGE, Austin, TX) and analyzed wet, before the deposition solvent had evaporated.

The response of rhodamine 6G was monitored using a selected dissociation reaction of the protonated species of m/z 443.3 Da to the dominant fragment of m/z 415.2 Da (i.e., selected reaction monitoring). The response of bradykinin was monitored using a selective ion monitoring of the doubly protonated species $[M + 2H]^{2+}$ of m/z 530.7 Da. The area of the peak chosen by Xcalibur's ICIS peak detection algorithm was used to compare responses and each experiment was repeated a minimum of five times to ensure consistency between mesh samples.

4.2.3 Fluorescence Microscopy

Analysis of residual rhodamine 6G was performed using either the 2.5X or 4X objective of an Olympus BX2 epifluorescent microscope equipped with a 12 bit CCD camera (DVC Co., Austin, TX) and high-pressure mercury bulb excitation source.

Excitation of rhodamine 6G occurred at 480 nm and emission was monitored at 535 nm. Photomicrographs were captured via DVC software with adjustable gain, offset, and exposure time. While various microscopy settings were used for different experiments based on the sensitivity of the instrument and the amount of residual analyte, all microscopy settings were consistent among the samples being compared.

4.3 Results and Discussion

Desorption electrospray ionization involves the interaction of an incoming electrospray plume with analytes adsorbed onto a surface. Desorption and ionization of these analytes is believed to proceed through a multistep droplet pick-up mechanism, where the initial step involves the formation of a thin solvent layer on the surface by the incoming solvent plume.[1,40] Adsorbed molecules eventually dissolve or migrate into the solvent layer and are subsequently desorbed by the momentum of the high velocity electrospray droplets that continue to contact the surface. Once the analytes are sequestered in the charged off-spring droplets, they are ionized by typical ESI mechanisms. Ultimately, the droplet pick-up mechanism depends not only on the characteristics of the electrospray but also on the physical and chemical characteristics of the surface. Specifically, the surface influences the formation of the solvent layer, spreading of the solvent layer, the ease with which off-spring droplets leave the surface and the migration rate of adsorbed molecules into the solvent layer. Therefore, experiments were designed to assess the impact of the mesh characteristics on electrospray transmission and desorption of solvated analytes.

4.3.1 Electrospray Transmission through Mesh Substrates

Numerous studies have investigated fundamental electrospray characteristics at various geometries, flow rates, gas pressures and applied voltages.[41-43] However, the

transmission of an electrospray through a material is not typically addressed. One way to probe the interaction is to compare the mass spectral response when an analyte is electrosprayed through the mesh with that when no mesh is present. Accordingly, a solution of rhodamine 6G (60 pg/μL in MeOH) was electrosprayed at a flow of 5 μL/min though each mesh material in Table 4.1 for 20 s, resulting in the analysis of a total of 100 pg of rhodamine 6G. Ten replicate experiments were conducted for each mesh material, each utilizing a new mesh for the analysis. The average response when the mesh was present was divided by the average response obtained in control experiments (i.e., no mesh present) performed immediately before and after each set of replicates, thereby resulting in an average percent recovery for rhodamine 6G. These results, along with the normalized percent recovery among the twenty different mesh substrates, are presented in Table 4.2.

The average recovery of rhodamine 6G varied from 2.0% to 48.8%, clearly indicating that the physical parameters of the mesh substrate had a dramatic impact on the transmission of the analyte. Examination of the entire dataset illustrates that the transmission of rhodamine 6G is not strictly favored for mesh materials with large open spaces, as materials such as PP 149 and ETFE 150 yield higher recoveries than PA66 500 or PETE 300, even though the open space is one-half to one-third as large. Furthermore, high recoveries were not strictly attributed to small strand diameters, as recoveries for PP 297 and PA66 500 are much larger than ETFE 105 and PA66 150, although the latter have much smaller strand diameters.

Table 4.2: Transmission through Mesh Materials

Mesh Material	Average Recovery (%)	Normalized Recovery (%)
PP 105	33.5	68.6
PP 129	40.3	82.6
PP 149	48.8	100.0
PP 250	27.9	57.2
PP 297	37.7	77.2
PP 500	23.0	47.2
PA66 110	15.6	31.9
PA66 130	22.5	46.1
PA66 150	7.1	14.5
PA66 250	3.7	7.6
PA66 310	8.0	16.3
PA66 500	2.0	4.1
PETE 105	10.8	22.2
PETE 132	5.1	10.5
PETE 150	4.5	9.2
PETE 250	12.0	24.6
PETE 300	10.0	20.5
PETE 500	13.6	27.9
ETFE 150	40.6	83.2
PEEK 300	24.5	50.3

When substrates are grouped based on their open space (e.g., PP 149, ETFE 150, PA66 150, PETE 150), it is apparent that PP, ETFE, and PEEK materials afford much

higher transmission than similarly sized PETE or PA66 substrates, especially for those with open spaces less than 300 μm. (Figure 4.3). These results are consistent throughout each size grouping and for both analytes, emphasizing the influence of the mesh material relative to the size characteristics of the mesh. However, the size characteristics are also an influential factor since the average recoveries for each mesh of a particular material were not equal.

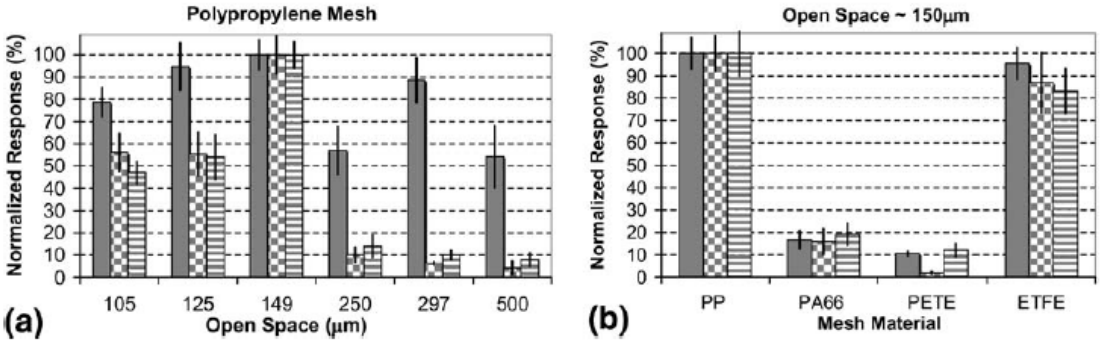

Figure 4.3: Normalized responses of rhodamine 6G and bradykinin using (a) polypropylene mesh materials with open spaces ranging from 105 to 500 μm and (b) meshes of different materials with open spaces of ~150 μm. Solid bars indicate transmission of rhodamine 6G electrosprayed through the mesh. Square patterned bars correspond to desorption of rhodamine 6G while horizontal striped bars correspond to desorption of bradykinin using TM-DESI analysis.

Rhodamine 6G that was not transmitted through the mesh to the mass spectrometer must have either adsorbed to the mesh or been scattered by the mesh away from the capillary inlet. Therefore, the mesh samples used for the transmission experiments were analyzed by fluorescence microscopy to determine the extent of analyte adsorption that occurred during the analysis. Furthermore, the transmission experiments were also repeated with a second sample holder containing a 5 mm x 10 mm

piece of paper placed ~6 mm behind the sample holder containing the mesh material but directly in front of the capillary inlet. In this case, the paper was used to collect rhodamine 6G analyte (i.e., ions and solvated neutrals) that was scattered by the various mesh substrates.

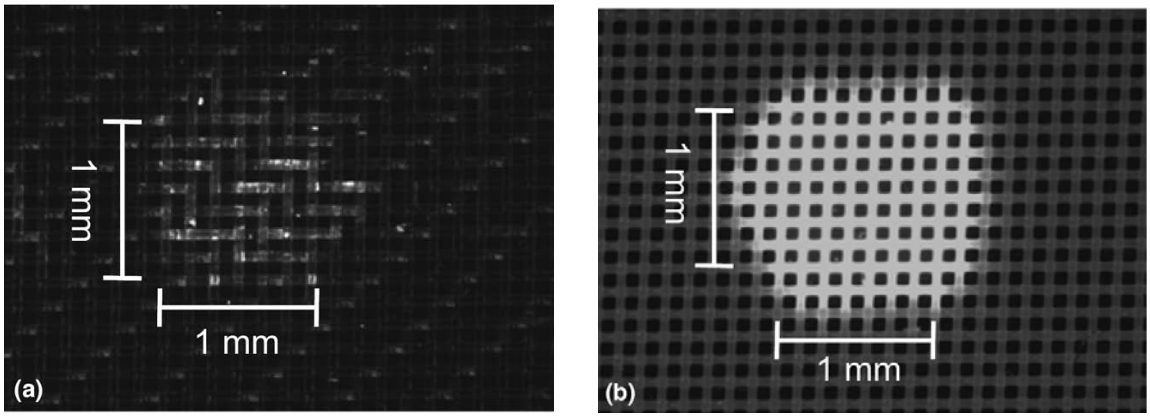

Figure 4.4: Fluorescence micrographs of mesh materials (a) PP 149(149 μm open space) and (b) PETE 150 (150 μm open space) following electrospray of rhodamine 6G (60 pg/μL) through the mesh for 20 s. Both micrographs were acquired using identical microscope gain and exposure settings.

As shown in Figure 4.4, there was a remarkable difference in the photomicrographs of the mesh materials. Materials such as PETE and PA66 tended to adsorb the rhodamine 6G while those composed of PP or ETFE did not. These results correlate directly with the recovery data and may be explained by either the porosity of the strands or the polarity and charging characteristics of the oligomeric materials since hydrophobic materials such as PP did not adsorb the dye nearly as much as the PA66 or PETE. Furthermore, the variation among the series of substrates of a particular material was at least partially explained by the amount of visible spreading of the adsorbed analyte. While the mesh materials with small open spaces and small strand diameters

showed little or no adsorption of analyte outside of the ~1 mm spot size, the meshes with large open spaces and correspondingly larger strand sizes were typically observed to have rhodamine 6G spread several mm across the mesh. These results suggest that the erosion effects typical in DESI[44] may also be present in TM-DESI, but only when the surface area of the mesh strands becomes too large for effective transmission.

The results of the scattering experiments (Figure 4.5) also demonstrated that mesh materials with larger strand sizes (i.e., those with open spaces ~150 to 315 μm) tended to facilitate scattering of the analytes as they passed through the mesh. For example; PP 250, PP 297, PETE 300, and PA66 310 all showed the distinct deposition of rhodamine 6G in multiple locations on the paper surrounding the capillary inlet. In contrast, transmission of the electrospray through mesh materials with smaller stand diameters (i.e., ~100 μm), such as PETE 105, PETE 50, ETFE 150, and PP 105, did not appear to produce any significant scattering.

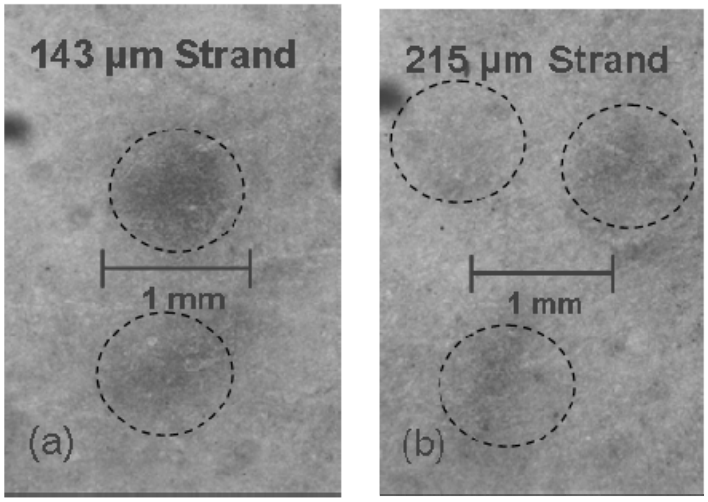

Figure 4.5: Images taken following electrospray of rhodamine 6G through mesh materials composed of (a) 143 μm strands and (b) 215 μm strands. Scattering of dye is visible in both samples. Similar images taken following experiments using strand sizes less than 100 μm produced no scattering.

4.3.2 Desorption of Liquid Samples from Mesh Substrates

Experiments were also performed to investigate the potential differences between desorption and transmission and their relationships to TM-DESI analysis of wet samples. Successful sample deposition for conventional DESI analyses involves balancing drying time and sample spreading. If low volatility solvents (e.g., water) are used, the drying time often becomes the rate limiting step of the analyses.[2, 15] If a more volatile solvent is used (e.g., methanol), the evaporation time may be reduced; however the low surface tension of the solvent makes uniform sample deposition more challenging.[2] Furthermore, sample analyses that utilize smooth surfaces are typically prone to erosion effects, thereby requiring alternative deposition onto porous or rough surfaces that retain the adsorbed analyte during the formation of the initial solvation layer.[2,37,39] The mesh materials used for TM-DESI overcome these difficulties by suspending both high and low volatility deposition solvents of varying surface tensions in the open space of a mesh. Like DESI, TM-DESI is also expected to proceed through a droplet pickup mechanism. However, a distinction can be drawn between TM-DESI analyses of dry samples versus wet samples. Analysis of dry samples should be completely analogous to traditional DESI as analytes are merely adsorbed onto a mesh strand instead of a hydrophobic spot or other surface. However, wet analyses present a different situation since the deposition solvent remains a component of the system and effectively acts as an abundant initial solvent layer.

Analyte molecules that remain suspended in the droplets are efficiently and rapidly desorbed into the electrospray, where surface active analytes may be ionized by heterogeneous charge-transfer between the electrospray droplets and the analyte or by typical ESI mechanisms following droplet fusion. Both of these mechanisms have been proposed previously for electrospray assisted desorption techniques such as ELDI and

MALDESI.[45-50] In contrast, analyte molecules that preferentially adsorb to the mesh substrate withstand the release of the deposition solvent droplets and instead are both desorbed and ionized by the spray solvent. The intricacies of the three component system (i.e., substrate, deposition solvent, electrospray solvent) are not entirely inconsequential as analyte response has been observed to depend on the identity of both the deposition and electrospray solvent. (See Chapter 3)

Experiments analogous to the transmission studies were performed to assess the influence of various mesh materials and mesh characteristics on the desorption and ionization process. In this case, methanol was used as both the deposition and electrospray solvents, thereby isolating the experiment from any solvent dependent mechanistic variations. Samples were prepared by depositing 1 μL of a solution of rhodamine 6G (100 pg/μL) or bradykinin (100 pg/μL) on the surface of a mesh substrate and analyzed before solvent evaporation by scanning a single pass across the visibly wet surface at a rate of 300 μm/s. Ten replicate experiments were conducted for each mesh material, each utilizing a new 5 mm x 10 mm mesh. The response of the 10 measurements was averaged and normalized to the maximum average response for the 20 mesh substrates. The normalized results for rhodamine 6G desorption are presented alongside the normalized transmission results in Table 4.3.

In general, the desorption of rhodamine 6G and bradykinin followed the trends established by the transmission experiments as the largest responses were observed for nonpolar mesh materials with moderate open space and small strand diameters. For both analytes, desorption from PP 149 and ETFE 150 resulted in the largest responses while much smaller signals were observed for substrates of different materials with similar mesh characteristics (e.g., PA66 150, PETE 150). Interestingly, results for other

relatively transmissive substrates such as PP 250, PP 297, PP 500, and PK 300 showed dramatic decreases in the relative efficiencies of desorption compared with transmission.

Table 4.3: Normalized Transmission and Desorption Results

Mesh Material	Transmission Recovery (%)	Desorption Recovery (%)
PP 105	68.6	56.1
PP 129	82.6	55.4
PP 149	100.0	100.0
PP 250	57.2	10.1
PP 297	77.2	6.3
PP 500	47.2	4.3
PA66 110	31.9	27.6
PA66 130	46.1	19.7
PA66 150	14.5	15.9
PA66 250	7.6	3.7
PA66 310	16.3	7.6
PA66 500	4.1	14.2
PETE 105	22.2	5.8
PETE 132	10.5	6.8
PETE 150	9.2	2.0
PETE 250	24.6	18.8
PETE 300	20.5	19.9
PETE 500	27.9	10.2
ETFE 150	83.2	86.9
PEEK 300	50.3	21.5

Figure 4.3a highlights the differences between the various polypropylene substrates and Figure 4.3b compares the responses for substrates with ~150 μm of open space. While the differences among the various mesh materials are of specific interest to this Chapter, the relative similarity of the normalized responses for rhodamine 6G and bradykinin desorption by TM-DESI are particularly significant because they indicate the potential transference between a model compound such as rhodamine 6G and broader molecular classes such as peptides. (see Chapter 5)

Fluorescence microscopy was again used to assess the impact of the mesh material by examining the extent of residual rhodamine 6G on the mesh after TM-DESI analysis. For example, Table 4.3 and Figure 4.3a indicate that the response of rhodamine 6G from PA66 via desorption was only 16% of the response from PP 149. Figure 4.6 depicts example micrographs taken on PP 149 and PA66 150 following these analyses. The differences clearly illustrate that the lower recovery is due to the preferential partitioning of the analyte between the substrate and the deposition solvent. In the case of PP 149, the rhodamine 6G remained dissolved in the methanol and was thus rapidly desorbed and ionized by the electrospray plume as it was scanned across the mesh. In contrast, the PA66 mesh material more strongly bound the analyte and less of the dye remained in the deposition solvent. In this instance, scanning across the mesh removed the deposition solvent but left a significant amount of the analyte behind.

Additional experiments to assess the decay rate of rhodamine 6G spotted onto PP 149 and PA66 150 were performed to expand on these observations. In this case the electrospray was not scanned across the 1 μL spot but instead moved rapidly to the position of the liquid droplet and held in place. The results for PP 149 echoed those previously reported for meshes of this material but of different size characteristics (Chapter 3) and showed a sharp initial response for PP 149 followed by rapid signal

decay. In contrast, the initial response from PA66 150 was much smaller and decayed more slowly, thereby indicating that the rhodamine 6G was gradually being desorbed from the mesh long after the initial deposition solvent had been incorporated into the electrospray plume.

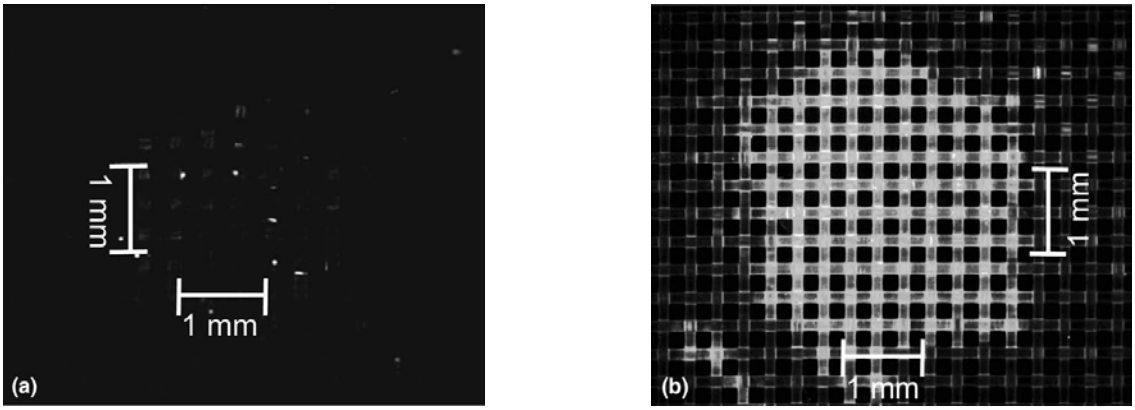

Figure 4.6: Fluorescence micrographs of mesh materials (a) PP 149 (149 μm open space) and (b) PA66 150 (150 μm open space) following TM-DESI analysis of a 1 μL sample of rhodamine 6G (100 pg/μL). Both samples were analyzed wet and micrographs were taken using identical gain and exposure settings.

4.4 CONCLUSIONS

The mass spectrometry and fluorescence microscopy results in this chapter illustrate the significance of the material of composition and the mesh characteristics on TM-DESI analyses. The transmission of the electrospray plume through the mesh depends highly on mesh characteristics such as open space and strand diameter. Substrates with open spaces less than 150 μm and accompanying minimal strand diameters produce less scattering of the plume and therefore favor transmission. Larger strand diameters typically encompass larger open spaces, but the increase in the surface

area of the strand increases both plume scattering and solvent and analyte spreading on the mesh.

Desorption of liquid samples from various mesh substrates is highly dependent on the material composition of the mesh and the relative affinity of the target analytes for the deposition solvent relative to the substrate material. Analytes that remain partitioned into the deposition solvent are rapidly desorbed into the electrospray plume where they undergo ionization via heterogeneous charge-transfer with other electrospray solvent droplets or by droplet fusion, charge redistribution and subsequent fission of the new progeny droplets. In contrast, analytes that have a higher affinity for the mesh substrate are desorbed more gradually from the surface following resolvation by the electrospray solvent in a typical droplet pickup mechanism. Experiments utilizing rhodamine 6G and bradykinin, typical model compounds for DESI analyses, clearly illustrate these effects as mesh materials composed of polypropylene and ethylene tetrafluoroethylene with open spaces of ~150 μm and strand diameters of ~100 μm afforded the most efficient desorption, and ultimately the greatest response for both analytes. The compilation of these results highlights the intricate chemistry that exists as the electrospray plume is transmitted through a mesh material, especially one containing a solvated sample.

4.5 REFERENCES

(1) Venter, A.; Nefliu, M.; Cooks, R. G. *Trends Anal. Chem.* **2008,** *27,* 284–290.

(2) Takats, Z.; Wiseman, J. M.; Cooks, R. G. *J. Mass Spectrom.* **2005,** *40,* 1261–1275.

(3) D'Agostino, P. A.; Hancock, J. R.; Chenier, C. L.; Lepage, J. *J. Chromatogr. A* **2006,** *1110,* 86–94.

(4) Ifa, D. R.; Gumaelius, L. M.; Eberlin, L. S.; Manicke, N. E.; Cooks, R. G.. *Analyst* **2007,** *132,* 461–467.

(5) Nyadong, L.; Green, M.D.; De Jesus, V. R.; Newton, P. N.; Fernandez, F. M. *Anal. Chem.* **2007,** *79,* 2150–2157.

(6) Cotte-Rodriguez, I.; Takats, Z.; Talaty, N.; Chen, H.; Cooks, R. G. *Anal. Chem.* **2005,** *77,* 6755–6764.

(7) Takats, Z.; Cotte-Rodriguez, I.; Talaty, N.; Chen, H.; Cooks, R. G. *Chem. Commun.* **2005,** 1950–1952.

(8) Justes, D. R.; Talaty, N.; Cotte-Rodriguez, I.; Cooks, R. G. *Chem. Commun.* **2007,** *21,* 2142–2144.

(9) Cotte-Rodriguez, I.; Hernandez-Soto, H.; Chen, H.; Cooks, R. G. *Anal. Chem.* **2008,** *80,* 1512–1519.

(10) Cotte-Rodriguez, I.; Cooks, R. G. *Chem. Commun*. **2006,** *28,* 2968–2970.

(11) D'Agostino, P. A.; Chenier, C. L.; Hancock, J. R.; Lepage, J. *Rapid Commun. Mass Spectrom.* **2007,** *21,* 543–549.

(12) Song, Y.; Cooks, R. G. *J. Mass Spectrom.* **2007,** *42,* 1086–1092.

(13) Cooks, R. G.; Ouyang, Z.; Takats, Z.; Wiseman, J. M. *Science* **2006,** *311,* 1566–1569.

(14) Ifa, D. R.; Wiseman, J. M.; Qingyu, S.; Cooks, R. G. *Int. J. Mass Spectrom.* **2007,** *259,* 8–15.

(15) Wiseman, J. M.; Ifa, D. R.; Venter, A.; Cooks, R. G. *Nat. Protocols* **2008,** *3,* 517–524.

(16) Chen, H; Talaty, N. N.; Takats, Z.; Cooks, R. G. *Anal. Chem.* **2005,** *77,* 6915–6927.

(17) Van Berkel, G. J.; Ford, M. J.; Deibel, M. A. *Anal. Chem.* **2005,** *77,* 1207–1215.

(18) Weston, D. J.; Bateman, R.; Wilson, I. D.; Wood, T. R.; Creaser, C. S. *Anal. Chem.* **2005,** *77,* 7752–7580.

(19) Williams, J. P.; Scrivens, J. H. *Rapid Commun. Mass Spectrom.* **2005,** *19,* 3643–3650.

(20) Hu, Q.; Talaty, N.; Noll, R. J.; Cooks, R. G. *Rapid Commun. Mass Spectrom.* **2006,** *20,* 3403–3408.

(21) Williams, J. P.; Patel, V. J.; Holland, R.; Scrivens, J. H. *Rapid Commun. Mass Spectrom.* **2006,** *20,* 1447–1456.

(22) Nyadong, L.; Green, M. D.; De Jesus, V. R.; Newton, P. N.; Fernandez, F. M. *Anal. Chem.* **2007,** *79,* 2150–2157.

(23) Ricci, C.; Nyadong, L.; Fernandez, F. M.; Newton, P. N.; Kazarian, S. G. *Anal. Bioanal. Chem.* **2007,** *387,* 551–559.

(24) Ifa, D. R.; Manicke, N. E.; Rusine, A. L.; Cooks, R. G. *Rapid Commun. Mass Spectrom.* **2008,** *22,* 503–510.

(25) Talaty, N.; Takats, Z.; Cooks, R. G. *Analyst* **2005,** *130,* 1624–1633.

(26) Jackson, A. T.; Williams, J. P.; Scrivens, J. H. *Rapid Commun. Mass Spectrom.* **2006,** *20,* 2717–2727.

(27) Williams, J. P.; Hilton, G. R.; Thalassinos, K.; Jackson, A. T.; Scrivens, J. H. *Rapid Commun. Mass Spectrom.* **2007,** *21,* 1693–1704.

(28) Chen, H.; Zhengzheng, P.; Talaty, N.; Raftery, D.; Cooks, R. G. *Rapid Commun. Mass Spectrom.* **2006,** *20,* 1577–1584.

(29) Kauppila, T. J.; Wiseman, J. M.; Ketola, R. A.; Kotiaho, T.; Cooks, R. G.; Kostiainen, R. *Rapid Commun. Mass Spectrom.* **2006,** *20,* 387–392.

(30) Pan, Z.; Gu, H.; Talaty, N.; Chen, H.; Shanaiah, N.; Hainline, B. E.; Cooks, R. G.; Raftery, D. *Anal. Bioanal. Chem.* **2007,** *387,* 539–549.

(31) Jackson, A. U.; Werner, S. R.; Talaty, N.; Song, Y.; Campbell, K.; Cooks, R. G.; Morgan, J. A. *Anal. Biochem.* **2008,** *375,* 272–281.

(32) Bereman, M. S.; Nyadong, L.; Fernandez, F. M.; Muddiman, D. C. *Rapid Commun. Mass Spectrom.* **2006,** *20,* 3409–3411.

(33) Shin, Y-S.; Drolet, B.; Mayer, R.; Dolence, K.; Basile, F. *Anal. Chem.* **2007,** *79,* 3514–3518.

(34) Bereman, M. S.; Williams, T. I.; Muddiman, D. C. *Anal. Chem.* **2007,** *79,* 8812–8815.

(35) Venter, A.; Cooks, R. G. *Anal. Chem.* **2007,** *79,* 6398–6403.

(36) Chipuk, J. E.; Brodbelt, J. S. *J. Am. Soc. Mass Spectrom.* **2008,** *19,* 1612.

(37) Kauppila, T. J.; Talaty, N.; Salo, P. K.; Kotiaho, T.; Kostiainen, R.; Cooks, R. G. *Rapid Commun. Mass Spectrom.* **2006,** *20,* 2143–2150.

(38) Volný, M.; Venter, A.; Smith, S. A.; Pazzi, M.; Cooks, R. G. *Analyst* **2008,** *133,* 525–531.

(39) Sen, A. K.; Nayak, R.; Darabi, J.; Knapp, D. R. *Biomed. Microdevices* **2008,** *10,* 531–538.

(40) Costa, A. B.; Cooks, R. G. *Chem. Commun.* **2007,** *38,* 3915–3917.

(41) Electrospray Ionization Mass Spectrometry: Fundamentals, Instrumentation, and Applications, Cole, R. B., Ed.; Wiley: New York, 1997.

(42) Cech, N. B.; Enke, C. G. *Mass Spectrom. Rev.* **2001,** *20,* 362–387.

(43) Page, J. S.; Kelly, R. T.; Tang, K.; Smith, R. D. *J. Am. Soc. Mass Spectrom.* **2007,** *18,* 1582–1590.

(44) Pasilis, S. P.; Kertesz, V.; Van Berkel, G. J. *Anal. Chem.* **2007,** *79,* 5956–5962.

(45) Shiea, J.; Huang, M.; Hsu, H.; Lee, C.; Yuan, C.; Beech, I.; Sunner, J. *Rapid Commun. Mass Spectrom.* **2005,** *19,* 3701–3704.

(46) Peng, I. X.; Shiea, J.; Loo, R. R. O.; Loo, J. A. *Rapid Commun. Mass Spectrom.* **2007,** *21,* 2541–2546.

(47) Shiea, J.; Yuan, C.-H.; Huang, M.-Z.; Cheng, S.-C.; Ma, Y.-L.; Tseng, W.-L.; Chang, H.-C.; Hung, W.-C. *Anal. Chem.* **2008,** *80,* 4845–4852.

(48) Sampson, J. S.; Hawkridge, A. M.; Muddiman, D. C. *J. Am. Soc.Mass Spectrom.* **2006,** *17,* 1712–1716.

(49) Sampson, J. S.; Hawkridge, A. M.; Muddiman, D. C. *Rapid Commun. Mass Spectrom.* **2007,** *21,* 1150–1154.

(50) Sampson, J. S.; Hawkridge, A. M.; Muddiman, D. C. *Anal. Chem.* **2008,** *80,* 6773–6778.

Chapter 5: Pairing Sample Preparation Methods and Applications in Transmission Mode Desorption Electrospray Ionization

5.0 Chapter Overview

Implementation of a transmission mode for desorption electrospray ionization mass spectrometry facilitates many potential applications. As illustrated in this chapter, sample preparation is also an important part of TM-DESI analysis. Examples of five different sample preparation methods; bulk material analysis; mesh immersion; sample deposition, substrate masking, and direct sample collection are paired with example applications to illustrate the flexibility of TM-DESI. While TM-DESI may be best suited to high speed screening applications, results presented for high throughput calibration; internal standardization and, improved precision may help elevate the analytical performance of the technique to a semi-quantitative status.

5.1 Introduction

Desorption electrospray ionization mass spectrometry (DESI-MS) has been employed in forensic analysis,[1-4] explosives detection,[5-7] chemical warfare agent detection,[2,8-10] pharmaceutical analysis,[11-19] natural product characterization,[1,20] polymer analysis,[21,22] metabolomics,[1,23,24,25] proteomics,[1,26,27] and glycomics.[28] In some of these applications, samples are ionized directly in their native environment without any pre-treatment (e.g., analysis of plant leaves)[20]. However, in many others the sample is extracted or otherwise prepared in a suitable solvent and ultimately transferred to a sample substrate, such as a glass slide, paper, metal, plastic, or TLC plate. Therefore, straightforward and reproducible sample preparation is essential to many DESI-MS applications.

Transmission mode desorption electrospray ionization (TM-DESI) is not typically used to analyze bulk materials (except in the case where the material happens to be mesh or grid-like), but rather in the analysis of samples deposited on or collected by a mesh

substrate. Since the transmission mode is first and foremost an alternate means of sample introduction for DESI-MS analysis, it is reasonable to expect the method to have a similar range of applications. Experiments discussed in this chapter were performed to investigate this hypothesis.

Clearly the distinguishing feature of TM-DESI is the sample mesh and the influence it has on the experimental arrangement and sample introduction. Aside from simplifying the geometry within the ionization region, the capability to desorb analytes from the surface of the mesh strands as well as from macro scale droplets held within their confines, facilitates analysis of both dried residues and liquid samples. In addition to improving the interface between the ionization source and the mass spectrometer, utilization of a mesh substrate results in a variety of sample preparation options. The examples discussed within the text showcase five alternate means of sample preparation: 1) direct analysis of bulk mesh-like materials; 2) mesh immersion for rapid sampling of bulk solutions; 3) deposition of individual sample spots; 4) sample deposition followed by substrate masking to create replicate subsamples, and 5) direct sample collection from surfaces using adhesive coated or solvated mesh materials. Although multiple techniques may be suitable for a particular class of analytes, the most appropriate preparation method for any particular analysis will be governed by the sample matrix and the desired analytical information. (i.e., qualitative vs. quantitative results)

5.2 EXPERIMENTAL

5.2.1 Materials

Bradykinin, nicotine, cotinine, gamma-amino butyric acid (GABA), creatine, deltamethrin, verapamil, quercetin, apigenin, and myricetin, were purchased from Sigma Aldrich. (St. Louis, MO). Neurotensin and Substance P were purchased from Bachem

(Torrence, CA). Pentaerithyritoltetranitrate (PETN) was purchased from Cerillient (Austin, TX) as a stock standard diluted in acetonitrile. High purity water, methanol, ethanol, acetonitrile and chloroform were purchased from Fisher Scientific (Hampton, NH). All materials were used without further purification.

5.2.2 Sample Preparation Methods

Five different methods were used for sample preparation. For analyses of bulk mosquito nets, the sample was held in place by affixing it to a 26 mm by 76 mm x 3 mm PEEK backing plate with an 8 mm by 38 mm slot cut into it to facilitate transmission of the electrospray through both the sample and the backing plate. For analyses requiring mesh immersion, materials were cut into 5 mm by 10 mm strips and immersed directly in the sample for several seconds before being affixed to a sample holder. For analyses requiring direct deposition of individual sample spots, a 5 μL syringe (SGE, Austin, TX) was used to deposit between 1μL and 3μL of solution directly onto a sample mesh. For analyses requiring sample deposition and subsequent sample masking, an Eppendorf pipetter (Hamburg, Germany) was used to deliver 25 μL of sample solution in a band several mesh cells wide across the length of the surface. The sample was allowed to dry and a sample mask was then placed over the mesh to create a series of subsamples. (Figure 5.1) A similar technique was used for preparation of the multi-layer bulk material samples. Finally, for analyses requiring direct sampling of surfaces, mesh materials were either pressed against an adhesive film (Tritech, Southport, NC) to transfer a portion of the adhesive to the mesh and then pressed against the desired surface (e.g., a laboratory bench top) to collect the sample, or saturated with ethanol and placed on the surface to facilitate analyte migration from the surface to the mesh as the solvent

evaporated. In this case the mesh is used as both a sampling device and a means of sample introduction.

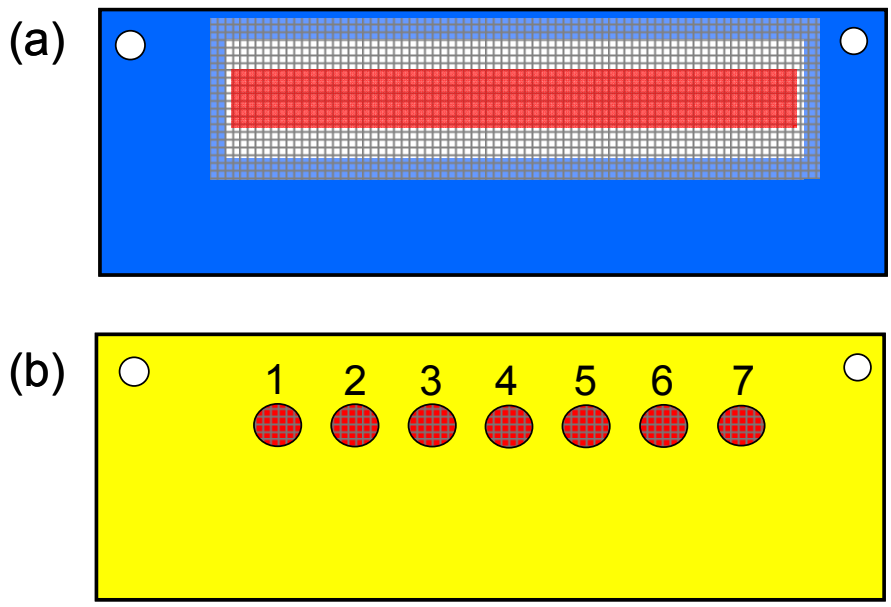

Figure 5.1: Sample preparation using sample deposition and sample masking. (a) A mesh substrate is affixed to a sample backing plate and 25 µL of sample solution is deposited in a band across the mesh. (b) After drying, a sample mask is overlaid on the backing plate to create replicate subsamples.

5.2.3 Mass Spectrometry

Either a manual scroll or one-dimensional automated scanning Omni Spray ion source (Prosolia, Inc., Indianapolis, IN) was mounted to a Thermo Fisher Scientific LTQ XL (Thermo Fisher Scientific Inc., Waltham, MA) and modified to allow a 0° angle between the electrospray tip and capillary inlet to the mass spectrometer. Various sample holders discussed in detail in Chapter 2 were used to introduce the sample. In all cases the distance between the electrospray tip and the mesh surface was 2 mm and the distance between the mesh sample and the capillary inlet of the mass spectrometer was 6 mm. A syringe pump (Harvard Apparatus, Holliston, MA) was used to deliver pure methanol; a 50:50 (v:v) mixture of water and methanol; a 50:50:1 (v:v:v) mixture of water, methanol, and formic acid; a 90:10:1 (v:v:v) mixture of acetonitrile, water, and ammonium acetate;

or a 5:1 mixture of acetonitrile and chloroform (v:v) as the electrospray solvent. The flow rate of the electrospray solvent and the nitrogen pressure varied based on the solvent identity. Typically, the solvent flow varied between 5 μL/min and 10 μL/min while the accompanying gas pressure varied between 100 psi and 120 psi. In all cases, the electrospray voltage was set to 4.0 kV, the ion accumulation time set to 10 ms and signal averaging set for three microscans. Mass spectra were acquired in either positive or negative mode, depending on the ionization affinity of the sample and acquired by scrolling the sample mesh perpendicularly into the electrospray plume between the spray tip and the capillary inlet. When the automated sampling stage was used, the scan rate was set to 500 μm/sec, except for the analysis of the bulk net materials, where the scan rate was 250 μm/sec.

5.3 Results and Discussion

The experimental results presented in the following sections illustrate both the potential applications of TM-DESI and the various means used to prepare TM-DESI samples. Furthermore, specific experiments were conducted to highlight the benefits of co-deposited internal standards; the capability to conduct high throughput calibration and sample screening; the potential for utilizing multi-layered sampling; and the ability to perform reactive TM-DESI experiments to increase selectivity and sensitivity

5.3.1 Pyrethroid Pesticides on Mosquito Nets (Bulk Sample)

Previous studies of pyrethroids, including deltamethrin and permethrin, using LC-ESI-MS demonstrated that the primary electrospray ionization pathway was cation adduction.[29-31] In particular, ammonium adducts were reported to dominate the LC-MS spectra and only a minimal amount of protonated species was observed.[29-31] A number of electrospray solvents (e.g., methanol, acetonitrile, water and methanol solutions) were

tested in the present study. Not surprisingly, the largest and most reproducible responses were observed when the electrospray solvent was doped with ammonium acetate to facilitate cation adduction and ultimately gas-phase ionization. This method of solvent doping is common in DESI and reactive DESI applications and takes advantage of the unique chemistry that exists when a desorbed neutral analyte is sequestered within a charged electrospray droplet containing other reactive species.[17,32]

The TM-DESI analyses were conducted on a linear ion trap (LIT) capable of performing multiple stages of tandem mass spectrometry. Thus, a consecutive reaction monitoring (CRM) strategy was developed to increase the reliability of deltamethrin identification. Figure 5.2 depicts an extracted ion chronogram for the TM-DESI analysis of a polyester bednet coated with 16 mg/m^2 of deltamethrin. The CRM method entailed collisionally induced dissociation (CID) of the most abundant isotope of the ammonium adduct (m/z 523) to generate protonated deltamethrin of *m/z* 506. Isolation and a second stage of CID generated the MS^3 product ion of *m/z* 281, whose proposed structure is shown in the inset. Analysis of both coated and impregnated nets produced reliable detections for deltamethrin at concentrations greater than or equal to 8 mg/ m^2. Deltamethrin was not detected on polyester nets with lower concentrations in these initial experiments.

The scanning capabilities of the ionization source made the TM-DESI analyses a useful tool for analyzing the distribution of the pesticide on the net material. As with all TM-DESI experiments, the characteristics of the mesh have an important influence on the transmission of the electrospray and ultimately on the observed mass spectrum. (See Chapter 4) In this case, the open space of the coated polyester bednet was on the order of 2 mm and the strand diameter was approximately 250 μm, resulting in a unit cell dimension of approximately 2500 μm x 2500 μm (calculated from the mesh open space

plus twice the strand radius). Moreover, the conditions used for the electrospray flow rate, nebulizing gas pressure, and distance from the electrospray tip to the sample resulted in an effective sampling diameter of approximately 1 mm. Since the unit cell dimension was greater than the sampling diameter, it was possible for the sampling area to exist entirely within the unit cell. Consequently, each strand of the polyester bednet could be interrogated independently if the scan rate was sufficiently slow (e.g., 250 μm/s).

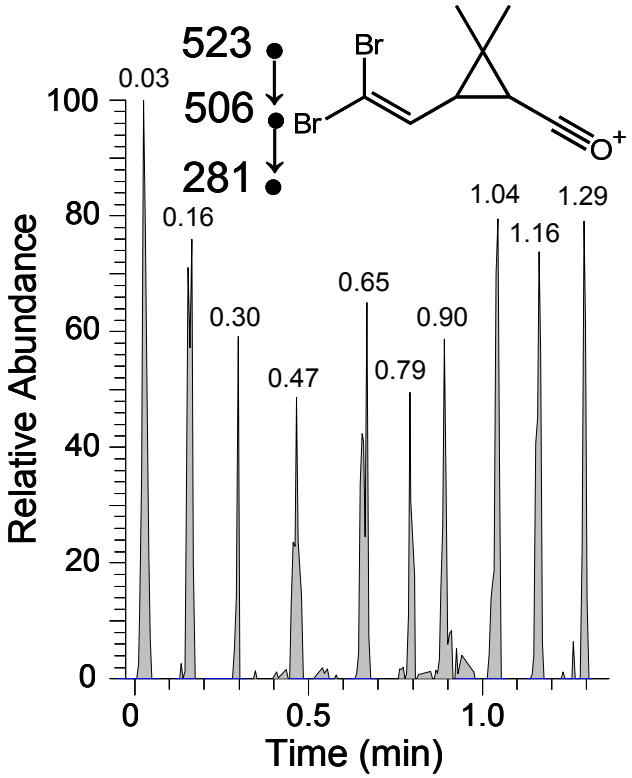

Figure 5.2: Extracted ion chronogram from a TM-DESI analysis of a polyester mosquito net coated with 16 mg/m^2 of deltamethrin. The consecutively monitored reaction encompassed CID of the most abundant isotope of the ammonium adduct (*m/z* 523) to the protonated species of *m/z* 506. Isolation and further CID generated the MS^3 product ion of *m/z* 281, whose proposed structure is shown in the inset. Since the unit cell dimension of the bednet (2 mm) is greater than the TM-DESI sampling diameter (~1 mm), each strand of the mosquito net was clearly discernable in the chronogram

The extracted ion chronogram in Figure 5.2 clearly shows that deltamethrin was detected at approximately 8 second (0.13 min) intervals during the bednet scan. At the specified scan rate this time interval is equivalent to 2000 μm between peak maxima. These results are well correlated with the measured unit cell dimensions of the net, especially when one considers that the sampling area is not a finite line but instead a circle with leading and trailing edges. While no further work to quantify deltamethrin via external calibration or through the inclusion of an internal standard was performed, the intensities observed in Figure 5.2 suggest that the distribution of deltamethrin on the nets is reasonably consistent.

While the difference between the unit cell dimension and sampling diameter facilitated investigation of the individual mosquito net strands, it also resulted in higher limits of detection since a relatively small portion of the surface area was exposed to the electrospray at any instant. Therefore, additional experiments were performed to assess a new aspect of TM-DESI; one in which multiple samples were interrogated simultaneously with the intention of increasing the observed response by effectively increasing the density of the target analyte within the sampling diameter. In this case, samples were constructed of one, two, three, four and five layers of net material offset such that the top layer of strands occupied the open space of the mesh layer beneath it. During these analyses, the electrospray sequentially traversed each layer of the surface on its way to the MS capillary inlet.

As shown in Figure 5.3, the resulting extracted ion chronograms for the multi-layered samples no longer contained completely resolved strands. Instead, overlapping contributions from the various strands composing the different layers were observed However, comparison of the average responses from the multi-layer analyses to those of the single layer sample showed that the observed intensity for the two and three layer

samples was increased. In contrast, deltamethrin was not detectable on the four and five layer samples, even though the total surface area and effective concentration of analyte was much larger. These results suggest two important conclusions: 1) it is possible to improve the detection limit of a TM-DESI-MS analysis by utilizing a multi-layer sample to introduce more surface area density (i.e., adsorbed sample) within the sampling diameter, and 2) the increase in sensitivity is ultimately limited by the ability of the electrospray to be efficiently transmitted through the sample. Therefore, as noted previously in the analysis of single layer materials, a balance between sample surface area and electrospray transmission must also be struck for multi-layer TM-DESI-MS analyses.

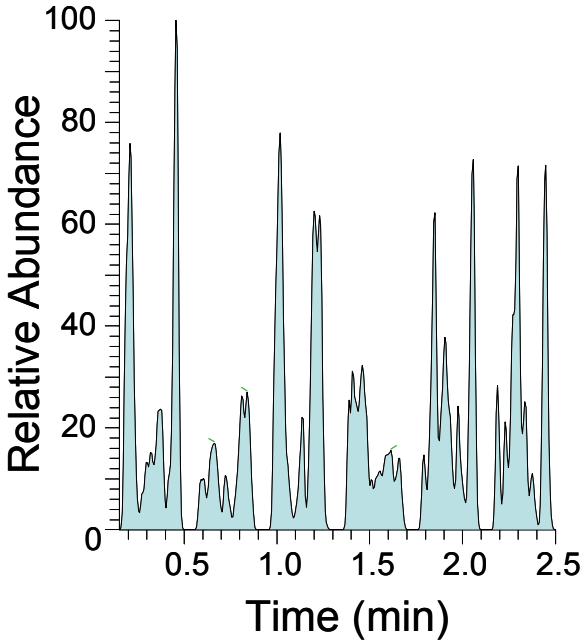

Figure 5.3: TM-DESI-MS analysis of a sample composed of three offset layers of deltamethrin coated polyester bednet (16 mg/m^2). Responses for individual strands that were observed in the single layer sample are no longer observed; however, the greater sample density results in increased response relative to a single layer sample

5.3.2 Peptides and Flavonoids (Mesh Immersion)

Proteomics is arguably the most common application of biological mass spectrometry. Bottom up proteomics in which the identity of the protein is elucidated by protein digestion and identification of its peptide components has grown enormously over the last several decades. Furthermore, the chemical structure of amino acids and peptides intrinsically contains at least one basic nitrogen atom, thereby facilitating protonation and analysis via electrospray ionization in the positive ion mode. As a class of natural products, flavonoids are abundant in most plants. Structurally, these molecules are substituted ring systems with many of the substitutions being hydroxyl groups. While not as acidic as carboxylic acids, these hydroxyl groups are deprotonated during electrospray ionization, thereby facilitating flavonoid analysis in the negative ion mode.

Mass spectra for mock mixtures of peptides and flavonoids obtained via TM-DESI-MS are depicted in Figure 5.4a and 5.4b. These spectra were acquired using the most straightforward sample preparation technique, mesh immersion. In this approach, the mesh is simply immersed in the sample solution for a few seconds, removed from the solution, affixed to the sample holder, and scrolled into the electrospray plume. While some chemical partitioning may take place, the primary sample transfer occurs by the suspension of the solution within the strands of the mesh. Therefore, the methodology relies heavily on the relationship between the open space of the mesh material and the surface tension of the sample solvent, making it primarily useful for analyses of samples in low surface tension solvents.

The principal benefit of the mesh immersion approach is speed. Sample throughput was very high and sample analysis, including preparation time, was routinely less than 20 seconds. Aside from the examples shown for peptides and flavonoids, this high speed qualitative screening technique could find additional applications where

sample volumes are not the limiting factor and quantitative analysis of the solution is not the primary objective.

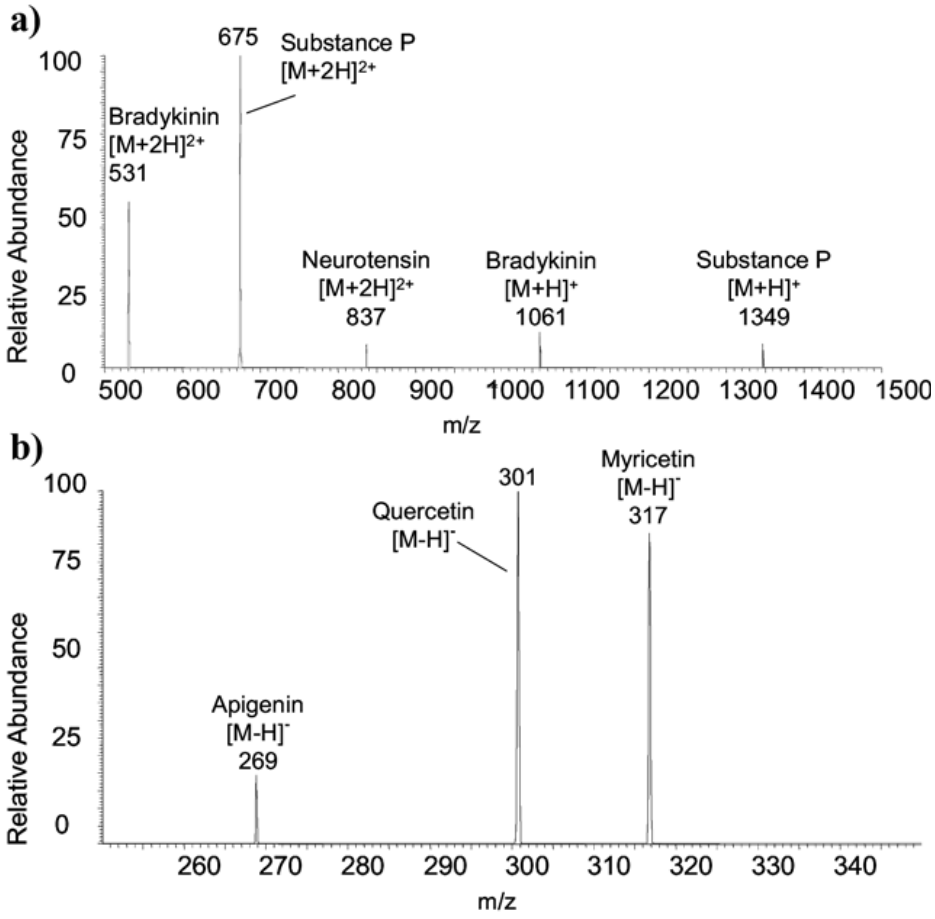

Figure 5.4: TM-DESI mass spectra for mixtures of (a) bradykinin, neurotension, and substance P (1 μM in methanol) and (b) apigenin, quercetin, and myricetin (100 μg/mL in methanol). Analysis was performed by immersing the mesh in the solution, affixing the mesh to the source, and scrolling the wet mesh into the electrospray plume.

5.3.3 Small Molecules and Metabolites (Sample Deposition)

Another potential application of TM-DESI is the analysis of small molecules that are either endogenous to the human body or otherwise introduced via deliberate or accidental

exposure. Among these analytes, many are specific metabolites that are monitored as indicators of health, disease, and drug abuse. Figure 5.5 depicts the mass spectrum obtained via TM-DESI-MS for a mock mixture that included a common neurotransmitter (GABA, 50 pg/μL), a common endogenous organic acid (creatine, 15 pg/μL), and a common exogenous stimulant (nicotine, 3 pg/μL) along with its primary urinary metabolite (cotinine, 2 pg/μL). In this case, the sample was prepared by direct deposition of 1μL of the methanolic mock mixture solution directly to a polypropylene sample mesh (open space of 149 μm, and strand diameter of 106 μm) and analyzed wet using a pure methanol electrospray.

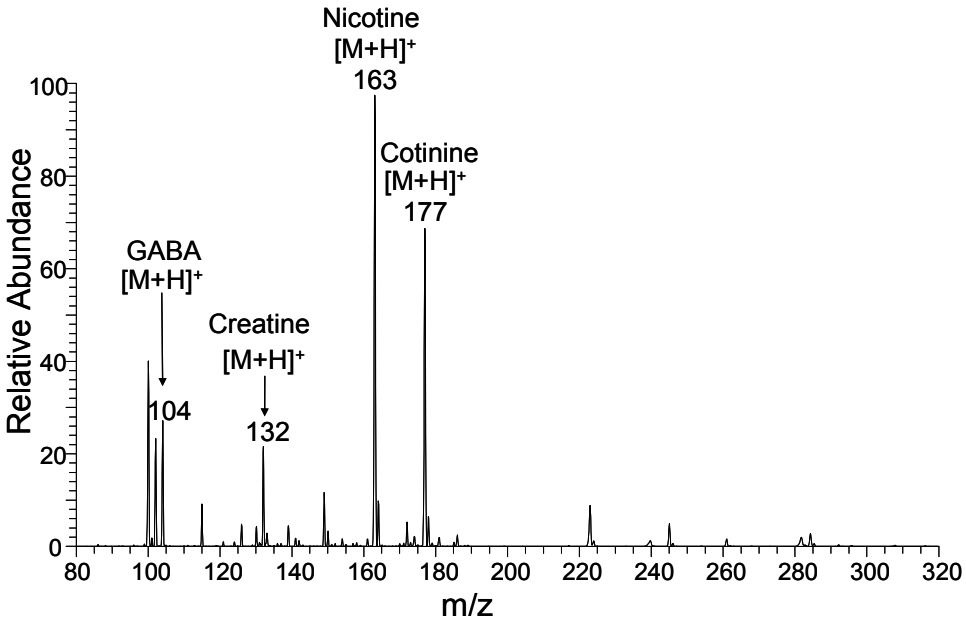

Figure 5.5: TM-DESI-MS spectrum of a mock mixture that included small molecule analytes typically found in biological matrices.

As expected, the most abundant ions were the protonated analyte species and the most basic analytes (i.e., nicotine, cotinine, and creatine) showed the largest response per unit mass. While GABA was successfully detected, the protonation of its primary amine was

obviously less facile than the protonation of the tertiary amines present in the other three analytes. Since the ionization mechanisms in DESI are inherent to electrospray ionization (ESI), this example demonstrates the competitive ionization often found in DESI and TM-DESI analyses. This concern is addressed in more detail in Chapter 6.

The investigation of biological metabolites present in the blood, urine and saliva is a common theme in metabolomics, a rapidly growing area for biological mass spectrometry. Therefore, the cotinine application was extended to a physiological matrix, urine. Fresh urine samples were collected and spiked with cotinine at a concentration of 100 pg/μL. Samples were spotted (1 μL) either directly onto a PEEK mesh and dried before analysis or diluted 1:100 with methanol and analyzed wet. Similar dilutions or sample extractions have been utilized in some [33] but not all [25,34] DESI studies involving urine. In the present study, direct analysis of the liquid urine samples without this dilution showed significant ion suppression by the urine matrix, presumably due to the remaining solvated salts. In accordance with published reports highlighting the high salt tolerance of conventional DESI experiments, TM-DESI of dried urine samples showed less ion suppression.[35]

Figure 5.6a depicts a representative mass spectra obtained in the analysis. The ion of *m/z* 177 corresponds to protonated cotinine, whereas the ion of *m/z* 199 corresponds to sodium-cationized cotinine. A MS-MS spectrum of the ion of *m/z* 177 was collected to confirm the presence of cotinine (Figure 5.6b). The major product ion (*m/z* 146) corresponds to the loss of CH_3NH_2. The ions of *m/z* 98 and *80* stem from cleavage of the bond between the pyridine and pyrrolidine rings. The resulting product ion spectrum matches previously reported results for analysis of cotinine by LC-MS[36,37] and illustrates that tandem mass spectrometry is also possible in TM-DESI analysis of wet samples, despite the relatively short-lived ion signal. Furthermore, the diluted concentration of 1

pg/μL in this analysis is above the detection limit of 0.156 pg/μL reported by LC-ESI-MS, but in the vicinity of the limit of quantitation (2.5 pg/μL) reported in the same study.[36] While TM-DESI did not produce a lower detection limit than LC-MS, the analysis was performed in seconds compared to the several minutes required for the LC-MS assay.

.

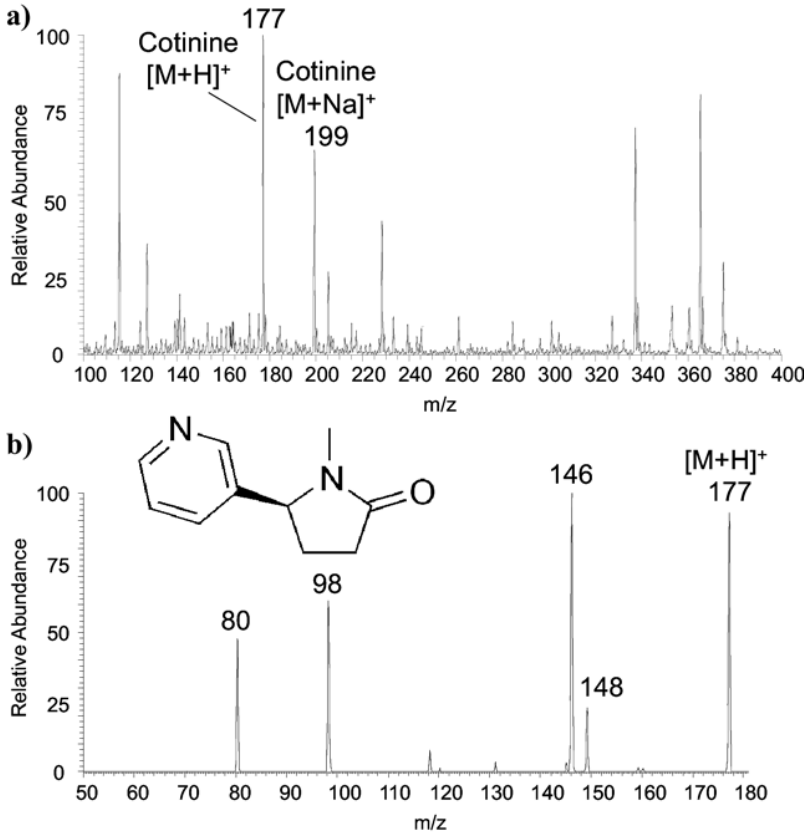

Figure 5.6: TM-DESI spectrum of (a) urine containing cotinine, the primary urinary metabolite of nicotine, and (b) MS-MS spectrum of the ion of *m/z* 177 used to confirm the presence of the protonated cotinine species.

The possibility of using a co-deposited internal standard for TM-DESI analysis of liquid samples was also explored. In this study nicotine (10 pg/μL) was added as an internal standard to cotinine standards (50 to 500 pg/μL) in methanol and analyzed immediately following deposition of 1 μL of sample on a PEEK mesh. Five replicate

measurements were taken at four concentrations of cotinine and the resulting calibration curve is shown in Figure 5.7. The %RSD for the individual points was reduced from an average of 16% without the internal standard to an average of 6.7% with it. Moreover, results reported by Ifa et al. describe similar success and suggest that further improvements may also come from using a deuterated internal standard.[38] Additionally, monitoring of selected transitions in MS-MS analyses or competitive reactions using reactive DESI may also help facilitate better quantitative capability.

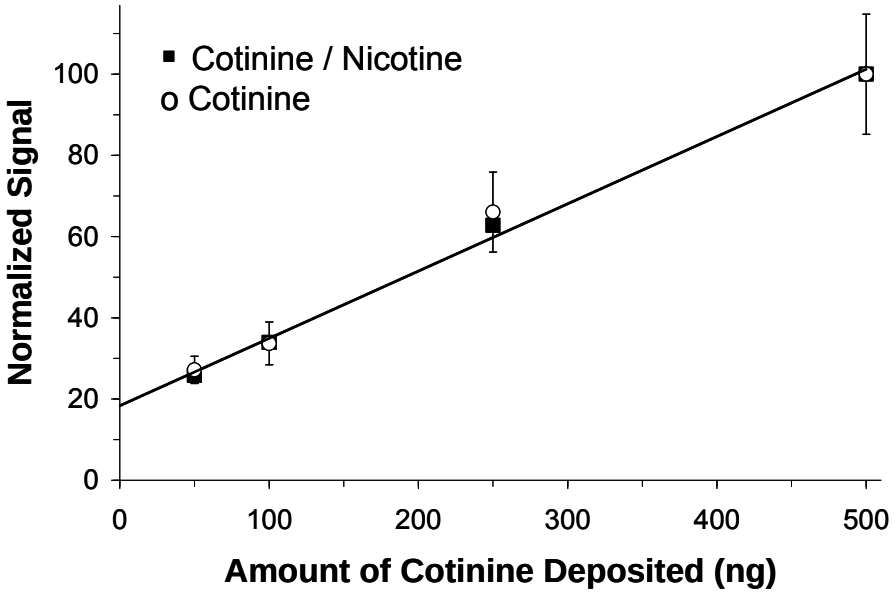

Figure 5.7: Calibration curve for cotinine with and without the use of nicotine as an internal standard. Error bars indicate one standard deviation of 5 replicate measurements of cotinine without adjustment to the internal standard.

5.3.4 Pharmaceuticals (Substrate Masking)

Rapid analysis of pharmaceuticals has been one of the most promising applications of DESI.[11-19] While the majority of these reports have focused on the direct analysis of formulated products, there is also a need to detect these types of molecules

either between stages of the production process or after they have been administered.[39] Most pharmaceutical analyses are especially demanding, requiring highly accurate and precise results to meet regulatory guidelines.[39,40] While it is desirable to obtain this accuracy and precision in a high throughput format, the trade off between the various performance criteria makes this goal difficult to achieve. Thus, the vast majority of pharmaceutical analyses utilize chromatographic separations to improve accuracy and precision, and in doing so, compromise analytical speed.[40] While this approach is clearly necessary to meet the demands of product validation, a high speed semi-quantitative screening approach that offers a balance between the competing metrics remains desirable.

A representative mass spectrum for verapamil (100 pg/uL) acquired by TM-DESI-MS is depicted in Figure 5.8. In this instance, 25 μL of a methanolic sample was deposited on a polypropylene mesh as a band several millimeters wide and allowed to dry. (See Figure 5.1). Prior to sample analysis a mask was overlaid on the mesh to create a series of equivalent subsamples. The mass spectrum in Figure 5.8 depicts the average response as the electrospray source was scanned over one of the transmissive spots.

The sample masking approach was primarily investigated as a means of increasing the precision of TM-DESI-MS analyses. Figure 5.9 shows a representative extracted ion chronogram when a selected ion monitoring experiment for verapamil was performed using this sample preparation method. Seven replicates experiments of this type were performed and the average percent relative standard deviation over the trials was 6.8%, a very reasonable result considering the total analysis time for each trial was approximately 40 seconds.

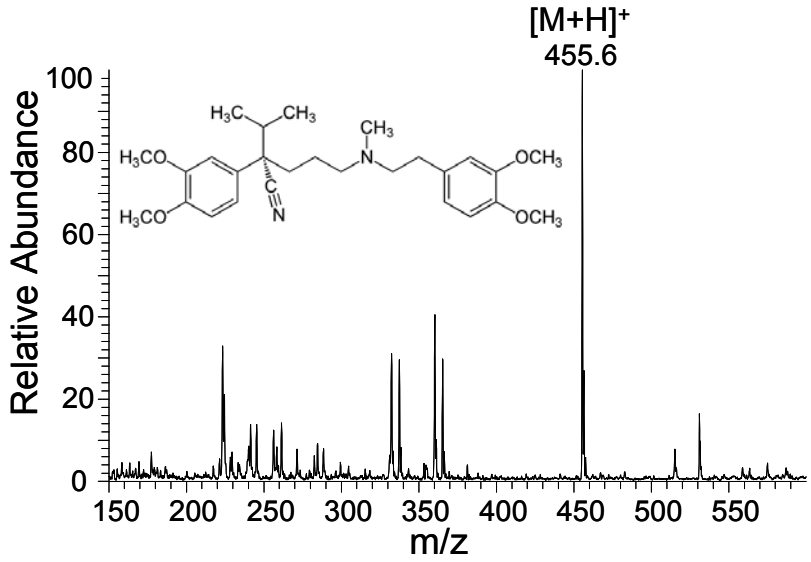

Figure 5.8: TM-DESI-MS spectrum of verapamil residue.

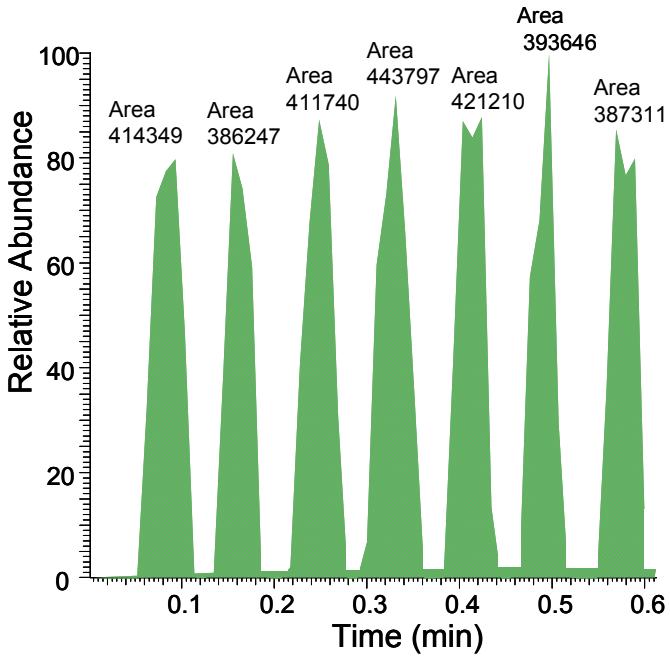

Figure 5.9: Extracted ion chronogram for verapamil analysis using sample masking.

In addition to providing a means for increasing precision the sample masking plates shown in Figure 5.1 can also be used as standardized guides for low volume (1-

3μL) sample deposition. As an example, a clean mesh was affixed to the sample backing plate and overlaid with a mask composed of 5 mm circles, thereby creating a sample introduction device reminiscent of a typical 96 well plate. Verapamil standards ranging from 25pg/μL to 2500 pg/μL in methanol were deposited as 2μL spots within the wells and allowed to dry. The extracted ion chronogram and calibration curve are shown in Figure 5.10. Of particular note are the correlation coefficient for the corresponding least squares fit (R^2= 0.994) and the total analysis time (~ 30 sec.). These results suggest that TM-DESI shows promise as a high throughput semi-quantitative screening method for pharmaceutical analysis.

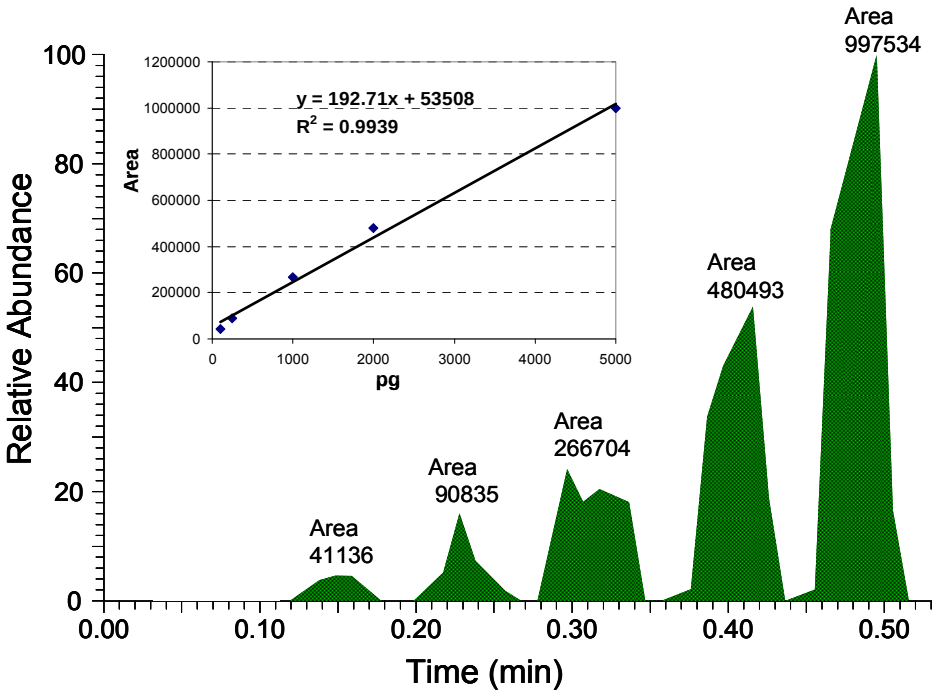

Figure 5.10: Calibration curve for the high speed TM-DESI calibration for verapamil.

5.3.5 Explosives (Direct Sample Collection)

The increase in terrorism over the last decade has been accompanied by a dramatic increase in the amount of research dedicated to the detection of energetic

materials.[41] In particular, the ease of explosives manufacture and the susceptibility of various infrastructure systems have made rapid screening and stand-off detection capabilities highly desirable.[41,42] To complicate the matter, many explosive materials have extremely low vapor pressures, thereby making their detection via gas-phase sampling techniques extremely difficult.[41,42] Furthermore, volatilization from the condensed phases is complicated by an inherent susceptibility to pyrolytic degradation.[42] While inorganic oxidizers such as nitrate, chlorate, and perchlorate salts and highly sensitive peroxides such as triacetone triperoxide (TATP), are commonly utilized in improvised explosive devices (IEDs)[41], a vast majority of military explosives are from three major chemical classes: 1) nitroaromatics; 2) nitramines, and 3) nitrate esters.[41,42] All of these compounds contain oxygen rich nitro- groups that impact not only their explosive activity, but also their detection.

Electrospray ionization is well suited to the analysis of common military explosives, with the most common ions being ion-molecule complexes of halogens or nitrate ions with the explosives;[42] these analytes are therefore typically detected in the negative ionization mode. Figure 5.11 depicts a mass spectrum obtained for pentaerythritoltetranitrate (PETN) a common nitrate ester via TM-DESI-MS. In this case the mesh was used not only as a sample introduction method, but also as a sampling device for extracting the sample from a surface. The adhesive coated mesh was prepared by exposing a polypropylene mesh to an adhesive coated material to remove a portion of the adhesive. The mesh material was then used to collect sample from a bench top that had been previously spiked with 10 μL of a 100 pg/μL solution of PETN in acetonitrile. The mass spectrum clearly shows the formation of chloride and nitrate adducts to the PETN. The chloride adducts were induced by the choice of the electrospray solvent, in this case a 5:1 mixture (v:v) of acetonitrile to chloroform. The nitrate adduct was created

by reaction of an intact PETN molecule with thermal decomposition product of another PETN molecule.[42] In this case thermal degradation was induced by the heat applied to the capillary inlet of the mass spectrometer (~ 200 °C). This particular example illustrates both the use of a reactive electrospray for TM-DESI and the use of mesh materials as sampling devices. The latter topic is discussed in detail in Chapter 6.

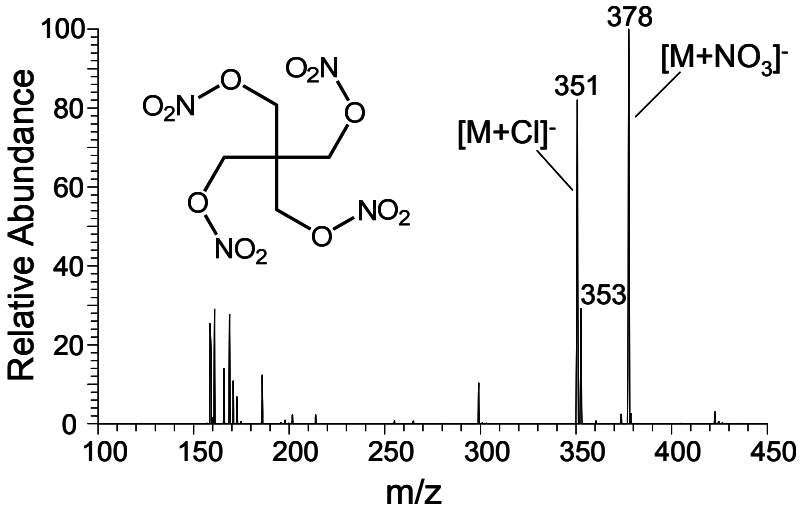

Figure 5.11: TM-DESI-MS spectrum of PETN obtained via the analysis of an adhesive coated sampling mesh that was used as a sample collection device. Chloride adducts were induced by incorporating chloroform into the reactive electrospray. The nitrate adduct was introduced by holding the temperature of the capillary inlet to the mass spectrometer at ~ 200 °C.

5.4 CONCLUSIONS

The successful analysis of small molecule metabolites, pharmaceuticals, flavonoids, peptides and explosives presented herein confirm the hypothesis that TM-DESI has a similar range of applications as DESI. Furthermore, the results discussed in this chapter also demonstrate that a variety of sample introduction methods are applicable to TM-DESI and that the technique can benefit from the use of internal standards and

reactive electrospray constituents. Ultimately, TM-DESI may be best suited to high speed screening applications. Thus, the results presented for high throughput calibration and improved precision following sample masking may help elevate the analytical performance of the technique to a semi-quantitative status.

5.5 REFERENCES

(1) Takats, Z.; Wiseman, J. M.; Cooks, R. G. *J. Mass Spectrom.* **2005,** *40,* 1261–1275.

(2) D'Agostino, P. A.; Hancock, J. R.; Chenier, C. L.; Lepage, J. *J. Chromatogr. A* **2006,** *1110,* 86–94.

(3) Ifa, D. R.; Wiseman, J. M.; Qingyu, S.; Cooks, R. G. *Int. J. Mass Spectrom.* **2007,** *259,* 8–15.

(4) Nyadong, L.; Green, M. D.; De Jesus, V. R.; Newton, P. N.; Fernandez,F. M.. *Anal. Chem.* **2007,** *79,* 2150–2157.

(5) Cotte-Rodriguez, I.; Takats, Z.; Talaty, N.; Chen, H.; Cooks, R. G.. *Anal. Chem.* **2005,** *77,* 6755–6764.

(6) Takats, Z.; Cotte-Rodriguez, I.; Talaty, N.; Chen, H.; Cooks, R. G. *Chem. Comm.* **2005**, 1950–1952.

(7) Justes, D. R.; Talaty, N.; Cotte-Rodriguez, I.; Cooks, R. G. *Chem. Commun*. **2007**, 2142–2144.

(8) Cotte-Rodriguez, I.; Cooks, R. G. *Chem. Commun.* **2006**, 2968–2970.

(9) D'Agostino, P. A.; Chenier, C. L.; Hancock, J. R.; Lepage, J. *Rapid Commun. Mass Spectrom.* **2007,** *21,* 543–549.

(10) Song, Y.; Cooks, R. G. *J.Mass Spectrom.* **2007,** *42,* 1086–1092.

(11) Chen, H.; Talaty, N.; Takats, Z.; Cooks, R. G. *Anal. Chem.* **2005,** *77,* 6915–6927.

(12) Van Berkel, G. J.; Ford, M. J.; Deibel, M. A. *Anal. Chem.* **2005,** *77,* 1207–1215.

(13) Weston, D. J.; Bateman, R.; Wilson, I. D.; Wood, T. R.; Creaser, C. S. *Anal. Chem.* **2005,** *77,* 7752–7580.

(14) Williams, J. P.; Scrivens, J. H. *Rapid Commun. Mass Spectrom.* **2005,** *19,* 3643–3650.

(15) Hu, Q.; Talaty, N.; Noll, R. J.; Cooks, R. G. *Rapid Commun. Mass Spectrom.* **2006,** *20,* 3403–3408.

(16) Williams, J. P.; Patel, V. J.; Holland, R.; Scrivens, J. H. *Rapid Commun. Mass Spectrom.* **2006,** *20,* 1447–1456.

(17) Nyadong, L.; Green, M. D.; De Jesus, V. R.; Newton, P. N.; Fernandez, F. M. *Anal. Chem.* **2007,** *79,* 2150–2157.

(18) Ricci, C.; Nyadong, L.; Fernandez, F. M.; Newton, P. N.; Kazarian, S. G. *Anal. Bioanal. Chem.* **2007,** *387,* 551–559.

(19) Ifa, D. R.; Manicke, N. E.; Rusine, A. L.; Cooks, R. G. *Rapid Commun. Mass Spectrom.* **2008,** *22,* 503–510.

(20) Talaty, N.; Takats, Z.; Cooks, R. G. *Analyst* **2005,** *130,* 1624–1633.

(21) Jackson, A. T.; Williams, J. P.; Scrivens, J. H. *Rapid Commun. Mass Spectrom.* **2006,** *20,* 2717–2727.

(22) Williams, J. P.; Hilton, G. R.; Thalassinos, K.; Jackson, A. T.; Scrivens, J. H. *Rapid Commun. Mass Spectrom*. **2007,** 21, 1693–1704.

(23) Chen, H.; Zhengzheng, P.; Talaty, N.; Raftery, D.; Cooks, R. G. *Rapid Commun. Mass Spectrom.* **2006,** *20,* 1577–1584.

(24) Kauppila, T. J.; Wiseman, J. M.; Ketola, R. A.; Kotiaho, T.; Cooks, R. G.;Kostiainen, R. *Rapid Commun. Mass Spectrom*. **2006,** 20, 387–392.

(25) Pan, Z.; Gu, H.; Talaty, N.; Chen, H.; Shanaiah, N.; Hainline, B. E.; Cooks, R. G.; Raftery, D. *Anal. Bioanal. Chem.* **2007,** *387,* 539–549.

(26) Bereman, M. S.; Nyadong, L.; Fernandez, F. M.; Muddiman, D. C. *Rapid Commun. Mass Spectrom.* **2006,** *20,* 3409–3411.

(27) Shin, Y.-S.; Drolet, B.; Mayer, R.; Dolence, K.; Basile, F. *Anal. Chem.* **2007,** *79,* 3514–3518.

(28) Bereman, M. S.; Williams, T. I.; Muddiman, D. C. *Anal. Chem.* **2007,** *79,* 8812–8815.

(29) Barranco-Martı´nez, D.; Parrilla-Va´zquez, P.; Martı´nez-Galera, M.; Gil Garcı´a, M.D. *Chromatographia* **2006**, 63(9/10), 487-491.

(30) Gil-Garcı´a, M.D; Barranco-Martı´nez, D.; Martı´nez-Galera, M.; Parrilla Va´zquez, P. R;; *Rapid Commun. Mass Spectrom. 2006, 20, 2395-2403.*

(31) Zimmer, D.; Philipowski, C.; Posner, B.; Gnielka, A.; Dirr, E.; Dorff, M. *J of AOAC Int*. **2006**, 89(3), 786-797

(32) Huang, G.; Chen, H.; Zhang, X.; Cooks, R.G.; Ouyang, Z. Anal Chem. 2007, 79, 8327-8332.

(33) Kauppila, T. J.; Talaty, N.; Kuuranne, T.; Kotiaho, T.; Kostiainen, R.;

Cooks, R. G. *Analyst* **2007**, 132, 868–875.

(34) Huang, G.; Chen, H.; Zhang, X.; Cooks, R. G.; Ouyang, Z. *Anal. Chem*. **2007**, 79, 8327–8332.

(35) Jackson, A. U.; Talaty, N.; Cooks, R. G.; Van Berkel, G. J. *J. Am. Soc. Mass Spectrom*. **2007**, 18, 2218–2225.

(36) Chadwick, C. A.; Keevil, B. *Ann. Clin. Biochem*. **2007**,44, 455–462.

(37) Murphy, S. E.; Villata, P.; Ho, S. W.; von Weymarn, L. B. *J. Chromatogr. B.* **2007**, 857, 1–8.

(38) Ifa, D. R.; Manicke, N. E.; Rusine, A. L.; Cooks, R. G. *Rapid Commun. Mass Spectrom*. **2008**, 22, 503–510.

(39) Chandran, S.; Singh, R.S.P. *Pharmazie* **2007** 62 1-14.

(40) Lim, C.K.; Lord, G. *Biol. Pharm. Bull.* **2002**, 25(5), 547-557.

(41) Moore, D.S. *Rev. Sci. Instrum*. **2004**, 75, 2499-2512.

(42) Yinon, J. *Trends Anal. Chem*. **2002**, 21(4), 292-301.

Chapter 6: Development of Surface Enhanced Transmission Mode Desorption Electrospray Ionization (TM-DESI)

6.0 Chapter Overview

This chapter discusses the development of surface-enhanced TM-DESI and illustrates its application toward a particular class of molecules, sulfhydryls. While these molecules are important to many fields, they are inherently more difficult to ionize than more basic or acidic molecules such as amines and carboxylic acids, thereby making them a suitable model set to demonstrate the benefits of a selective capture and enrichment technique. Mesh materials for surface-enhanced TM-DESI have been fabricated using an acid-catalyzed hydrolysis of polyamide mesh (nylon 6,6). Following the coupling of a neutravidin binding layer, a capture agent containing a photolabile biotinylated linker is attached. Mesh materials are then immersed in samples to capture sulfhydryls. Following analyte capture and rinsing, the mesh is exposed to UV light and cleavage of the photolabile unit releases the mass tagged analyte to the matrix-free mesh. Samples are then analyzed immediately by TM-DESI-MS without any additional sample preparation. In addition to providing a method of releasing the covalently bound target analyte, cleavage of the photolabile linker also provides a means of tagging the analyte with an easily ionizable tag that facilitates electrospray ionization and subsequent tandem mass spectrometry experiments.

6.1 Introduction

A new era of high-throughput mass spectrometry emerged with the nearly simultaneous introduction of two ambient ionization techniques: desorption electrospray ionization (DESI)[1] and direct analysis in real time (DART).[2] Recognition of the enormous potential of these ionization methods has resulted in a growing number of

related techniques, including ones that integrate laser desorption, the use of plasmas, and extraction methods.[3-5] Although many variations of ambient ionization techniques have been developed since the initial report of DESI in 2004, the original DESI method continues to find the most extensive use, with an expanding list of applications that range from small molecule analysis to proteomics to imaging.[4,5]

In the DESI process, ions are produced by directing charged solvent droplets from an electrospray source toward a sample that is either a bulk material or one that has been deposited onto a sampling surface. As discussed in previous chapters, transmission mode desorption electrospray ionization (TM-DESI), is a new mode of operation for DESI in which the sample is adsorbed onto the strands of a mesh or otherwise suspended as macro scale droplets within its confines. Samples are analyzed by scrolling the mesh orthogonally into the path of an electrospray plume positioned coaxial to the inlet capillary of the mass spectrometer, thereby resulting in the transmission of the ionizing plume directly through the material. The transmission mode results in desorption and ionization typical of DESI, but with the added benefits of a simpler experimental geometry and the convenient analysis of both dry (i.e., following evaporation of the deposition solvent) and wet (i.e., solvated) samples from smooth substrates.

The most compelling motivations for ambient ionization mass spectrometry are the ability to analyze surfaces directly, the speed of the analysis and the elimination of difficult or time consuming sample preparation steps. Most ambient ionization methods require only seconds per sample, which is a substantial improvement in throughput compared to the multiple minutes required to separate and analyze components in GC-MS and LC-MS analyses. Moreover, most of the cumbersome sample preparation steps such as derivatization reactions and extensive sample cleanup protocols are alleviated. Although one of the major benefits touted for ambient ionization mass spectrometric

methods is the direct analysis of complex samples, the elimination of chromatographic separation generally results in reduced specificity and ion suppression for low concentration species. A recent variation of DESI, termed reactive DESI invokes the addition of specific reagents to the electrospray solvent to facilitate ion/molecule reactions with analytes of interest, thereby resulting in improved performance metrics for some classes of targeted molecules.[6-9] While reactive DESI-MS has shown promise in particular situations, it is not universally applicable and thus it is generally recognized that one set of performance metrics (i.e., specificity and/or sensitivity) has been compromised for another (i.e., analytical speed) in desorption-based ambient ionization mass spectrometry.

Selective capture of target molecules from solution for subsequent analysis via mass spectrometry continues to be a burgeoning field.[10-12] While it has been explored most prominently in the field of proteomics,[13-20] techniques such as surface-enhanced laser desorption ionization (SELDI) [10-23,] and its related component surface-enhanced affinity capture (SEAC)[15] are in theory applicable to virtually any application.[12] In the SELDI process a surface is modified with an affinity probe designed to capture either a specific molecule via antibody-antigen interactions, [24-30] or a broader class of molecules such as bacteria or microorganisms[31-32] After capture, samples are rinsed to remove interferences, thereby providing not only a concentrated sample but also increased specificity.[10-12] Analysis is completed by subjecting the sample to laser desorption ionization (LDI) either directly, or following the addition of a suitable matrix (i.e., MALDI).[10-12,33,34]

Surfaces for SELDI-MS have taken a variety of forms including polyvinylidene difluoride (PVDF),[34-38] alkane thiol self assembled monolayers,[25,26,39-41] dextran,[25] polyethylene[36] and polyester.[38] However, one particularly effective SELDI surface

utilizes immobilized metals to selectively bind various important classes of compounds such as phosphorylated peptides.[10-12,44,45] This technique, immobilized metal affinity chromatography (IMAC) has been commercialized and the use of IMAC SELDI biochips has been reported in numerous studies, especially those targeting post translational modifications and disease biomarkers. [10,11,45-49]

Aside from SELDI-MS, several other analytical techniques employ affinity capture to provide increased specificity and improved sensitivity. In particular, enzyme linked immunosorbent assays (ELISA) and other protein microarrays are highly utilized in biomedical applications as they provide an efficient mode to quantify the presence of target molecules in complex samples.[50-51] In the case of ELISA, the preferred detection method is fluorescence, primarily due to its inherent sensitivity and simplicity. Another common affinity capture application is surface plasmon resonance (SPR), in which the binding of a particular analyte to a substrate is detected by the change in the refractive index of the surface. [52-58] Perhaps the most intriguing aspect of SPR is its capability to study the binding kinetics of the system, while simultaneously concentrating the analyte. Once the assay is complete, the target molecules can be removed from the substrate and subsequently analyzed via mass spectrometry to give a qualitative identification. The coupling of SPR and MS, deemed biomolecular ineraction mass spectrometry (BIA-MS) has become an integral part of proteomics studies.[59-62]

The experiments discussed in Chapter 4 demonstrated that the chemical characteristics of the mesh strands can influence the ability to desorb species from the surface during TM-DESI analysis. The present chapter expands on those observations by demonstrating that the specificity of TM-DESI analyses can be dramatically increased by fabrication and utilization of mesh materials that have been designed to capture selected analyte molecules from solution (Figure 6.1). Subsequent interaction of the mesh with

UV light results in cleavage of a photolabile unit linking the mesh to the captured analyte. The mesh materials are then analyzed immediately by TM-DESI-MS without any additional sample preparation. In addition to providing a method of releasing the covalently bound target analyte, cleavage of the photolabile linker also provides a means of tagging the analyte with an easily ionizable mass tag that facilitates electrospray ionization and subsequent tandem mass spectrometry experiments. This surface-enhanced TM-DESI-MS strategy is a tunable approach and can be extended to the selective capture, release, and analysis of targeted molecules from complex mixtures, thus uniting the analytical merits of specificity and speed for many classes of analytes.

This chapter discusses the development of surface-enhanced TM-DESI and illustrates its application toward a particular class of molecules, sulfhydryls. These molecules are important to many fields including metabolomics, pharmaceuticals, environmental science, and proteomics. However, they are inherently more difficult to ionize than more basic or acidic molecules such as amines and carboxylic acids, thereby making them a suitable model set to demonstrate the benefits of a selective capture and enrichment technique.

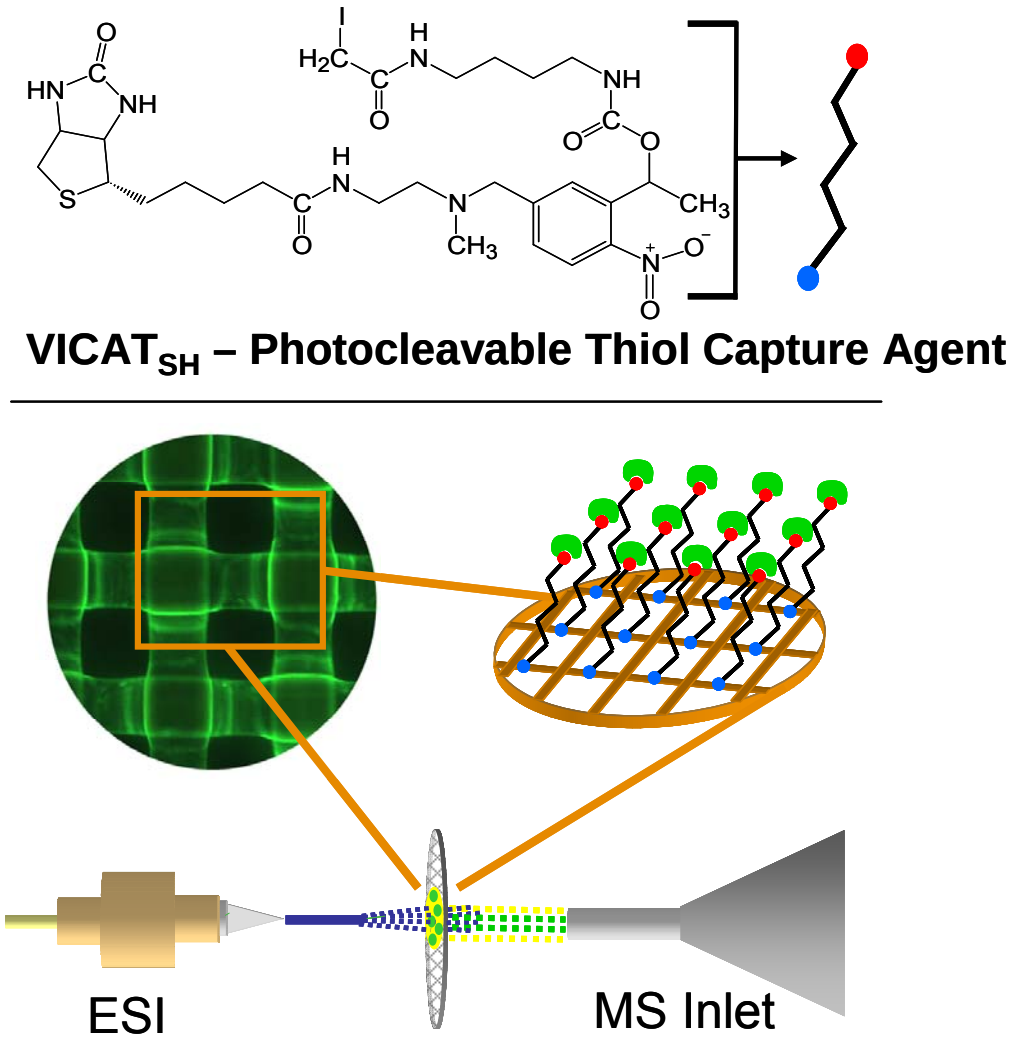

Figure 6.1: Schematic view of surface-enhanced transmission mode desorption electrospray ionization mass spectrometry employing VICAT$_{SH}$ as a sulfhydryl capture reagent attached to a neutravidin-coated mesh.

6.2 EXPERIMENTAL

6.2.1 Materials

Hydrochloric acid, sodium hydroxide, sodium chloride, potassium chloride, methanol, acetonitrile, and water (HPLC grade) were purchased from Fisher Scientific (Hampton, NH). N-acetyl-L-cysteine, captopril, creatinine, cysteamine, fluorescein(sodium salt), 6-mercaptopurine, MES hydrate, methyl violet 10B (crystal violet), penicillamine, CMC 4-[2-[(Cyclohexylcarbonimidoyl)amino]ethyl]-4-methylmorpholinium p-toluenefulfonate, and phosphate buffered saline were purchased from Sigma Aldrich (St.Louis, MO). Neutravidin (a deglycosylated form of avidin) and fluorescein isothiocyanate (FITC) derivatized neutravidin were purchased from Pierce Biotechnology (Rockford, IL). Biotin-4-fluorescein was purchased from Anaspec (San Jose, CA) and Synthrapol dying detergent from Dharma Trading Company (San Rafael, CA). Polyamide mesh sheets (nylon-6,6) with a strand diameter of 125 μm encompassing an open space of 190 μm were purchased from Small Parts Inc. (Miramar, Fl.) $VICAT_{SH}$, a biotinylated molecule incorporating an iodoacetaminyl group for the selective capture of sulfhydryls and a photolabile o-nitrobenzyl linkage between the biotin and the capture agent was synthesized in the laboratory of Dr. Michael Gelb at the University of Washington using previously reported procedures.[63,64]

6.2.2 Fabrication of Enhanced Mesh Materials

Mesh materials were marked, cut into 1 cm squares and cleaned thoroughly with methanol to remove any residual ink. The mesh pieces were then sonicated in an aqueous solution of Synthrapol (1%) to remove any remaining surface contaminants. Following a thorough rinse with DI H_2O, the cleaning procedure was completed by sonicating the

materials in an acetonitrile and water solution (50:50 v:v) for five minutes. Batches of cleaned materials were stored in HPLC grade H_2O for future use.

Acid-catalyzed hydrolysis of polyamide (nylon-6,6) materials to expose carboxyl groups was performed using a 3 M solution of HCl for approximately 24 hours at temperatures between 25 °C and 40 °C. Following hydrolysis, mesh materials were rinsed with HPLC grade H_2O to remove any residual acid, blown dry with air, and stored dry in a sealed glass or PTFE containers.

Derivatization of the hydrolyzed mesh materials with neutravidin was performed using a two step procedure for carbodiimide mediated coupling of surface carboxyl groups to the primary amines of the protein. In the first step, the free carboxyl groups of the hydrolyzed mesh were reacted with a room temperature solution of CMC (108 mM) in MES coupling buffer (pH = 5) for 15 min. After rinsing the mesh materials in phosphate buffered saline (pH=7.4), neutravidin (either in its FITC derivatized or native form) was coupled to the mesh materials by immersion of the meshes (20 per 5 mL batch) for at least 2 hours in a 0.2 mg/mL (3.3 μM) solution of the protein in PBS (pH=7.4). Following protein derivatization, the mesh materials were rinsed free of excess protein with additional PBS and immersed in a 100 μg/mL solution of $VICAT_{SH}$ for at least 2 hours in the dark. At this stage, the meshes present neutravidin surfaces suitable for capturing biotinylated molecules, such as the $VICAT_{SH}$ reagent shown in Figure 6.1. The biotin group of $VICAT_{SH}$ binds to neutravidin, thus anchoring $VICAT_{SH}$ to the mesh, while the iodoacetaminyl capture agent of $VICAT_{SH}$ remains available to react specifically with analytes containing free sulfhydryl groups.

6.2.3 Mass Spectrometry

A one-dimensional automated scanning Omni Spray ion source (Prosolia, Inc., Indianapolis, IN) was mounted to a Thermo Fisher Scientific LTQ XL (Thermo Fisher Scientific Inc., Waltham, MA) and modified to allow a 0° angle between the electrospray tip and capillary inlet to the mass spectrometer. The sample holder used in previous chapters was modified to accommodate mesh materials designed for surface-enhanced TM-DESI analysis. In this case, a transmissive sample stage with a 2 cm square cutout was constructed of 2.3 mm thick high density polyethylene (HDPE) and mounted orthogonally to the Omni Spray ion source. Mesh samples were affixed to 3.5 cm x 6.5 cm slides constructed of 0.77 mm thick oriented polyester with 8 mm square cutouts to accommodate transmission through the mesh sample, slide and transmissive sample stage. All analyses were conducted at a distance of 2 mm between the electrospray tip and the mesh surface and a distance of 6 mm between the mesh sample and the capillary inlet of the mass spectrometer. Methanol at a flow rate of 10 μL/min was used as the electrospray solvent and nitrogen at a pressure of 110 psi was used as the nebulizing gas. The electrospray voltage was set to 4.0 kV, the ion accumulation time set to 10 ms and signal averaging set for three microscans. Mass spectra were acquired in the positive ion mode by scanning the sample at a rate of 500 μm/sec.

6.2.4 Fluorescence Microscopy and Fluorimetry

Analysis of the distribution of fluorescently labeled neutravidin on derivatized mesh materials was performed using the 2.5X objective of an Olympus BX2 epifluorescent microscope equipped with a 12 bit CCD camera (DVC Co., Austin, TX) and high pressure mercury bulb excitation source. Excitation of the fluorescein isothiocyanate tag occurred at 480 nm and emission was monitored at 535 nm.

Photomicrographs were captured via DVC software with adjustable gain, offset, and exposure time.

The reproducibility of key mesh derivatization processes (i.e., polyamide hydrolysis, neutravidin coupling, and biotin binding) was assessed through a series of fluorimetric assays that utilized the chemical functionalities present in common dyes such as fluorescein and fluorescein isothiocyanate to provide fluorescent markers for each derivatization reaction. Thus, each batch of materials underwent a quality control assessment following each key derivatization step. All assays were performed on a Perkin Elmer Victor 3 fluorimeter equipped to read samples presented in 24 well plates. Aqueous samples (1 mL) were deposited in the plate wells and the analysis time was optimized to provide maximum fluorescence intensity for positive control samples while maintaining minimal signal intensity from control blanks. For experiments involving fluorescein or fluorescein isothiocyanate excitation and emission were modulated using filters of 485 nm and 535 nm, respectively. Additional experimental details of each assay are presented alongside the results discussed in the text.

6.2.5 Execution of Surface Enhanced TM-DESI Analysis

With respect to the analytical strategy for utilizing the derivatized mesh materials described in Section 6.2.2, Figure 6.2 summarizes the steps involved in manufacturing the mesh materials and provides a schematic overview of the workflow in surface-enhanced TM-DESI-MS. First, the pH of the sample is adjusted to the appropriate range for the capture agent (e.g., ~9.5 for $VICAT_{SH}$ capture of sulfhydryls), and the mesh is submerged in the sample solution to capture sulfhydryl-containing analytes. In the case of sulfhydryls, analyte capture by the iodoacetaminyl unit of the $VICAT_{SH}$ reagent was complete in approximately 5 minutes. Next, the mesh is removed from the sample

solution, rinsed thoroughly with water or methanol to remove matrix interferences (e.g., salts) and non-sulfhydryl-containing compounds and placed under a UV lamp for 10 minutes to induce photocleavage of the o-nitrobenzyl linkage. The meshes are then placed in line with the electrospray and analyzed directly by TM-DESI-MS using methanol as the electrospray solvent. As an example, the photocleavage of a sulfhydryl analyte captured by $VICAT_{SH}$ is shown in Figure 6.3. It should be noted that the current study was not aimed at optimizing the quantitative aspects of the analysis, but instead was focused primarily on developing the technique for capture, release, and analysis of sulfhydryl-containing compounds for screening applications. Once the technique is fully implemented, a disulfide reduction step utilizing TCEP will likely be inserted.

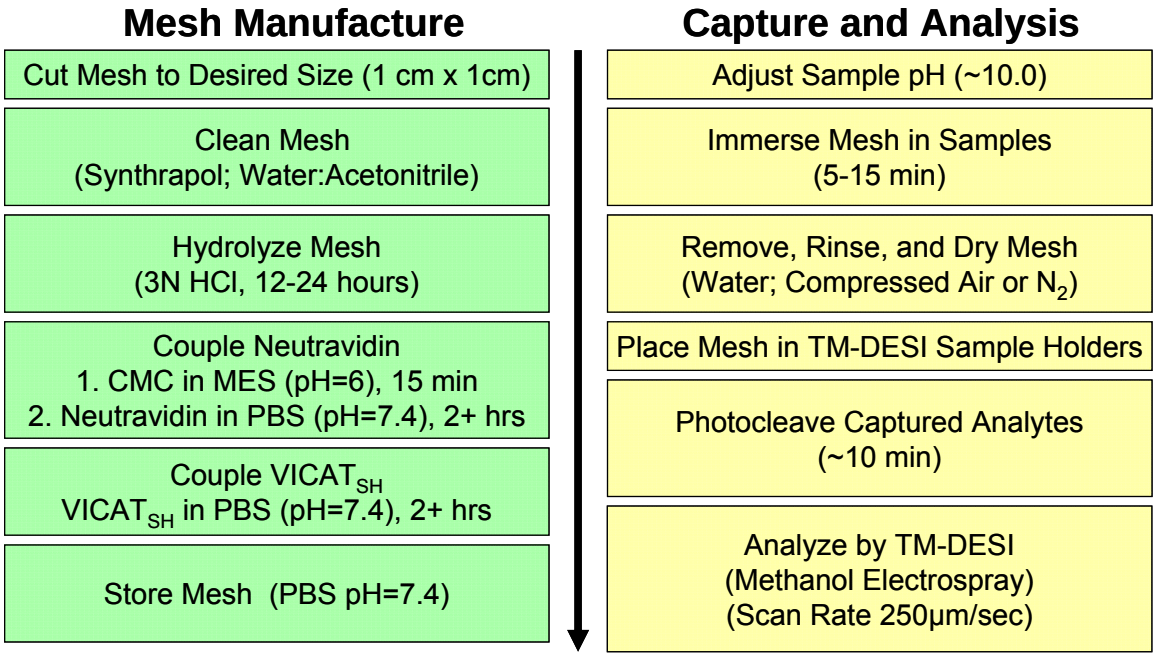

Figure 6.2: Work flow summary for surface-enhanced mesh preparation and TM-DESI analysis of sulfhydryl analytes. Required manufacturing steps are shown in green, while required sample analysis steps are shown in yellow. Quality control steps during the mesh manufacturing process are shown in gray.

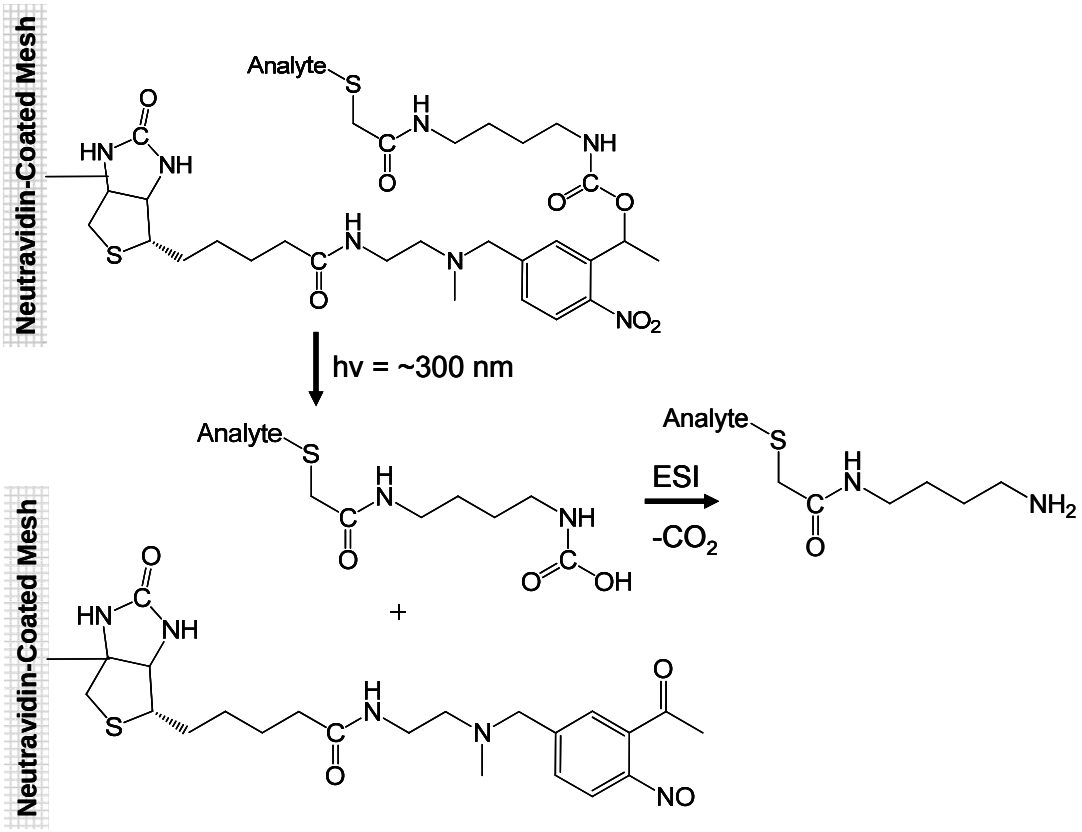

Figure 6.3: Schematic overview of the photocleavage reaction for a sulfhydryl-containing analyte captured by VICAT$_{SH}$. The biotinylated linker molecule remains attached to the mesh surface the mass tagged analyte is released.

6.3 RESULTS AND DISCUSSION

Experiments discussed in Chapter 3 demonstrated that the sampling area for TM-DESI is essentially circular and that the diameter of the sampling spot is on the order of 1 mm when the electrospray tip is held 2 mm from the mesh surface and the flow rate of the electrospray solvent is 5 μL/min. When TM-DESI is used to analyze deposited samples, the mesh material acts as a support for analytes adsorbed to the mesh strands or suspended as macro-scale droplets within the unit cells of the mesh. In either case, the analytes are desorbed by the incoming electrospray as the sampling spot is scanned across the mesh. Thus, the analysis is primarily impacted by two factors: 1) the ability of

the mesh to transmit the electrospray, and 2) the partitioning of free analytes between the deposition solvent or electrospray solvent and the mesh material. Consequently, sensitivity in TM-DESI analysis of deposited samples is maximized by using a chemically inert mesh with high transmission efficiency.

Chapter 5 highlighted four different approaches for sample preparation in TM-DESI, one of which relied on utilizing the sample mesh as a surface sampling device. A similar approach is used in surface-enhanced TM-DESI. In this case, the mesh substrate selectively extracts analytes from a sample solution and concentrates them on the surface of the mesh. Therefore, the sensitivity of the approach depends directly on the surface density of the capture agent, which in turn is impacted by the number of active derivatization sites on the mesh and ultimately correlated with the total surface area of the sampling material. In contrast to the results presented in Chapter four and five, inert mesh materials such as polypropylene and ETFE that are optimal for TM-DESI analysis following sample deposition are not effective for surface-enhanced analyses. Instead, the mesh material must be reactive itself or modified to include exposed reactive groups to allow attachment of the reactive capture agents. Non-conducting and readily activated polymers, such as polyamides, are well suited for manufacturing surfaced enhanced TM-DESI substrates.

There are several important considerations for optimizing a surface-enhanced approach: 1) the exposed surface area of the mesh material must be balanced with the ability to transmit the electrospray; 2) the number of active derivatization sites per unit area should be maximized without sacrificing material integrity during the derivatization process; 3) the surface density of the capture agent should be maximized by providing an efficient linkage between the capture agent and the mesh derivatization sites, and; 4) the accessibility of the exposed surface area to the UV light during the photocleaveage and to

the electrospray during the analysis should be maximized to facilitate efficient detection of a high proportion of the captured analytes. This investigation therefore sought to determine the surface area of potential mesh materials, the accessibility of the surface area, and the reproducibility of the mesh hydrolysis and derivatization reactions. Ultimately, these results are expected to be necessary for optimizing the derivatization and manufacturing process.

6.3.1 Calculation of Mesh Surface Area

The surface area of a woven mesh material can be derived from the diameter of the strands composing the mesh, d, and the open space between the mesh strands, o. As illustrated in Figure 6.4, these parameters enable the assignment of a unit cell and the calculation of the number of unit cells in a mesh of known size (i.e., X by Y). The unit cell has two lengths, U_x and U_y, which can be calculated by taking the open space of the mesh and adding the radius of the strand on both sides of the open space. (see Figure 6.4).

Eq. 6.1: $U_x = o + r + r = o + d$ and $U_y = o + r + r = o + d$

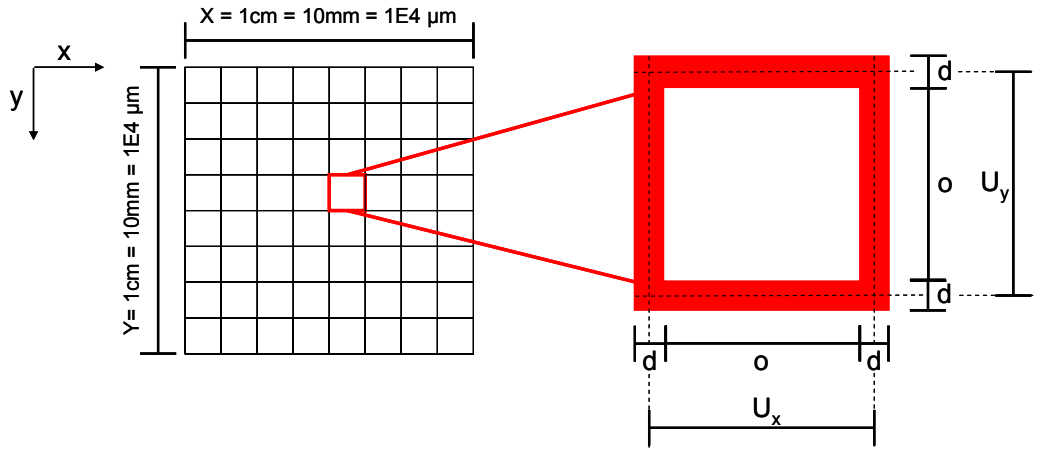

Figure 6.4: Calculation of mesh surface area via definition of unit cells.

If the length in each dimension is known, then the number of unit cells in each dimension, N_x and N_y, can be determined by taking the total length and dividing it by the appropriate unit cell length. (Eq. 6.2) Since each unit cell is composed of two strands in each direction, the number of strands, S_x and S_y, is therefore given by the number of unit cells in that dimension plus one. (Eq. 6.3) Furthermore, if the mesh material under consideration is square, then the strands composing the vertical and horizontal portions of the mesh are equivalent (i.e., the same length) and the total number of strands in the mesh, S_T, is equal to the sum of the strands in each dimension. (Eq. 6.4)

Eq. 6.2: $N_x = X / U_x$ and $N_y = Y / U_y$

Eq. 6.3: $S_x = N_x + 1$ and $S_y = N_y + 1$

Eq. 6.4: $S_T = S_x + S_y$

If the mesh strands are assumed to be circular, then the circumference of the stands can be derived directly from the diameter. Since, the length of the strands is given by X or Y, the surface area of a representative strand, SA_n, can be calculated by multiplying the circumference of the strand by the length. (Eq. 6.5) Thus, multiplying the surface area of one strand, SA_n, by the total number of strands, S_T, provides the total surface area of all the strands composing the mesh, SA_T. (Eq. 6.6)

Eq. 6.5: $SA_n = \pi d \times Y$

Eq. 6.6: $SA_T = SA_n \times S_T$

Calculation of the total surface area, SA_T, results in an overestimation of the effective surface area because it includes the entire surface without considering the three dimensional structure of the woven mesh and the loss of exposed surface area at points where the mesh strands overlap. Since the number of overlap points is equal to the number of strands used to compose the mesh, the amount of surface area that is lost to strand overlap, SA_{OV}, can be readily approximated by determining an intersection area,

Ai, from the strand diameter (Eq. 6.7) and multiplying it by the total number of strands used to form the mesh, S_T. (Eq. 6.8). Ultimately, the exposed surface area, SA_{EXP}, is equal to the total surface area, SA_T, less the surface area lost to strand overlap, SA_{OV}. (Eq. 6.9)

Eq. 6.7: $A_i \approx d \times d$

Eq. 6.8: $SA_{OV} = 2 \times S_T \times A_i$ (exposed area is lost from both strands)

Eq. 6.9: $SA_{EXP} = SA_T - SA_{OV}$

The exposed surface areas of the 1 cm x 1 cm polyamide mesh materials considered for the development of surface-enhanced TM-DESI are given in Table 6.1.

As discussed in Chapter 4, substrates with open spaces less than 150 μm and accompanying minimal strand diameters produce less scattering of the electrospray plume and therefore favor transmission. Larger strand diameters typically encompass larger open spaces, but the increase in the surface area of the strand increases both plume scattering and solvent and analyte spreading on the mesh. Thus, the mesh composed of 125 μm diameter strands and an open space of 190 μm (shown in bold) was used throughout the surface-enhanced development because it provided the best balance between exposed surface area and the mesh characteristics shown in Chapter 4 to provide optimal electrospray transmission.

Table 6.1. Calculated Surface Area of Polyamide Mesh Materials

Strand Diameter (μm)	Open Space (μm)	Total Surface Area (mm^2)	Overlap Surface Area (mm^2)	Exposed Surface Area (mm^2)
50	130	175.9	0.6	175.3
83	165	213.8	1.1	212.7
125	**190**	**251.3**	**2.0**	**249.3**
155	210	272.7	2.7	270.0
151	310	208.7	2.0	206.7
240	350	256.3	3.9	252.4

6.3.2 Accessibility of Mesh Surface Area

The adaptation of DESI to a transmission mode effectively replaces relatively planar surfaces such as glass, PMMA, or PTFE slides with transmissive mesh materials. As shown in Table 6.1, square mesh materials (1cm x 1cm) may have exposed surface areas on the order of 250 mm^2. For comparison, one side of a glass slide of the same size would have an accessible surface area of approximately 100 mm^2, which is 60 percent less than the calculated mesh surface area. (Note: both of these calculations assume that the surface is uniform, therefore neglecting any surface porosity.) While this result may seem counterintuitive, it follows from the perception of each object; that is, in the preceding calculation the mesh was treated as a three dimensional object with a completely accessible surface while the glass or PMMA slide was treated as a two dimensional object with only one plane exposed to the electrospray. It is certainly reasonable to assume that only one side of the glass slide is accessible to the electrospray in the conventional DESI mode in which the spray bounces off the solid surface. In

contrast, preliminary studies conducted using the TM-DESI mode indicated that deposition of samples on either side of the mesh produced similar results, suggesting that analytes could be desorbed from the front or back side. Additional experiments were conducted here to determine whether the exposed surface area of the mesh was accessible and whether the electrospray could interact with and ionize analytes from both the front (i.e., facing the electrospray tip) and back (i.e., facing the mass spectrometer) of the mesh.

In one set of experiments, the entire surface of polyamide mesh materials was coated with methyl violet B (crystal violet), a highly basic dye well suited to electrospray and desorption electrospray ionization. TM-DESI analysis of these mesh materials produced large responses for the protonated dye species and an examination of the mesh post analysis showed a distinctly clear trace where the dark violet dye had been removed by the electrospray as it was scanned across the surface. Most importantly, the clear trace was observed on both sides of the material indicating that the dye was indeed removed from both the front and back of the mesh. Additional studies were conducted in which one side of the mesh was masked prior to coating with the crystal violet stain, thereby creating mesh materials that were stained on only one side. When these materials were analyzed by TM-DESI, the observed mass spectral intensity was essentially equal regardless of the orientation of the mesh (i.e. stained side facing the electrospray or stained side facing the mass spectrometer). These results confirm that the electrospray does interact with both sides of the mesh and indicate that a majority of the exposed surface area is accessible during the analysis.

Further detailed studies are necessary to confirm the mechanism by which the electrospray interacts with each portion of the exposed surface. However, it is plausible that some of the electrospray droplets contact and wet the front of the mesh, migrate to

the back of the mesh via their momentum, and are subsequently released from the material under the influence of the nebulizing gas. In this way analytes sequestered on both sides of the mesh can be solvated and readily desorbed into the vapor phase.

6.3.3 Efficiency of Mesh Derivatization

Hydrolysis

In general, the amount and accessibility of the exposed surface area are fundamentally critical factors for numerous surface-enhanced methods. However, the development of affinity capture techniques is also intrinsically dependent on the number and density of the reactive sites used to tether capture agents to the surface. Due to incomplete polymerization, some reactive carboxyl and primary amino terminal groups are present in most polyamides. However, the number and density of these groups can be dramatically increased by partially hydrolyzing the material, thereby cleaving surface amide bonds and creating reactive carboxyl and amino groups in their place. While polyamide hydrolysis can be accomplished under both acidic and basic conditions,[65-70] the studies reported here utilized an acid-catalyzed hydrolysis with 3N HCl. This concentration was reported to be optimal for several forms of nylon[66-69] and found here to be the highest tolerable concentration the 125 μm mesh strands could withstand. Increasing the concentration beyond 3N either dissolved the material completely or resulted in severe loss of structural integrity.

Cleavage of polyamide bonds with HCl results in the formation of carboxylic acids and protonated amine chloride salts. When exposed to water, carboxylic acids on the surface of the hydrolyzed mesh dissociate (pKa ~5) to produce the associated carboxylate ions. Therefore, submersion of the mesh materials in aqueous solutions resulted in an increase of hydrogen ion concentration and an associated decrease in

solution pH. In addition to gross measurements taken using standard pH paper, more accurate measurements were made using a fluorimetric assay.

It is well known that the fluorescence intensity of an aqueous fluorescein solution is dependent on the equilibrium created amongst its cationic, neutral, anionic, and dianionic forms.[71] In the case of fluorescein, the dianion and anion having much larger extinction coefficients and quantum yields than the neutral molecule.[71] As the pH decreases and more protons are available in solution, the shift of the equilibrium from primarily anions and dianions under neutral conditions to a greater number of anions and neutral species results in a large decrease in solution fluorescence.[71] Thus, an assay that utilized the change in fluorescence of aqueous solutions of fluorescein following exposure to hydrolyzed mesh materials was developed as a fast and accurate way to study the efficiency and reproducibility of the hydrolysis reaction.

In this case, a total of twenty representative mesh samples were taken from five replicate reaction batches conducted under various time and temperature conditions. Each of the mesh materials was weighed, added to 1 mL of an aqueous fluorescein solution (1 μM) contained in a 24 well plate and allowed to equilibrate for 10 minutes. The fluorescence intensity at 535 nm (excitation 485 nm) was then measured for 100 ms, and mass corrections were applied to account for any differences in mesh surface area. Since the additional free carboxyl groups will dissociate in the aqueous solution and shift the equilibrium of fluorescein toward its less fluorescent forms, a decrease in the fluorescence intensity indicated a higher acid content and more complete hydrolysis of the mesh. As shown in Table 6.2, raising the temperature increased the amount of hydrolysis observed at a particular reaction time. However, similar results were also obtained when the reaction was run for 24 hours at room temperature. Furthermore, the

reproducibility of the reaction was acceptable (RSD ~ 5%) and appeared to be independent of the reaction conditions.

Table 6.2: Decrease in aqueous 1M fluorescein fluorescence following exposure to mesh materials hydrolyzed for varying times and at temperatures

Time (hrs)	Temperature (°C)	Intensity (counts)	RSD (%)
2	25	7604	5.7
2	40	5268	4.6
8	25	5567	6.1
8	40	4780	5.0
24	25	4479	4.7
24	40	4385	5.2

An additional set of experiments was also conducted to quantify the reduction of the fluorescence and equate it to the additional H^+ concentration in the solution. In this case, a series of aqueous fluorescein solutions were treated with known amounts of 1 M HCl and the reduction in fluorescence was measured to form the calibration curve depicted in Figure 6.5. When the reduction in fluorescence of identical solutions exposed to the various mesh samples was measured and compared to the calibration curve, it was determined that mesh samples hydrolyzed for 2 hours at 40 °C produced a fluorescence that was equivalent to adding 2.6 μmoles of H^+ from the strong acid. Mesh samples that were hydrolyzed for 24 hours, whether at room temperature or at 40 °C, produced a response that was equivalent to adding 3.6 μmoles of H^+. Along with the data presented in Table 6.2, these results suggest that hydrolysis was more complete after the additional exposure time. While the determination of the equivalent moles of H^+ was not necessary for determining the reproducibility of the hydrolysis reaction, it will be critical for

standardization of the manufacturing process and determination of the total number of hydrolyzed sites available for further derivatization.

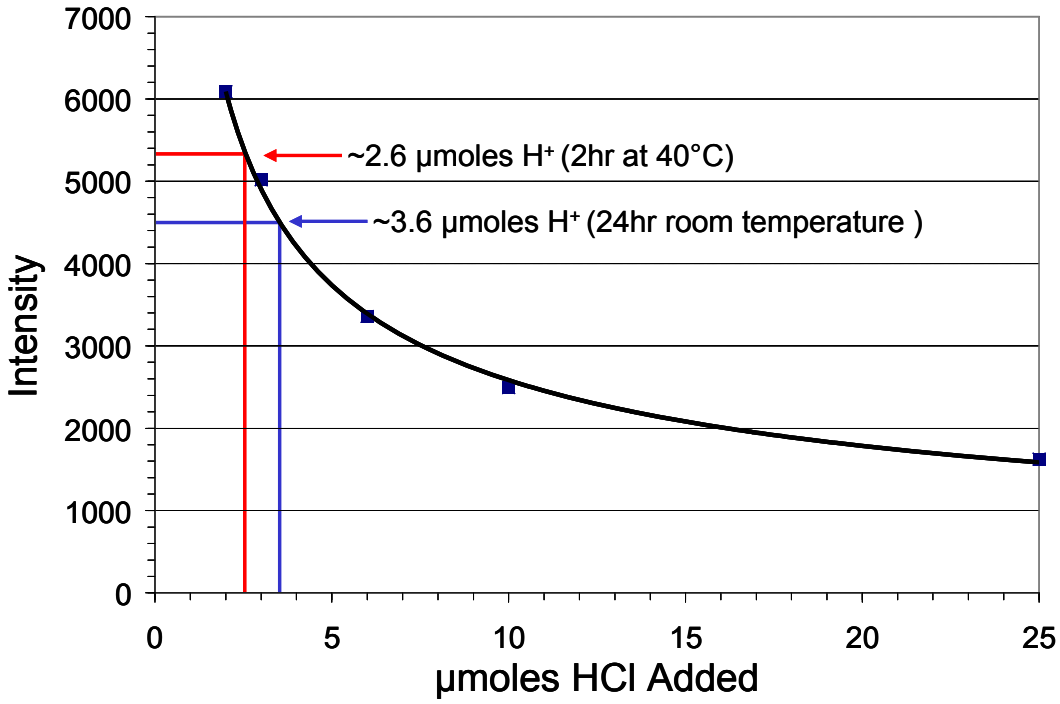

Figure 6.5: Calibration curve for fluorescence intensity versus the addition of HCl (i.e., varying pH.). The calibration curve (shown in black) was obtained by adding known amounts of 1 M HCl to 1 mL of 1 µM aqueous fluorescein solutions. When mesh samples hydrolyzed for 2 hours at 40 °C were immersed in identical solutions, the resulting measured solution fluorescence was equivalent to adding 2.6 µmoles of H^+ (red). When identical solutions were exposed to mesh samples that were hydrolyzed for 24 hours (at room or elevated temperatures), the resulting measured fluorescence was equivalent to adding 3.6 µmoles of H^+.

Neutravidin Coupling

In the present study, neutravidin was coupled directly to the hydrolyzed mesh to form a binding layer for subsequent attachment of the biotinylated photocleavable reactive capture agent, VICAT $_{SH}$. Because the performance of surface-enhanced TM-DESI is ultimately dependent on the total number of accessible reactive capture agent sites on the mesh, it is critical that the neutravidin surface layer be uniform, robust and reproducible. To evaluate the preparation of the neutravidin-modified meshes prior to modification with the biotinylated reactive capture agent, the performance of the neutravidin-coupling method was assessed by fluorescence microscopy using FITC-labeled neutravidin. Figure 6.6 depicts a fluorescent micrograph of a polyamide mesh successfully derivatized with FITC-labeled neutravidin alongside a control mesh that was cleaned and hydrolyzed, but not derivatized with the protein. The comparison provides convincing evidence that the neutravidin coupling was both successful and relatively uniform.

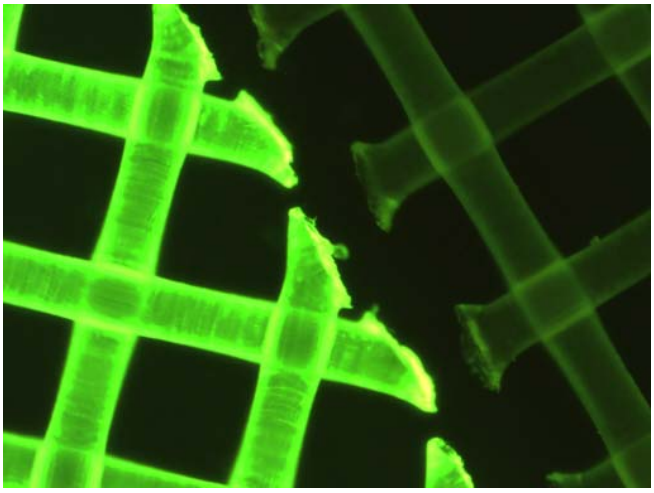

Figure 6.6: Fluorescent micrograph comparing neutravidin (FITC) derivatized and underivatized polyamide mesh materials.

In addition, the reproducibility of the neutravidin coupling to the mesh was determined by quantifying the fluorescence of representative meshes taken from five preparation batches. In this case, the mesh samples were removed from the reaction flask, rinsed with water, allowed to dry, weighed and placed flat in the bottom of a 24 well plate. The fluorescence was then measured using the same excitation and emission wavelengths used in the previous fluorescein-based hydrolysis assay.

The results shown in Figure 6.7 suggest that the derivatization procedure was fairly reproducible as nine of the ten mesh materials produced very similar responses; further investigation would be necessary to determine why the coupling efficiency for sample six was much lower than the others. Perhaps more importantly, the non-destructive nature of the fluorescence assay facilitated a quality control measure which enabled the confident identification and removal of a poorly performing mesh substrate before it was used for sample analysis.

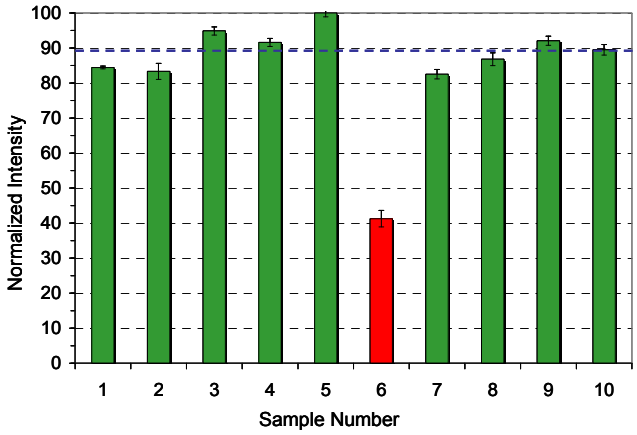

Figure 6.7: Fluorescence comparison for ten mesh materials derivatized with FITC labeled neutravidin. Two mesh samples were taken from five separate production batches and nine of the ten mesh materials produced comparable fluorescence. The mean of the green bars is shown as the dashed blue line. Error bars indicate one relative standard deviation taken from five replicate fluorescence measurements for each sample.

Biotin Binding

As was the case with the coupling of neutravidin to the mesh, quality control assays were conducted to determine the reproducibility of the subsequent attachment of biotinylated molecules and the distribution of the biotin binding sites across the mesh surface. Six mesh materials from the previously described neutravidin coupling assay were used to study the reproducibility, while the other three meshes were used to assay the distribution of the biotin binding sites.

To evaluate the reproducibility, each of the neutravidin-derivatized meshes was submerged in 1 mL of 150 nM biotin-4-fluorescein, a fluorescent conjugate of biotin selected to serve as a probe for the successful attachment of the biotinylated ligand to the mesh. Binding of the biotinylated probe to the neutravidin-derivatized mesh resulted in extraction of the probe from the solution, which ultimately caused a measurable decrease in solution fluorescence. The average intensity was determined to be 28.8% less than the control solution, but more importantly, the %RSD of the six sample analyses was less than 5% overall. Since the extent of biotin binding is directly proportional to the amount of neutravidin on the mesh, the results were also normalized to the relative intensities observed in the previous neutravidin coupling assay (i.e., adjusted for the relative fluorescence in Figure 6.7). After this correction, the relative standard deviation for the biotin binding assay was approximately 2%. Ultimately, these results suggest that the binding of biotin to neutravidin-derivatized mesh materials was very reproducible; perhaps an unsurprising result when one considers the popularity of the avidin-biotin system for immunoassay development.

When biotin-4-fluorescein binds to an avidin, streptavidin or neutravidin substrate, the fluorescence of the fluorescein-based probe is quenched.[72,73] Thus, it was not possible to utilize biotin-4-fluorescein to conduct microscopy experiments that

paralleled those described earlier for the neutravidin (FITC) coupling. Instead, the success of the attachment of the $VICAT_{SH}$ to the neutravidin-derivatized mesh was assayed by TM-DESI-MS using $VICAT_{SH}$ as a probe molecule in the absence of any sulfhydryl analytes. In this case, three neutravidin-modified meshes were immersed in solutions containing $VICAT_{SH}$ (100 μg/mL) for two hours; removed from the solution; rinsed with water and methanol; and placed under a UV lamp for 10 minutes to induce photocleavage of the bound $VICAT_{SH}$. The meshes were then subjected to TM-DESI-MS to detect the release of N-(4-aminobutyl)-2-iodoacetamide from the photocleaved $VICAT_{SH}$. N-(4-aminobutyl)-2-iodoacetamide was detected by selected reaction monitoring for conversion of the N-(4-aminobutyl)-2-iodoacetamide precursor ion of *m/z* 257 to the product ion of *m/z* 240 upon CID. A representative chronogram from the three replicates is shown in Figure 6.8.

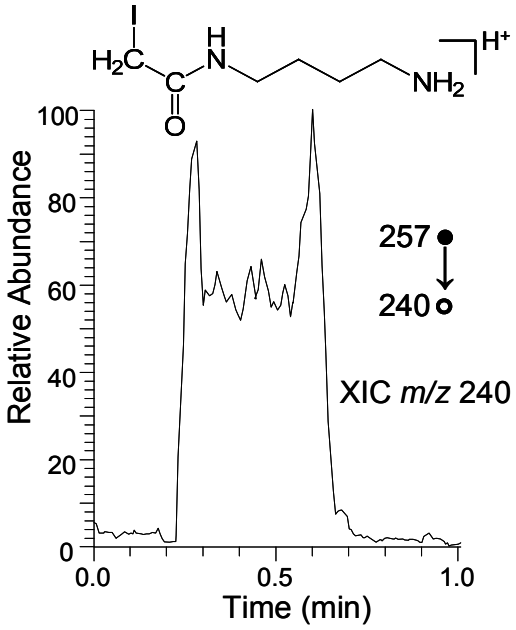

. **Figure 6.8:** The distribution of $VICAT_{SH}$ across the derivatized mesh was monitored by TM-DESI-MS. Photocleavage of unreacted $VICAT_{SH}$ produces the ion of *m/z* 257. The extracted ion chromatogram of ion *m/z* 240 obtained via CID corresponds to the loss of ammonia from the precursor ion

In general, the extracted ion chronograms showed a reasonable distribution of the photocleaved $VICAT_{SH}$ across the center portion of the mesh, indicating that the biotin binding sites are fairly well distributed. However, in all cases, larger responses were observed near the edges of the mesh. Mesh samples were scanned multiple times across the same path and while the intensity of the extracted ion chronogram decreased with each pass, the shape was relatively consistent. There are several possible causes for these edge effects: 1) they are attributable to the analysis method (i.e., there is a difference in the manner in which the electrospray interacts with the mesh at the edges); 2) the mesh materials had more reactive carboxyl groups on the edges due to more complete hydrolysis of the cut strand cross-section; 3) the materials had more neutravidin on the edges of the mesh due to increased efficiency or non-specific binding on the cut edges, or 4) there was increased biotin binding efficiency at the edges. Options one, two, or three seem the most logical, but further studies are necessary before conclusions can be drawn.

6.3.4 Capture and Analysis of Sulfhydryl Compounds

Sulfhydryl containing compounds are prevalent in pharmaceuticals and human metabolism. Captopril, acetylcysteine, penicillamine, and mercaptopurine are all well established drugs that are used to treat a variety of diseases ranging from hypertension to leukemia, whereas compounds such as cysteamine, homocysteine, glutathione, nitrosoglutathione, and mercaptolactic acid are meaningful components of the human metabolome. Thus it is not surprising that significant efforts have been made to analyze sulfhydryl compounds in both biological and environmental matrices.[75-89] The five compounds shown in Figure 6.9 were chosen as a model set to illustrate the application of surface-enhanced TM-DESI for the selective capture and analysis of sulfhydryl compounds. While these model analytes are primarily pharmaceuticals, the surface-

enhanced technique can easily be extended to endogenous metabolites, other xenobiotics, or environmental contaminants containing the reactive thiol. It should be noted that the current study was not aimed at optimizing the quantitative aspects of the analysis, but instead was focused primarily on developing the technique for capture, release, and analysis of sulfhydryl-containing compounds for screening applications. Thus, no additional steps to reduce disulfide bonds or otherwise counteract the high reactivity of the thiols were included in the work flow diagram in Figure 6.2

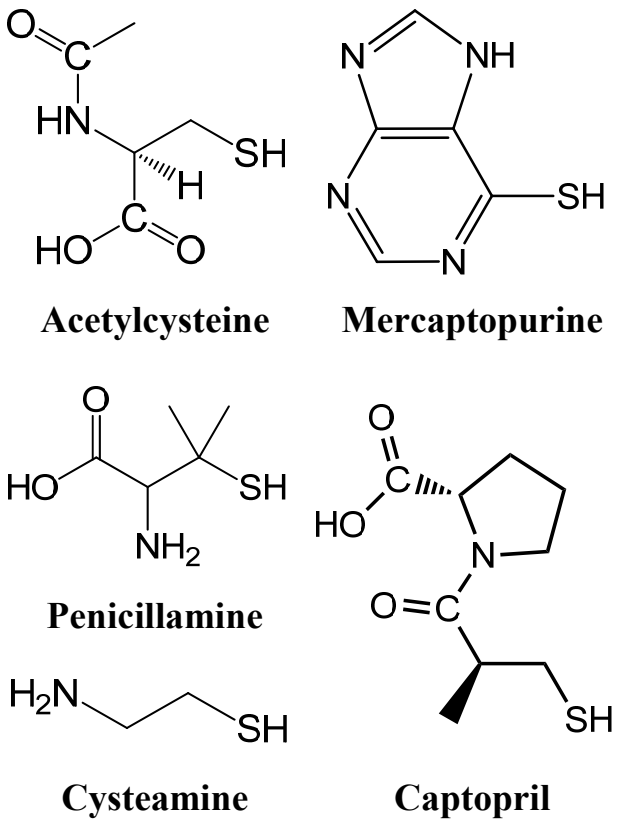

Figure 6.9: Sulfhydryl analyte structures.

Optimization of Capture and Analysis Conditions

Initial experiments to optimize the capture conditions were conducted in matrix-free aqueous solutions (100 μM) of each of the five model compounds. A series of experiments were performed to assess the impact of the sample pH (7 to 10) and the reaction time (1 min. to 40 min) on the capture efficiency. In this case the derivatization reaction of the sulfhydryl analyte and $VICAT_{SH}$ was performed in both aqueous solution and after $VICAT_{SH}$ had already been attached to the mesh. A selected reaction monitoring reaction from each of the precursor ions shown in Table 6.3 to the most abundant product ion was used to measure the performance.

Results showed that the pH had a tremendous impact on the reaction as no capture was observed at pH values less than 9. However, when the pH exceeded 9, the reaction was very efficient and no unreacted $VICAT_{SH}$ was observed during the TM-DESI analyses. In contrast, capture was found to be insensitive to the reaction time as similar results were obtained when reactive capture of the sulfhydryl-containing analytes was allowed to occur for as little as 5 min. or as long as 40 min.

One primary advantage of the surface-enhanced approach is the capability to rinse away the sample matrix prior to sample analysis. The covalent capture of target analytes was expected to create a robust method that would allow for relatively rigorous rinsing and removal of salts and other easily ionized interferences. Thus, experiments were conducted to investigate the impact of rinsing the mesh with various solvents (water, methanol, acetonitrile) prior to photocleavage. In this case, derivatized mesh materials were immersed in a 1 mM aqueous solutions (pH = 9.5) of captopril for 10 minutes to provide an abundance of analyte and favorable reaction conditions. Materials were then removed from the reaction solution and immersed in PBS buffer solution for 5 minutes. Following removal from the salt buffer, mesh materials were rinsed with the

aforementioned solvents and allowed to dry prior to UV photocleavage and subsequent analysis by TM-DESI. A selected reaction monitoring method for mass tagged captopril precursor of *m/z* 346 to the most abundant product ion of *m/z* 231 (Table 6.3) was used to monitor the impact of the solvent rinse. As expected, unbound (non-sulfhydryl) compounds were readily removed by rinsing without noticeable differences in recovery of the covalently-bound sulfhydryl compounds. Ultimately, water was chosen as an initial rinse solvent while methanol was chosen as a secondary rinse to facilitate rapid drying of the mesh before photocleavage.

The o-nitrobenzyl group incorporated in $VICAT_{SH}$ has been used in a number of photolabile probes and crosslinking agents, some of which have become staples of oligonucleotide synthesis schemes.[90-105] Previous reports concerning the use of $VICAT_{SH}$ for quantifying absolute amounts of proteins in cell lysates [63,64] utilized photocleavage times of 16 min[64] while other reports discussing similar o-nitrobenzyl photolabile compounds used exposure times as low as 5 min to induce photocleavage. [91] Therefore, the impact of photocleavage time on surface-enhanced TM-DESI-MS was also investigated by conducting a series of experiments where the exposure time was varied (5 min to 20 min). Results showed that photocleavage times of approximately 8 to 10 minutes were sufficient. Photocleavage is also dependent on the wattage and flux of the UV source. In this study, the UV lamp was a 20 Watt lamp with a wavelength of 365 nm and the sample was placed approximately 5 cm from the lamp.

CID Spectra of Mass Tagged Analytes

As depicted in Figure 6.3, photocleavage of $VICAT_{SH}$ results in the introduction of an easily ionized amine-terminated mass tag to the target sulfhydryl compound. In the gas phase, the resulting protonated species should undergo common dissociation

pathways upon collisional activation, thus allowing ready identification of the sulfhydryl compounds by MS/MS analysis. Figure 6.10 depicts both a full scan and CID mass spectrum for cysteamine captured from an aqueous solution by $VICAT_{SH}$ and analyzed by TM-DESI-MS. In this case, the mass tag provides an appreciable increase in mass from 77 Da prior to derivatization, to a tagged ion of *m/z* 206.

Upon CID, the mass-tagged cysteamine undergoes cleavage of the amide linkage to produce a fragment ion of m/z 89 and also undergoes the loss of water. The amide cleavage and water loss routes are expected to be common to many of the tagged sulfhydryls upon collisional activation, and thus should serve as consistent pathways for selected reaction monitoring of $VICAT_{SH}$-captured compounds. Furthermore, while the structural identity of the analyte cannot be unequivocally determined by the CID spectrum alone, the $VICAT_{SH}$ tag adds a mass of 129, meaning that the capture analyte has a molecular weight of 77, again consistent with cysteamine. Thus, additional confidence in the identification of cysteamine could be inferred from the surface-enhanced TM-DESI-MS analysis.

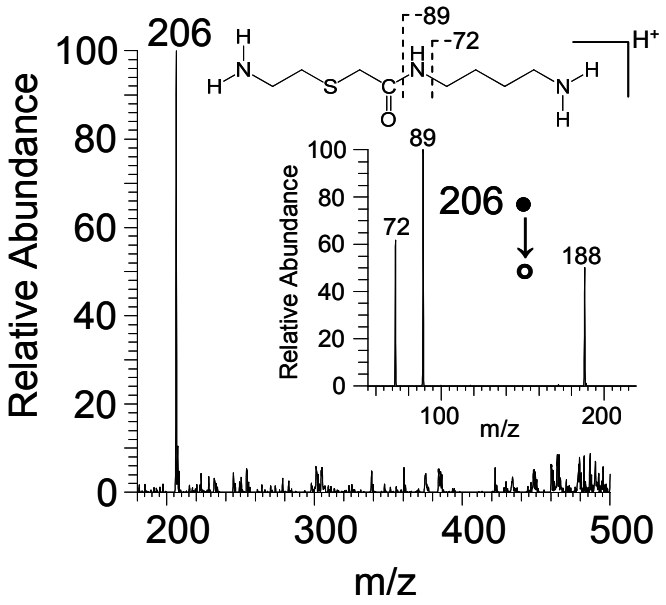

Figure 6.10: Surface-enhanced TM-DESI mass spectrum of cysteamine captured from water. The photocleaved product has a mass of 206 Da. The inset depicts the CID spectrum of the mass tagged and protonated cysteamine.

As an additional example, Figure 6.11 presents the surface-enhanced TM-DESI mass spectrum and CID mass spectrum for mercaptopurine captured from an aqueous solution by a $VICAT_{SH}$–derivatized mesh and analyzed by TM-DESI-MS. In this case, the CID spectrum shows the same favored fragmentation pathways (i.e., cleavage of the amide bond and ammonia loss). However, the amide bond cleavage results not only in the ion of *m/z* 89 which is indicative of the mass tag, but also favors the production of the ion of *m/z* 193, which is indicative of the analyte. Table 6.3 summarizes the three dominant fragment ions obtained upon CID of each analyte captured on a $VICAT_{SH}$-derivatized mesh. While extensive detection limit studies were not carried out here, solutions containing 100 ng to 400 ng of sulfhydryl analyte consistently produced positive detections.

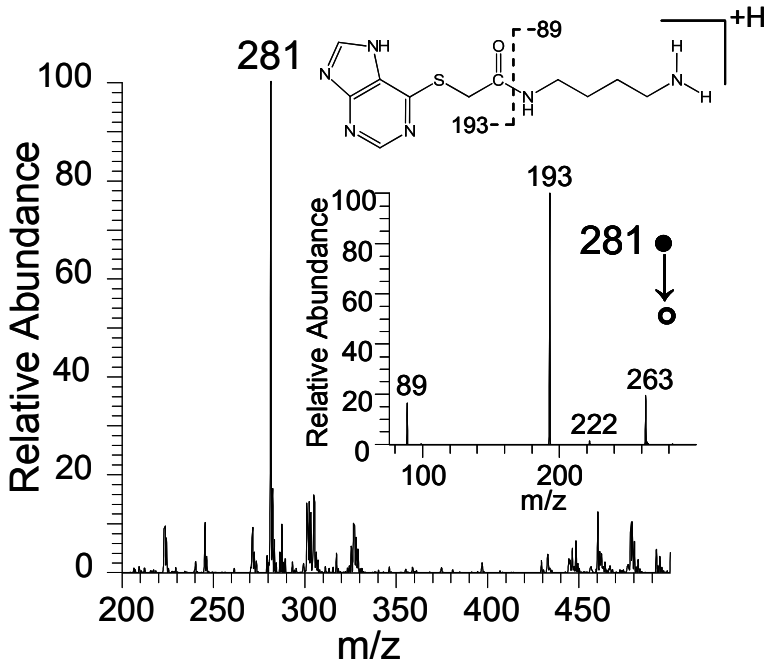

Figure 6.11: Surface enhanced TM-DESI full scan and CID mass spectra for mercaptopurine captured from water. The photocleaved product has a mass of 281 Da.

Table 6.3. VICAT$_{SH}$-Derivatized Analyte CID Fragment Ions

	Precursor	Product Ions (Relative %)		
Analyte(mass in Da)	**Ion m/z**	**Ion 1 m/z(%)**	**Ion 2m/z(%)**	**Ion 3 m/z(%)**
Mercaptopurine (152)	281	193(100)	263(20)	89(16)
Acetylcysteine (163)	292	275(100)	187(50)	232(35)
Captopril (217)	346	231(100)	249(48)	213(18)
Cysteamine (77)	206	89(100)	72(60)	188(48)
Penicillamine (149)	278	89(100)	260(70)	217(10)

Overcoming Sample Interferences with Surface Enhanced TM-DESI

Instances where complex sample matrices obscure or preclude analyte detection are abundant not only in the field of mass spectrometry, but throughout the discipline of analytical chemistry. In general, separation science, which includes sample partitioning, multiple forms of chromatography, and electrophoretic separations, aims to overcome the same recurring problem, sample interferences. These interferences ultimately degrade analytical performance by decreasing selectivity, increasing limits of detection, and reducing confidence in the accuracy and precision of the analytical method. Within the field of mass spectrometry, and specifically the areas of sample introduction and ionization, two types of interferences dominate: ion suppression and matrix effects. In the case of electrospray ionization the most common difficulties are associated with high salt or inorganic content and ion suppression due to disparities in acidity and basicity of the various analytes.

Therefore experiments were designed to demonstrate the ability of surface-enhanced TM-DESI to overcome these obstacles. The results for one of these studies are summarized in Figure 6.12. The sample in this experiment was an aqueous solution (2 mL) containing nicotine (1 μM), captopril (10 uM), sodium chloride (10 mM) and potassium chloride (10 mM), a composition chosen to mimic a physiological solution containing an easily ionizable but potentially non-targeted interference (nicotine). The sample was analyzed by direct infusion electrospray, TM-DESI without surface enhancement, and TM-DESI using a mesh derivatized with $VICAT_{SH}$. When analyzed directly by ESI, the resulting mass spectrum was dominated by the ions of *m/z* 163 and *m/z* 185, which correspond to protonated and sodium-cationized nicotine. Captopril was not observed (protonated captopril has a *m/z* of 218).

Similar results, albeit with reduced salt interference, were obtained by TM-DESI-MS analysis of sample aliquots spotted and dried on an underivatized nylon mesh. (Figure 6.12A) In this case, the presence of the nicotine, with its high basicity and high ESI efficiency, precluded detection of captopril. In contrast, successful detection and confirmation via collision induced dissociation (CID) of captopril from the same solution was easily obtained using $VICAT_{SH}$- with TM-DESI-MS analysis. In this case, protonated nicotine (m/z 163) was not detected in the TM-DESI mass spectrum, indicating that the mesh material was selective against the non-thiol containing alkaloid. Furthermore, CID of the ion of *m/z* 346 produced the spectrum displayed in Figure 6.12B. This spectrum is indicative of the mass tagged version of captopril (*m/z* 346), confirming the successful capture and release of this thiol-containing analyte. The extracted ion chronogram of *m/z* 231, an ion that corresponds to loss of the pyrrolidine carboxylic acid group, in Figure 6.12C illustrates the distribution of the captured analyte across the mesh (Analysis time = 0.25 min to 0.65min).

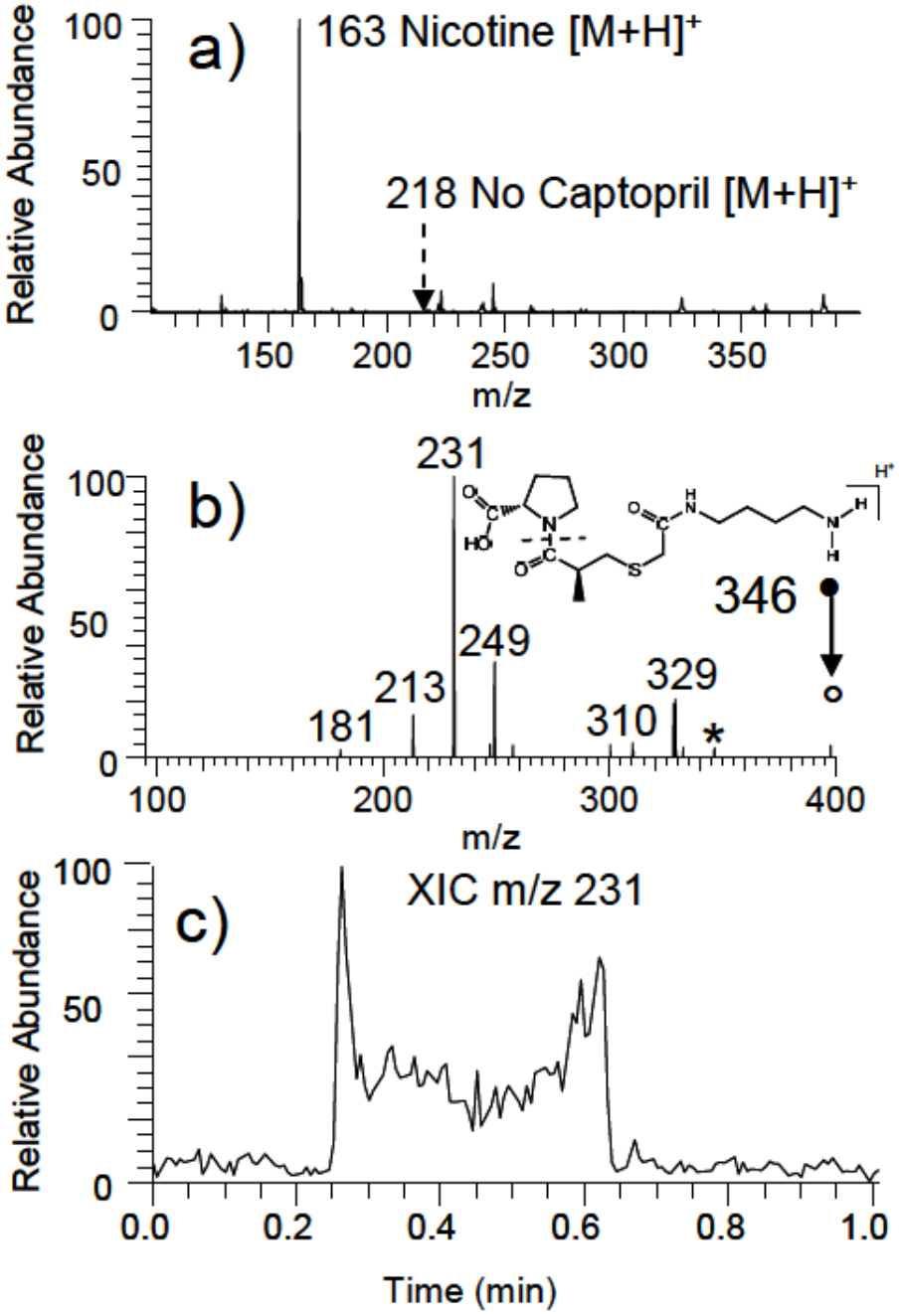

Figure 6.11: (a) TM-DESI-MS of a mock sample containing nicotine (1 μM), captopril (10 μM), sodium chloride (10 mM), and potassium chloride (10 mM) from an underivatized nylon mesh. (b) CID spectrum for captured and tagged captopril (precursor m/z 346 Da) (c) Extracted ion chronogram for ion m/z 231 indicating the distribution of the captured analyte across the mesh.

This example clearly illustrates the ability of surface-enhanced TM-DESI to overcome the presence of highly basic interferences that typically result in ion suppression and false negative detection for lower abundance, lower basicity analytes in standard direct infusion ESI and DESI analyses. The results of these studies suggest that analyte capture directly from biological matrices, such as urine, plasma, and saliva, is a logical and real possibility for advancing the scope of ambient ionization mass spectrometry.

6.4 CONCLUSIONS

Mesh materials for surface-enhanced TM-DESI-MS analyses have been fabricated using an acid-catalyzed hydrolysis of a polyamide mesh (nylon 6,6). This reaction provides a pathway to both accessible primary amines and carboxyl groups for further surface derivatization. In this work, neutravidin is coupled directly to the acid-hydrolyzed mesh surface, and then a photocleavable, biotinylated reactive capture agent is tethered to the mesh via interaction with neutravidin. There are many other potential derivatization pathways for the preparation of meshes selective for the capture and release of targeted analytes.

The surface-enhanced TM-DESI-MS method relies on the preparation of robust reactive capture materials. To achieve this goal, several issues are critical. Foremost is the creation and standardization of rapid, sensitive and accurate quality control assays that will ultimately bring high confidence to the mesh manufacturing process and by extension, to the analytical results. Without these measures it is impossible to maintain control over a rigorous experimental design and valuable resources may be lost to bad materials. Finally, extension of the surface-enhanced approach to other compound classes and ultimately to high throughput, selective analyses in complex biological

matrices will require an even better understanding of the fundamental physical chemistry behind transmitting an ionizing electrospray through a reactive mesh surface. In particular, there is a need for a more complete understanding of the complex balance that occurs as the spray penetrates, solvates, and desorbs analytes from the mesh surface.

6.5 REFERENCES

(1) Takats, Z.; Wiseman, J.M.; Gologan, B.; Cooks, R.G. *Science* **2004**, 306, 471-473.

(2) Cody, R.B.; Laramee, J.A.; Durst, H.D. *Anal. Chem.* **2005**, 77, 2297-2302.

(3) Venter, A.; Nefliu, M.; Cooks, R.G. *Trends Anal. Chem*. **2008**, 27, 284-290.

(4) Chen, H.; Gamez, G.;Zenobia, R. *J Am Soc Mass Spectrom* **2009**, 20, 1947–1963

(5) Ifa, D. R.; Jackson, A. U.; Paglia, G; Cooks, R. G. *Anal. Bioanal. Chem*. **2009**, 394, 1995–2008.

(6) Cooks, R.G.; Ouyang, Z.; Takats, Z.; Wiseman, J.M. *Science* **2006**, 311, 1566-1569.

(7) Huang, G., Chen, H., Zhang, X, Cooks, R.G., Ouyang, Z. *Anal. Chem*. **2007** ,79, 8327-8332.

(8) Nyadong, L., Green, M.D., De Jesus, V.R., Newton, P.N., Fernandez, F.M., *Anal. Chem*. **2007**, 79, 2150-2157.

(9) Wu, C., Ifa, D.R., Manicke, N.E., Cooks, R.G., *Anal. Chem*. **2009**, 81, 7618-7624.

(10) Nelson, R.W.; *Mass Spec. Rev*. **1997**, 16, 353-376.

(11) Merchant, M.; Weinberger, S.R. *Electrophoresis* **2000**, 21, 1164-1177.

(12) Tang, N.; Tornatore, P.; Weinberger, S.R. *Mass Spec. Rev*. **2004**, 23, 34-44.

(13) Weinberger, S.R.; Dalmasso, E.A.; Fung, E.T. *Curr. Opin. Chem. Biol*. **2001**, 6, 86-91.

(14) Weinberger, S.R.; Morris, T.S.; Pawlak, M. *Pharmacogenomics* **2000**, 1, 1462-1482.

(15) Roy, P.; Shukla, Y. *Cancer Therapy* **2008**, 6, 841-856.

(16) Uversky, V.N.; Permyakov, E.A. *Meth. Prot. Struct. Stab. Anal.* **2007**, Part D, 121-174.

(17) Vekey, K.; Telekes, A.; Vertes, A. *Med. App. of Mass Spectrom*. **2008**, 379-406.

(18) Bulman, A. *Amer. Biotech. Lab*. **2008**, 26(2), 14-16.

(19) Kiehntopf, M.; Siegmund, R.; Deufel, T. *Clin. Chem. Lab. Med*. **2007**, 45(11), 1435-1449.

(20) Petricoin, E. F.; Liotta, L. A. Edited by Liebler, D.C. *Prot. in Cancer Res*. **2005**, 117-131.

(21) Hutchens, T.W.; Yip, T.T. *Rapid. Comm. Mass Spectrom*. **1993**, 7, 576-580.

(22) Lomas, Lee O.; Weinberger, Scot R. Edited by Marks, R.S. *Handbook of Biosensors and Biochips* **2007**, 2, 885-894.

(23) Grizzle, William E.; Semmes, O. John; Bigbee, William L.; Malik, Gunjan; Miller, Elizabeth; Manne, Barkha; Oelschlager, Denise K.; Zhu, Liu; Manne, Upender Edited by Patrinos, George P.; Ansorge, Wilhelm *Molecular Diagnostics* **2005**, 211-222.

(24) Austens, B. Frears, E.R.; Davies, H. *J. Pept. Sci. Sep*. **2000**, 6, 459-460.

(25) Brockman, A.H.; Orlando, R. *Rapid. Comm. Mass Spectrom*. **1994**, 10, 1688-1692.

(26) Brockman, A.H.; Orlando, R. *Anal. Chem*. **1995**, 67, 4581-4585.

(27) Papac, D.I.; Hoyes, J.T.; Tomer, K.B. *Anal. Chem.* **1994**, 66, 2609-2613.

(28) Davies, H.; Lomas, L.; Austen, B. *Biotechniques* **1999**, 27, 1258-1261.

(29) Yip, T.T.; Van de Water, J.; Gershwin, M.E.; Coppel, R.L.; Hutchens, T.W. *J.Biol. Chem*. **1996**, 271, 32825-32833.

(30) Liang, J.; Zhang, Z.; Rosenzweig, R.; Wang, Y.Y.; Chan, D.W. *Anal. Chem*. **1998**, 70, 498-503.

(31) Bundy, J.; Fenselau, C. *Anal. Chem*. **1999**, 71, 1460-1463.

(32) Bundy, J.; Fenselau, C. Anal. Chem. **2001**, 73, 751-757.

(33) Worsoe-Jorgensen, A.L.; Juul-Madsen, H.R.; Stagsted, J. *J. Mass. Spectrom*. **2009**, 44, 338-345.

(34) Hillenkamp, F.; Strupat, K.; Karas, M.; Eckerskorn, C.; Lottspeich, F. *Anal. Chem*. **1994**, 464-470.

(35) Vestling, M.M.; Fenselau, C. *Anal. Chem.* **1994**, 66, 471–477.

(36) Blackledge, J.A.; Alexander, A.J. *Anal. Chem.* **1995**, 67, 843–848.

(37) Worrall, T.A.; Cotter, R.J.; Woods, A.S.; *Anal. Chem. **1998**, 70, 750-756.*

(38) Wang, H.; Tseng, K.; Lebrilla, C.B. *Anal. Chem*. **1999**. 71, 2014-2020.

(39) Marin, V.L.; Bayburt, T.H.; Sligar, S.G.; Mrksich, M. *Angew. Chem. Int. Ed*. **2007**, 46, 8796-8798.

(40) Patrie, S.M.; Mrksich, M. *Anal. Chem.* **2007**, 79, 5878-5887.

(41) Mrksich, M. *ACS Nano* **2008**, 2(1), 7-18.

(42) Hutchens, T.W.; Yip, T.T. *J Chromatogr*. **1992**, 604, 133–141.

(43) Kwon, S.W.; Kim, S.C.; Jaunbergs, J.; Falck, J.R. Molec. Cell. Proteomics 2003, 2, 242-247.

(44) Suen, S-Y.; Liu, Y-C.; Chang, C-S.; *J. Chrom. B*, **2003**, 797, 305–319.

(45) Raska, C.S.; Parker, C.E.; Dominski, Z.; Marzluff, W.F.; Glish, G.L.; Pope, M.R.; Borchers, C.H.; *Anal. Chem.* **2002**, 74, 3429–3433.

(46) Tetsuyuki, A.; Takao, Y. *Proteome Science* **2009**, 7, 14-17.

(47) Hogstrand, C.; Balesaria, S.; Glover, C.N. *Comp. Biochem. Physiol. B*. **2002**, 133, 523–535.

(48) Li, J.; Zhang, Z.; Rosenzweig, R.; Wang, Y.Y.; Chan, D.W. *Clin. Chem. J.* **2002**, 48, 1296–1304.

(49) Batorfi, J.; Ye, B.; Mok, S.C.; Cseh, I.; Berkowitz, R.S.; Fulop, V. *Gyneco.l Onco.* **2003,** 8, 424-428.

(50) The ELISA Guidebook. Crowther, J.R.; Editor , Humana, Totowa, N. J. 2001.

(51) ELISA: Theory and Practice. In Methods Mol. Biol. Totowa, N. J., 1995.

(52) Lai, N.-S.; Wang, C.-C.; Chiang, H.-L.; Chau, L.-K.; *Anal. Bioanal. Chem*. **2007**, 388, 901-907.

(53) Chau, L.-K.; Lin, Y.-F.; Cheng, S.-F.; Lin, T.-J. *Sens. Actuators B* **2006**, 113, 100-105.

(54) Smith, E.A.; Corn, R.M. *Appl. Spectroscopy*, **2003**, 57, 320A-332A.

(55) Aslan, K.; Lakowicz, J.R.; Geddes, C. *Current Opinion in Chemical Biology*, **2005**, 9, 538–544.

(56) Yu, L-P; Sun, Y-Z; Z, Z-X. *Current Pharmaceutical Analysis* **2009**, 5(2), 112-119.

(57) Kaliyaperumal, A.; Jing, S. *Current Pharmaceutical Biotechnology* **2009**, 10(4), 352-358.

(58) Anker, J.N.; Hall, W.P; Lyandres, O.; Shah, N.C.; Zhao, J.; Van Duyne, R.P. *Nature Materials* **2008**, 7, 442 – 453.

(59) Nelson, R.W.; Krone, J.R.; Bieber, A.L.; Williams, P.*Anal Chem* **1995**, 67, 1153–1158.

(60) Nelson, R.W.; *Mass Spectrom Rev.* **1997***, 1*6, 353–376.

(61) Nedelkov, D.; Nelson, R.W. *J Mol Recog* **2000**, 13, 40–145.

(62) Nedelkov, D. Nelson, R.W. In Neuropeptide research New York: John Wiley & Sons, Inc., 2002.

(63) Bottari, P.; Aebersold, R.; Turecek, F.; Gelb, M.H. *Bioconjugate Chem*. **2004**, 15 (2), 380-388.

(64) Lu, Y.; Bottari, P.; Turecek, F.; Aebersold, R.; Gelb, M.H. *Anal. Chem*. **2004**, 76, 4104-4111.

(65) Haslam, J.; Swift, S.D. *Analyst* **1954**, 79, 82-85.

(66) Edelman, G.M.; Rutishauser, U.; Millette, C.F. *Proc. Nat. Acad. Sci. USA* **1971**, 68, 2153-2157.

(67) Jasiewicz, M.L.; Schoenberg, D.R.; Mueller, G.C. Exp. Cell Res. **1976**, 100, 213-217.

(68) Hendry, R.M.; Herrmann, J.E. Journal *of Immunological Methods* **1980**, 35, 285-296.

(69) Isgrove, F.H.; Williams, R.J.H.; Niven, G.W.; Andrews, A.T. *Enzyme and Microbial Technology* **2001**, 28, 225–232.

(70) Tang, J.; He, N.; Nie, L.; Xiao, P.; Chen, H. *Surface Science* **2004**, 550, 26-34.

(71) Sojback, R.; Nygren, J.; Kubista, M. *Spectrochimica Acta Part A* **1995**, 51, L7-L21.

(72) Kada, G.; Falk, H.; Gruber, H.J *Biochimica et Biophysica* Acta **1999**, 1427 33-43.

(73) Kada, G.; Kaiser, K.; Falk, H.; Gruber, H.J. *Biochimica et Biophysica Acta* **1999**, 1427, 44-48.

(75) Seiwert, B.; Karst, U. *Anal. Chem*. **2007**, 79 (18), 7131-7138.

(76) Liang, S.C.; Wang, H.; Zhang, Z.M.; Zhang, H-S. *Anal. Bioanal. Chem.* **2005**, 381,1095–1100.

(77) Kuśmierek, K.; Glowacki, R.; Bald, E. *Anal Bioanal Chem* **2006**, 385, 855–860.

(78) Kusmierek, K.; Bald, E. *Chromatographia* **2007**, 66, 71-74.

(79) Kusmierek, K.; Bald, E *Chromatographia* **2008**, 67, 23-29.

(80) Fiskerstrand, T.; Refsum, H.; Kvalhehn, G.; Ueland, P.M.; *Clin. Chem*. **1993**, 39(2), 263-271.

(81) Pastore, A.; Massoud, R.; Motti, C.; Russo, A.L.; Fucci, G.; Cortese, C.; Federici1, G. *Clin. Chem*. **1998**, 44(4), 825–832.

(82) Andersson, A.; Isaksson, A.; Brattstrom, Hultberg, B. Clin. **1993**, 39(8),1590-1597.

(83) Inoue, T.; Kirchhoff, J.R. *Anal. Chem*. **2002**, 74 (6), 1349-1354.

(84) Zacharisa, C.K.; Tzanavaras, P.D.; Themelisa, D.G. *J. of Pharm.Biomed. Anal.* **2009**, 50 384–391.

(85) Du, M. *Anal.l Let.* **2007**, 40, 3245-3255.

(86) Srinivas, N.R.; Mamidi, R.N.V.S. *Biomed. Chromatogr*. **2003**, 17, 285–291.

(87) Favaro, G.; Fiorani, M. *Anal. Chim. Acta* **1996**, 332, 249-255.

(88) Y. Fujita,; I. Morri, T. Yamaguchi. *Anal. Sciences* **2002**, 18, 981-985.

(89) Bald, E.; Sypniewski, S. *Fresenius J. Anal. Chem.* **1997**, 358, 554–555.

(90) Piggott, A.M.; Karuso, P. *Tetrahedron Lett*. **2005**, 46, 8241–8244.

(91) Olejnik, J.; Sonar, S.; Krzymañska-Olejnik, Rothschild, K.J. *Proc. Natl. Acad. Sci*. **1995**, 92, 7590-7594.

(92) Milburn, T.; Matsubara, N.; Billington, A. P.; Udgaonkar, J. B.; Walker, J. W.; Carpenter, B. K.; Webb, W. W.; Marque, J.; Denk,W.; McCray, J. A; Hess, G. P. *Biochemistry*, **1989**, 28, 49-55.

(93) Walker, J. W.; Reid, G. P.; McCray, J. A.; Trentham, D. R. *J. Am. Chem. Soc*. **1988**, 110, 7170-7177.

(94) Zhou, H.; Ranish, J.A.; Watts, J.D.; Aebersold, R. N*ature Biotech* **2002**, 19, 512-515.

(95) Bai, X.; Li, Z.; Jockusch, S.; Turro, N. J.; Ju, J. *Proc. Natl. Acad. Sci*. **2003**, 100(2), 409-413.

(96) Beecher, J.E.; Cameron, J. F.; Frechet, J. M. J. *Polym. Materials Science and Engineering* **1991**, 64, 71-2.

(97) Bai1, X.; Sobin, K.; Zengmin, L.; Nicholas, J.T.; Jingyue, J. *Nuc. Acids Res*. **2004**, 32, (2), 535-541.

(98) Holmes, C.P. *J. Org. Chem*., **1997**, 62, 2370-2380.

(99) Pandori, M.W.; Hobson, D.A.; Olejnik, J.; Sonar, S.; Krzymañska-Olejnik, E.; Rothschild, K.J.; Palmer, A.A.; Phillips, R.J.; Sano, T. *Chem. Biol*. **2002**, 9, 567-573.

(100) Olejnik, J.; Krzymañska-Olejnik, E.; Rothschild, K.J. *Nuc. Acids Res* **1998**, 26, 3572-3576.

(101) Olejnik, J.; Lüdemann, H.-C. ; Krzymañska-Olejnik, E.; Berkenkamp, S.; Hillenkamp, F.; Rothschild, K.J. *Nuc. Acids Res* **1999**, 27, 4626-4631.

(102) Olejnik, J.; Krzymanska-Olejnik, E.; Rothschild, K.J. *Methods in Enzymology* **1998**, 291, 135-154.

(103) Olejnik, J.; Krzymanska-Olejnik, E.; Rothschild, K.J. *Nuc. Acids Res* 1996, 24, 361-366.

(104) Dormán, G.; Prestwich, G.D.; *Trends in Biotech.*, **2000**, 8, 64-77.

(105) Ordoukhanian, P.; Taylor, J-S. *J. Am. Chem. Soc*. **1995**, 117, 9570-9571.

.

Chapter 7: Conclusions and Future Directions

7.1 Conclusions

The field of ambient ionization mass spectrometry has grown rapidly since the first reports of desorption electrospray ionization (DESI)[1] in 2004 and direct analysis in real time (DART)[2] in 2005. By 2009 more than 25 ambient ionization methods have been reported in the literature[3] and interest in the field remains very high. While a number of applications including bulk material analysis[4-7], human screening,[8,9] and imaging[10-12] involve the direct interrogation of the sample in its native environment, many other applications involve the collection and/or deposition of a sample onto a substrate before it is introduced to the ionization source. Just as many forms of ionization exist for mass spectrometry, there are also numerous methods of sample introduction.

This dissertation summarizes the development and optimization of a transmission mode of operation for ambient ionization mass spectrometry, in this case, specifically for desorption electrospray ionization. In the transmission mode, the sample is either deposited on, or otherwise collected by a mesh substrate that is subsequently introduced orthogonally to an electrospray ionization source, thereby permitting the transmission of the electrospray through the material. Analytes that are adsorbed on the surface of the mesh strands or suspended within its confines as macroscale droplets are solvated by the electrospray; desorbed by the momentum of the incoming droplets; and transferred to the gas phase where they undergo ionization via typical electrospray ionization mechanisms.

The transmission mode was designed to overcome specific challenges associated with DESI regarding the complexity of the experimental arrangement and sample deposition. By making the sampling surface transparent to the ionizing spray, the new technique aimed to convert the triangular experimental arrangement of conventional

DESI to a linear one, thus simplifying and increasing the robustness of the method. Furthermore, the choice of a grid-like substrate was intended to reduce sample spreading by allowing the surface tension of the deposition solvent to effectively suspend the sample between the mesh strands.

The results presented in chapter 3 detail the initial development and optimization of the technique, focusing primarily on the various distances within the experimental arrangement; the variables associated with the electrospray; and the impact of the deposition and electrospray solvents. The results show that TM-DESI is capable of producing high quality mass spectral data for both solid residues and liquid samples in very short periods of time and that the bulk of the analytical variability is defined by the factors affecting the desorption process: the electrospray solvent, the deposition solvent, the substrate material, and the target analyte. Ultimately, it was concluded that partitioning of target analytes between the various solvents and the material used as the mesh substrate creates a potentially useful microscale separation; however, further experiments were necessary to investigate these interactions in detail.

Chapter four describes experiments aimed at understanding the influence of the geometric and material characteristics of the mesh substrate on TM-DESI. A combination of mass spectrometry and fluorescence microscopy was used to study both the transmission of the electrospray plume through the mesh and the partitioning of analytes between the mesh strands and the deposition/electrospray solvent system. Results suggested that there is a balance between mesh surface area and electrospray transmission as specific mesh strand diameters and open spaces facilitated greater response by maximizing transmission and desorption versus scattering and solvent spreading. It was also confirmed that the identity of the mesh material has a tremendous impact on the performance of the substrate as polar analytes such as dyes and peptides

are preferentially desorbed from non-polar materials. Furthermore, the details in chapter 4 demonstrate that an intricate chemistry exists as the electrospray plume is transmitted through a mesh material, especially one containing a solvated sample

Application of the transmission mode and options for sample preparation are presented in chapter 5. Successful analysis of small molecule metabolites, pharmaceuticals, flavonoids, peptides and explosives confirms the hypothesis that TM-DESI has a similar range of applications as DESI. Furthermore, four methods of sample preparation are highlighted, each of which can be paired with various applications. Experiments detailing a high throughput calibration and improved precision are discussed that may help elevate the DESI from a screening experiment to a high throughput semi-quantitative status. These results could prove to be especially important for pharmaceutical or target metabolomics applications.

Finally chapter 6 details the initial development of surface-enhanced TM-DESI. This technique aims to improve the selectivity and sensitivity of DESI by utilizing mesh materials that are specifically designed to capture target analytes from solution. Details regarding theoretical considerations, mesh fabrication and quality control assays are discussed. The chapter culminates by demonstrating the capability of the technique to overcome interferences that have typically required chromatographic separations using LC-MS or have been insurmountable using ambient ionization methods. The impact of the surface-enhanced method could be tremendous as it may ultimately unite the competing metrics of analytical speed and specificity for ambient ionization mass spectrometry.

7.2 FUTURE DIRECTIONS

Continued development of the transmission mode technique can be divided into four areas: hardware development; fundamental research; technique optimization, and advanced applications. The work presented in this dissertation was primarily performed using home-built sample introduction devices. However, the results were significant enough to warrant the recent delivery of professionally machined prototypes specifically designed for TM-DESI. Thus, additional work should focus on testing and refining these prototypes, understanding their benefits, and ultimately providing enough validation to warrant commercialization of a transmission mode specific ionization source.

While chapter 4 began the study of the interaction of an electrospray with a mesh material, there is certainly much more to learn about the physics and chemistry of this interface. Additional investigation would not only increase the understanding of experimental results, but also provide valuable information for constructing optimized mesh surfaces. In addition, preliminary studies have shown that an electrospray can be transmitted through multiple mesh materials, thereby opening up potential opportunities for increasing accuracy via external standard calibration and decreasing detection limits via multi-mesh sampling.

Above all, the most promising avenue for continued research lies in the optimization and development of surface-enhanced materials. The potential to couple increased selectivity and sensitivity with the already rapid sample analysis provided by DESI or DART could prove to have an incredible impact on high throughput screening. Application opportunities range from metabolomics and biomarker screening to homeland security and environmental monitoring. In conjunction, the melding of sample collection with sample introduction via design of transmission mode suitable collection materials will continue to facilitate real-world application of the technique.

7.3 REFERENCES

(1) Takats, Z.; Wiseman, J.M.; Gologan, B.; Cooks, R.G. *Science* **2004**, 306, 471-473.

(2) Cody, R.B.; Laramee, J.A.; Durst, H.D. *Anal. Chem.* **2005**, 77, 2297-2302.

(3) Chen, H.; Gamez, G.;Zenobia, R. *J Am Soc Mass Spectrom* **2009**, 20, 1947–1963.

(4) Chen, H.; Talaty, N.; Takats, Z.; Cooks, R.G. *Anal. Chem*. **2005**,77, 6915-6927.

(5) Talaty, N.; Takats, Z.; Cooks, R.G. *Analyst*, **2005**, 130, 1624-1633.

(6) McEwen, C.N.; McKay, R.G.; Larsen, B.S. *Anal. Chem*. **2005**, 77, 7826-7831.

(7) Andrade, F. J.; Shelley, J. T.; Wetzel, W. C.; Webb, M. R.; Gamez, G.; Ray,S. J.; Hieftje, G. M.. *Anal. Chem*. **2008**, 80, 2646–2653.

(8) Justes, D. R.; Talaty, N.; Cotte-Rodriguez, I.; Cooks, R.G. *Chem. Comm*. **2007**, 132, 868-875.

(9) Chen, H.; Hu, B.; Hu, Y.; Huan,Y. Zhou, Z.; Qiaoc, X. *J Am Soc Mass Spectrom* **2009**, 20, 719–722.

(10) Cooks, R. G.; Ouyang, Z.; Takats, Z.; Wiseman, J. M. *Science* **2006,** *311,* 1566–1569.

(11) Wiseman, J.M.; Ifa, D.R.; Venter, A.; Cooks, R.G. *Nat. Protocols* **2008**, 3, 517-524.

(12) Ifa, D.R.; Wiseman, J.M.; Qingyu, S.; Cooks, R.G. *Int. J. Mass Spectrom*. **2007**, 259, 5-15.

References

Andersson, A.; Isaksson, A.; Brattstrom, Hultberg, B. Clin. **1993**, 39(8),1590-1597.

Andrade, F. J.; Shelley, J. T.; Wetzel, W. C.; Webb, M. R.; Gamez, G.; Ray, S. J.; Hieftje, G. M. *Anal. Chem.* **2008,** *80*, 2646–2653.

Andrade, F.J.; Shelley, J.T.; Wetzel, W.C.; Webb, M.R.; Gamez, G.; Ray, S.J.; Hieftje, G.M. *Anal. Chem*. **2008**, 80, 2646-2653.

Anker, J.N.; Hall, W.P; Lyandres, O.; Shah, N.C.; Zhao, J.; Van Duyne, R.P. *Nature Materials* **2008**, 7, 442 – 453.

Aslan, K.; Lakowicz, J.R.; Geddes, C. *Current Opinion in Chemical Biology*, **2005**, 9, 538–544.

Austens, B. Frears, E.R.; Davies, H. *J. Pept. Sci. Sep*. **2000**, 6, 459-460.

Bai, X.; Li, Z.; Jockusch, S.; Turro, N. J.; Ju, J. *Proc. Natl. Acad. Sci*. **2003**, 100(2), 409-413.

Bai1, X.; Sobin, K.; Zengmin, L.; Nicholas, J.T.; Jingyue, J. *Nuc. Acids Res*. **2004**, 32, (2), 535-541.

Bald, E.; Sypniewski, S. *Fresenius J. Anal. Chem.* **1997***,* 358, 554–555.

Batorfi, J.; Ye, B.; Mok, S.C.; Cseh, I.; Berkowitz, R.S.; Fulop, V. *Gyneco.l Onco.* **2003,** 8, 424-428.

Beecher, J.E.; Cameron, J. F.; Frechet, J. M. J. *Polym. Materials Science and Engineering* **1991**, 64, 71-2.

Bereman, M. S.; Nyadong, L.; Fernandez, F. M.; Muddiman, D. C. *Rapid Commun. Mass Spectrom.* **2006,** *20,* 3409–3411.

Bereman, M. S.; Williams, T. I.; Muddiman, D. C. *Anal. Chem.* **2007,** *79,* 8812–8815.

Blackledge, J.A.; Alexander, A.J. *Anal. Chem.* **1995**, 67, 843–848.

Bottari, P.; Aebersold, R.; Turecek, F.; Gelb, M.H. *Bioconjugate Chem*. **2004**, 15 (2), 380-388.

Brockman, A.H.; Orlando, R. *Anal. Chem*. **1995**, 67, 4581-4585.

Brockman, A.H.; Orlando, R. *Rapid. Comm. Mass Spectrom*. **1994**, 10, 1688-1692.

Bulman, A. *Amer. Biotech. Lab*. **2008**, 26(2), 14-16.

Bundy, J.; Fenselau, C. *Anal. Chem*. **1999**, 71, 1460-1463.

Bundy, J.; Fenselau, C. Anal. Chem. **2001**, 73, 751-757.

Cech, N. B.; Enke, C. G. *Mass Spectrom. Rev*. **2001**, 20, 362–387.

Chadwick, C. A.; Keevil, B. *Ann. Clin. Biochem*. **2007**,44, 455–462.

Chandran, S.; Singh, R.S.P. *Pharmazie* **2007** 62 1-14.

Chau, L.-K.; Lin, Y.-F.; Cheng, S.-F.; Lin, T.-J. *Sens. Actuators B* **2006**, 113, 100-105.

Chen, H. W.; Venter, A.; Cooks, R. G. *Chem. Commun*. **2006,** 2042-2044.

Chen, H. W.; Wortmann, A.; Zhang, W. H.; Zenobi, R. *Angew. Chem. Int. Ed*. **2007**, 46, 580–583.

Chen, H.; Gamez, G.;Zenobia, R. *J Am Soc Mass Spectrom* **2009**, 20, 1947–1963.

Chen, H.; Hu, B.; Hu, Y.; Huan,Y. Zhou, Z.; Qiaoc, X. *J Am Soc Mass Spectrom* **2009**, 20, 719–722.

Chen, H.; Talaty, N.; Takats, Z.; Cooks, R. G. *Anal. Chem.* **2005,** *77,* 6915–6927.

Chen, H.; Venter, A.; Cooks, R.G. *Chem. Commun*. **2006**, 2042–2044.

Chen, H.; Zhengzheng, P.; Talaty, N.; Raftery, D.; Cooks, R. G. *Rapid Commun. Mass Spectrom.* **2006,** *20,* 1577–1584.

Cheng, S. C.; Cheng, T. L.; Chang, H. C.; Shiea, J. *Anal. Chem.* **2009,** *81*, 868–874.

Chingin, K.; Chen, H.; Gamez, G.; Zhu, L.; Zenobi, R. *Anal. Chem.* **2009,** *81*, 123–129.

Chingin, K.; Gamez, G.; Chen, H. W.; Zhu, L.; Zenobi, R. *Rapid Commun. Mass Spectrom*. **2008**, 22, 2009–2014

Cody, R.B.; Laramee, J.A.; Durst, H.D. *Anal. Chem*. **2005**, 77, 2297-2302.

Cole, R. B., Ed. Electrospray Ionization Mass Spectrometry: Fundamentals, Instrumentation, and Applications; Wiley: New York, 1997.

Cooks, R. G.; Ouyang, Z.; Takats, Z.; Wiseman, J. M. *Science* **2006,** *311,* 1566–1569.

Costa, A. B.; Cooks, R. G. *Chem. Commun.* **2007,** *38,* 3915–3917.

Cotte-Rodriguez, I.; Cooks, R. G. *Chem. Commun*. **2006,** *28,* 2968–2970.

Cotte-Rodriguez, I.; Hernandez-Soto, H.; Chen, H.; Cooks, R. G. *Anal. Chem.* **2008,** *80,* 1512–1519.

Cotte-Rodriguez, I.; Takats, Z.; Talaty, N.; Chen, H.; Cooks, R. G.. *Anal. Chem.* **2005,** *77,* 6755–6764.

Covey, T.R.; Lee, E.D.; Bruins, A.P.; Henion, J.D. *Anal. Chem*. **1986**, 58, 1451A-1461A.

Crowther, J.R.; Editor The ELISA Guidebook. , Humana, Totowa, N. J. 2001.

D'Agostino, P. A.; Chenier, C. L.; Hancock, J. R.; Lepage, J. *Rapid Commun. Mass Spectrom.* **2007,** *21,* 543–549.

D'Agostino, P. A.; Hancock, J. R.; Chenier, C. L.; Lepage, J. *J. Chromatogr. A* **2006,** *1110,* 86–94.

Davies, H.; Lomas, L.; Austen, B. *Biotechniques* **1999**, 27, 1258-1261.

Dixon, R. B.; Sampson, J. S.; Muddiman, D. C. *J. Am. Soc. Mass Spectrom.* **2009,** *20*, 597–600.

Dole, M.; Mack, L. L.; Hines, R. L.; Mobley, R. C.; Ferguson, L. D.; Alice, M. B.*J. Chem. Phys.* **1968**, *49*, 2240-2249.

Dormán, G.; Prestwich, G.D.; *Trends in Biotech.*, **2000**, 8, 64-77.

Douglas, D.J.; Frank, A.J.; Mao, D. Mass Spec. Rev. 2005, 24(1), 1-29.

Du, M. *Anal.l Let.* **2007**, 40, 3245-3255.

Edelman, G.M.; Rutishauser, U.; Millette, C.F. *Proc. Nat. Acad. Sci. USA* **1971**, 68, 2153-2157.

ELISA: Theory and Practice. In Methods Mol. Biol. Totowa, N. J., 1995.

Favaro, G.; Fiorani, M. *Anal. Chim. Acta* **1996**, 332, 249-255.

Fiskerstrand, T.; Refsum, H.; Kvalhehn, G.; Ueland, P.M.; *Clin. Chem*. **1993**, 39(2), 263-271.

Ford, M.j.; Van Berkel, G.J. *Rapid Commun. Mass Spectrom*. **2004**, 18,1303–1309.

Fujita,Y; Morri,I.;Yamaguchi, T.. *Anal. Sciences* **2002**, 18, 981-985.

Green, F.M.; Stokes, P.; Hopley, C.; Seah, M.P.; Gilmore, I.S.; O'Connor, G. *Anal. Chem*. **2009**, 81, 2286–2293.

Grizzle, William E.; Semmes, O. John; Bigbee, William L.; Malik, Gunjan; Miller, Elizabeth; Manne, Barkha; Oelschlager, Denise K.; Zhu, Liu; Manne, Upender Edited by Patrinos, George P.; Ansorge, Wilhelm *Molecular Diagnostics* **2005**, 211-222.

Gross, M.; Pramanik, B. N.; Ganguly, A.K. Applied Electrospray Mass Spectrometry, Marcel Dekker: New York, 2002.

Haddad, R.; Sparrapan, R.; Eberlin, M. N. *Rapid Commun. Mass Spectrom.* **2006,** *20*, 2901–2905.

Harper, J. D.; Charipar, N. A.; Mulligan, C. C.; Zhang, X. R.; Cooks, R. G.; Ouyang, Z. *Anal. Chem.* **2008,** *80*, 9097–9104.

Harrison, A.G. Chemical Ionization Mass Spectrometry, CRC Press: Boca Raton, FL, 1992.

Haslam, J.; Swift, S.D. *Analyst* **1954**, 79, 82-85.

Hendry, R.M.; Herrmann, J.E. Journal *of Immunological Methods* **1980**, 35, 285-296.

Hillenkamp, F.; Strupat, K.; Karas, M.; Eckerskorn, C.; Lottspeich, F. *Anal. Chem*. **1994**, 464-470.

Hogstrand, C.; Balesaria, S.; Glover, C.N. *Comp. Biochem. Physiol. B.* **2002**, 133, 523–535.

Holmes, C.P.; *J. Org. Chem*., **1997**, 62, 2370-2380.

Hu, Q.; Talaty, N.; Noll, R. J.; Cooks, R. G. *Rapid Commun. Mass Spectrom.* **2006,** *20,* 3403–3408.

Huang, G., Chen, H., Zhang, X, Cooks, R.G., Ouyang, Z. *Anal. Chem*. **2007** ,79, 8327-8332.

Hutchens, T.W.; Yip, T.T. *J Chromatogr*. **1992**, 604, 133–141.

Hutchens, T.W.; Yip, T.T. *Rapid. Comm. Mass Spectrom*. **1993**, 7, 576-580.

Ifa, D. R.; Gumaelius, L. M.; Eberlin, L. S.; Manicke, N. E.; Cooks, R. G.. *Analyst* **2007,** *132,* 461–467.

Ifa, D. R.; Jackson, A. U.; Paglia, G; Cooks, R. G. *Anal. Bioanal. Chem*. **2009**, 394, 1995–2008.

Ifa, D. R.; Manicke, N. E.; Rusine, A. L.; Cooks, R. G. *Rapid Commun. Mass Spectrom.* **2008,** *22,* 503–510.

Ifa, D. R.; Wiseman, J. M.; Qingyu, S.; Cooks, R. G. *Int. J. Mass Spectrom.* **2007,** *259,* 8–15.

Inoue, T.; Kirchhoff, J.R. *Anal. Chem*. **2002**, 74 (6), 1349-1354.

Iribarne, J. V.; Thomson, B. A. *J. Chem. Phys*. **1976**, 64, 2287-2294.

Isgrove, F.H.; Williams, R.J.H.; Niven, G.W.; Andrews, A.T. *Enzyme and Microbial Technology* **2001**, 28, 225–232.

Jackson, A. T.; Williams, J. P.; Scrivens, J. H. *Rapid Commun. Mass Spectrom.* **2006,** *20,* 2717–2727.

Jackson, A. U.; Talaty, N.; Cooks, R. G.; Van Berkel, G. J. *J. Am. Soc. Mass Spectrom*. **2007**, 18, 2218–2225.

Jackson, A. U.; Werner, S. R.; Talatly, N.; Song, Y.; Campbell, K.; Cooks, R. G.; Morgan, J. A. *Anal. Biochem.* **2008,** *375,* 272–281.

Jasiewicz, M.L.; Schoenberg, D.R.; Mueller, G.C. Exp. Cell Res. **1976**, 100, 213-217.

Justes, D. R.; Talaty, N.; Cotte-Rodriguez, I.; Cooks, R. G. *Chem. Commun*. **2007**, 2142–2144.

Kada, G.; Falk, H.; Gruber, H.J *Biochimica et Biophysica* Acta **1999**, 1427 33-43.

Kada, G.; Kaiser, K.; Falk, H.; Gruber, H.J. *Biochimica et Biophysica Acta* **1999**, 1427, 44-48.

Kaliyaperumal, A.; Jing, S. *Current Pharmaceutical Biotechnology* **2009**, 10(4), 352-358.

Karas, M.; Bachmann, D.; Hillenkamp, F. *Anal. Chem*. **1985,** 57, 2935–2939.

Kauppila, T. J.; Talaty, N.; Salo, P. K.; Kotiaho, T.; Kostiainen, R.; Cooks, R. G. *Rapid Commun. Mass Spectrom.* **2006,** *20,* 2143–2150.

Kauppila, T. J.; Wiseman, J. M.; Ketola, R. A.; Kotiaho, T.; Cooks, R. G.;Kostiainen, R. *Rapid Commun. Mass Spectrom*. **2006,** 20, 387–392.

Kauppila, T.J.; Kotiaho, T.; Kostiainen, R.; Bruins, A.P. *J Am Soc Mass Spectrom.* **2004**, 15, 203-211

Kauppila, T.J.; Talaty, N.; Kuuranne, T.; Kotiaho, T.; Kostiainen,R.; Cooks, R.G. *Analyst.* **2007**, 132, 868–875.

Kiehntopf, M.; Siegmund, R.; Deufel, T. *Clin. Chem. Lab. Med*. **2007**, 45(11), 1435-1449.

Kusmierek, K.; Bald, E *Chromatographia* **2008**, 67, 23-29.

Kusmierek, K.; Bald, E. *Chromatographia* **2007**, 66, 71-74.

Kuśmierek, K.; Glowacki, R.; Bald, E. *Anal Bioanal Chem* **2006**, 385, 855–860.

Kwon, S.W.; Kim, S.C.; Jaunbergs, J.; Falck, J.R. Molec. Cell. Proteomics 2003, 2, 242-247.

Lai, N.-S.; Wang, C.-C.; Chiang, H.-L.; Chau, L.-K.; *Anal. Bioanal. Chem*. **2007**, 388, 901-907.

Laiko, V.V.; Baldwin, M.A., Burlingame, A.L. *Anal. Chem*. **2000**, 72(4), 652-657.

Li, J.; Zhang, Z.; Rosenzweig, R.; Wang, Y.Y.; Chan, D.W. *Clin. Chem. J.* **2002**, 48, 1296–1304.

Liang, J.; Zhang, Z.; Rosenzweig, R.; Wang, Y.Y.; Chan, D.W. *Anal. Chem*. **1998**, 70, 498-503.

Liang, S.C.; Wang, H.; Zhang, Z.M.; Zhang, H-S. *Anal. Bioanal. Chem.* **2005**, 381,1095–1100.

Lim, C.K.; Lord, G. *Biol. Pharm. Bull.* **2002**, 25(5), 547-557.

Lomas, Lee O.; Weinberger, Scot R. Edited by Marks, R.S. *Handbook of Biosensors and Biochips* **2007**, 2, 885-894.

Lu, Y.; Bottari, P.; Turecek, F.; Aebersold, R.; Gelb, M.H. *Anal. Chem*. **2004**, 76, 4104-4111.

March, R.E. *Int. J. Mass Spectrom*. **2000**, 200, 285-312

Marin, V.L.; Bayburt, T.H.; Sligar, S.G.; Mrksich, M. *Angew. Chem. Int. Ed*. **2007**, 46, 8796-8798.

McEwen, C. N.; McKay, R. G.; Larsen, B. S. *Anal. Chem.* **2005,** *77,* 7826–7831.

Merchant, M.; Weinberger, S.R. *Electrophoresis* **2000**, 21, 1164-1177.

Milburn, T.; Matsubara, N.; Billington, A. P.; Udgaonkar, J. B.; Walker, J. W.; Carpenter, B. K.; Webb, W. W.; Marque, J.; Denk,W.; McCray, J. A; Hess, G. P. *Biochemistry*, **1989**, 28, 49-55.

Moore, D.S. *Rev. Sci. Instrum*. **2004**, 75, 2499-2512.

Mrksich, M. *ACS Nano* **2008**, 2(1), 7-18.

Mulligan, C.C.; Talaty, N.; Cooks, R.G. *Chem. Commun*. **2006**, 1709-1711.

Murphy, S. E.; Villata, P.; Ho, S. W.; von Weymarn, L. B. *J. Chromatogr. B.* **2007**, 857, 1–8.

Nedelkov, D. Nelson, R.W. In Neuropeptide research New York: John Wiley & Sons, Inc., 2002.

Nedelkov, D.; Nelson, R.W. *J Mol Recog* **2000**, 13, 40–145.

Nefliu, M.; Smith, J. N.; Venter, A.; Cooks, R. G. *J. Am. Soc.Mass Spectrom*. **2008**, 19, 420–427.

Nefliu, M.; Venter, A.; Cooks, R.G. *Chem. Commun*. **2006**, 888–890.

Nelson, R.W.; Krone, J.R.; Bieber, A.L.; Williams, P.*Anal Chem* **1995**, 67, 1153–1158.

Nelson, R.W.; *Mass Spec. Rev*. **1997**, 16, 353-376.

Nemes, P.; Vertes, A. *Anal. Chem*. **2007**, 79, 8098-8106.

Nyadong, L., Green, M.D., De Jesus, V.R., Newton, P.N., Fernandez, F.M., *Anal. Chem*. **2007**, 79, 2150-2157.

Olejnik, J.; Krzymanska-Olejnik, E.; Rothschild, K.J. *Methods in Enzymology* **1998**, 291, 135-154.

Olejnik, J.; Krzymanska-Olejnik, E.; Rothschild, K.J. *Nuc. Acids Res* **1996**, 24, 361-366.

Olejnik, J.; Krzymañska-Olejnik, E.; Rothschild, K.J. *Nuc. Acids Res* **1998**, 26, 3572-3576.

Olejnik, J.; Lüdemann, H.-C. ; Krzymañska-Olejnik, E.; Berkenkamp, S.; Hillenkamp, F.; Rothschild, K.J. *Nuc. Acids Res* **1999**, 27, 4626-4631.

Olejnik, J.; Sonar, S.; Krzymañska-Olejnik, Rothschild, K.J. *Proc. Natl. Acad. Sci*. **1995**, 92, 7590-7594.

Ordoukhanian, P.; Taylor, J-S. *J. Am. Chem. Soc*. **1995**, 117, 9570-9571.

Page, J. S.; Kelly, R. T.; Tang, K.; Smith, R. D. *J. Am. Soc. Mass Spectrom.* **2007,** *18,* 1582–1590.

Pan, Z.; Gu, H.; Talaty, N.; Chen, H.; Shanaiah, N.; Hainline, B. E.; Cooks, R. G.; Raftery, D. *Anal. Bioanal. Chem.* **2007,** *387,* 539–549.

Pandori, M.W.; Hobson, D.A.; Olejnik, J.; Sonar, S.; Krzymañska-Olejnik, E.; Rothschild, K.J.; Palmer, A.A.; Phillips, R.J.; Sano, T. *Chem. Biol*. **2002**, 9, 567-573.

Papac, D.I.; Hoyes, J.T.; Tomer, K.B. *Anal. Chem.* **1994**, 66, 2609-2613.

Pasilis, S. P.; Kertesz, V.; Van Berkel, G. J. *Anal. Chem*. **2007**, 79, 5956–5962.

Pastore, A.; Massoud, R.; Motti, C.; Russo, A.L.; Fucci, G.; Cortese, C.; Federici1, G. *Clin. Chem*. **1998**, 44(4), 825–832.

Patrie, S.M.; Mrksich, M. *Anal. Chem.* **2007**, 79, 5878-5887.

Paul, W.; Steinwedel, H. Zeitschrift fur Naturforschung 1953, 8(7), 448-450.

Peng, I. X.; Loo, R. R. O.; Shiea, J.; Loo, J. A. *Anal. Chem.* **2008,** *80*, 6995–7003.

Peng, I. X.; Shiea, J.; Loo, R. R. O.; Loo, J. A. *Rapid Commun. Mass Spectrom.* **2007,** *21,* 2541–2546.

Petricoin, E. F.; Liotta, L. A. Edited by Liebler, D.C. *Prot. in Cancer Res*. **2005**, 117-131.

Piggott, A.M.; Karuso, P. *Tetrahedron Lett*. **2005**, 46, 8241–8244.

Raska, C.S.; Parker, C.E.; Dominski, Z.; Marzluff, W.F.; Glish, G.L.; Pope, M.R.; Borchers, C.H.; *Anal. Chem.* **2002**, 74, 3429–3433.

Ricci, C.; Nyadong, L.; Fernandez, F. M.; Newton, P. N.; Kazarian, S. G. *Anal. Bioanal. Chem.* **2007,** *387,* 551–559.

Robb, D.B.; Covey, T.R.; Bruins, A.P. *Anal. Chem*. **2000**, 72(15), 3653-3659.

Roy, P.; Shukla, Y. *Cancer Therapy* **2008**, 6, 841-856.

Sampson, J. S.; Hawkridge, A. M.; Muddiman, D. C. *Anal. Chem.* **2008,** *80*, 6773–6778.

Sampson, J. S.; Hawkridge, A. M.; Muddiman, D. C. *Rapid Commun. Mass Spectrom.* **2007,** *21,* 1150–1154.

Sampson, J.S.; Hawkridge, A.M.; Muddiman, D.C. *J Am Soc Mass Spectrom* **2006**, 17, 1712–1716.

Schwartz, J.C.; Senko, M.W.; Syka, J.E.P; J Am Soc Mass Spectrom. 2002, 13 659-669.

Seiwert, B.; Karst, U. *Anal. Chem*. **2007**, 79 (18), 7131-7138.

Sen, A. K.; Nayak, R.; Darabi, J.; Knapp, D. R. *Biomed. Microdevices* **2008,** *10,* 531–538.

Shelley, J. T.; Wiley, J. S.; Chan, G. C. Y.; Schilling, G. D.; Ray, S. J.;Hieftje, G. M. *J. Am. Soc. Mass Spectrom.* **2009,** *20*, 837–844.

Shiea, J.; Huang, M. Z.; Hsu, H. J.; Lee, C. Y.; Yuan, C. H.; Beech, I.; Sunner, J. *Rapid Commun.Mass Spectrom.* **2005,** *19*, 3701–3704.

Shiea, J.; Yuan, C.-H.; Huang, M.-Z.; Cheng, S.-C.; Ma, Y.-L.; Tseng, W.-L.; Chang, H.-C.; Hung, W.-C. *Anal. Chem.* **2008,** *80,* 4845–4852.

Shieh,I-F,; Lee,C-Y.; Shiea, J, *J. Proteome Research* **2005**, 4, 606-612.

Shin, Y.-S.; Drolet, B.; Mayer, R.; Dolence, K.; Basile, F. *Anal. Chem.* **2007,** *79,* 3514–3518.

Smith, E.A.; Corn, R.M. *Appl. Spectroscopy*, **2003**, 57, 320A-332A.

Sojback, R.; Nygren, J.; Kubista, M. *Spectrochimica Acta Part A* **1995**, 51, L7-L21.

Song, Y.; Cooks, R. G. *J. Mass Spectrom.* **2007,** *42,* 1086–1092.

Song, Y.; Cooks, R.G. *Rapid Comm. Mass Spectrom.* **2006**, 20, 3130-3138.

Srinivas, N.R.; Mamidi, R.N.V.S. *Biomed. Chromatogr*. **2003**, 17, 285–291.

Suen, S-Y.; Liu, Y-C.; Chang, C-S.; *J. Chrom. B*, **2003**, 797, 305–319.

Takats, Z.; Cotte-Rodriguez, I.; Talaty, N.; Chen, H.; Cooks, R. G. *Chem. Comm.* **2005**, 1950–1952.

Takats, Z.; Wiseman, J. M.; Cooks, R. G. *J. Mass Spectrom*. **2005**, 40, 1261–1275.

Takats, Z.; Wiseman, J.M.; Gologan, B.; Cooks, R.G. *Science.* **2004**, 306, 471-473.

Talaty, N.; Takats, Z.; Cooks, R. G. *Analyst* **2005,** *130,* 1624–1633.

Tanaka, K.; Waki, H.; Ido, Y.; Akita, S.; Yoshida, Y.; Yoshida, T. *Rapid Commun Mass Spectrom.* **1988**, 2 (20), 151–153.

Tang, J.; He, N.; Nie, L.; Xiao, P.; Chen, H. *Surface Science* **2004**, 550, 26-34.

Tang, N.; Tornatore, P.; Weinberger, S.R. *Mass Spec. Rev*. **2004**, 23, 34-44.

Tetsuyuki, A.; Takao, Y. *Proteome Science* **2009**, 7, 14-17.

Thomson, B.A. *J. Am. Soc. Mass Spectrom*. **1998**, 9(3), 187-193.

Uversky, V.N.; Permyakov, E.A. *Meth. Prot. Struct. Stab. Anal.* **2007**, Part D, 121-174.

Van Berkel, G. J.; Ford, M. J.; Deibel, M. A. *Anal. Chem.* **2005,** *77,* 1207–1215.

Vekey, K.; Telekes, A.; Vertes, A. *Med. App. of Mass Spectrom*. **2008**, 379-406.

Venter, A.; Cooks, R. G. *Anal. Chem.* **2007,** *79,* 6398–6403.

Venter, A.; Nefliu, M.; Cooks, R. G. *Trends Anal. Chem.* **2008,** *27,* 284–290.

Venter, A.; Sojka, P.E.; Cooks, R.G. *Anal. Chem*. **2006**, 78, 8549-8555.

Vestling, M.M.; Fenselau, C. *Anal. Chem.* **1994**, 66, 471–477.

Volný, M.; Venter, A.; Smith, S. A.; Pazzi, M.; Cooks, R. G. *Analyst* **2008,** *133,* 525–531.

Walker, J. W.; Reid, G. P.; McCray, J. A.; Trentham, D. R. *J. Am. Chem. Soc*. **1988**, 110, 7170-7177.

Wang, H.; Tseng, K.; Lebrilla, C.B. *Anal. Chem*. **1999**. 71, 2014-2020.

Weinberger, S.R.; Dalmasso, E.A.; Fung, E.T. *Curr. Opin. Chem. Biol*. **2001**, 6, 86-91.

Weinberger, S.R.; Morris, T.S.; Pawlak, M. *Pharmacogenomics* **2000**, 1, 1462-1482.

Weston, D. J.; Bateman, R.; Wilson, I. D.; Wood, T. R.; Creaser, C. S. *Anal. Chem.* **2005,** *77,* 7752–7580.

Willard, H.H.; Merritt, L.L.; Dean, J.A.; Settle, F.A. Instrumental Methods of Analysis, Wadsworth: Belmont, CA, 1988.

Williams, J. P.; Hilton, G. R.; Thalassinos, K.; Jackson, A. T.; Scrivens, J. H. *Rapid Commun. Mass Spectrom*. **2007,** 21, 1693–1704.

Williams, J. P.; Patel, V. J.; Holland, R.; Scrivens, J. H. *Rapid Commun. Mass Spectrom.* **2006,** *20,* 1447–1456.

Williams, J. P.; Scrivens, J. H. *Rapid Commun. Mass Spectrom.* **2005,** *19,* 3643–3650.

Williams, J.P.; Patel, V.J.; Holland, R.; Scrivens, J.H.. *Rapid Commun. Mass Spectrom.* **2006**, 20, 1447-1456.

Wiseman, J. M.; Ifa, D. R.; Venter, A.; Cooks, R. G. *Nat. Protocols* **2008**, 3, 517–524

Worrall, T.A.; Cotter, R.J.; Woods, A.S.; *Anal. Chem. **1998**, 70, 750-756.*

Worsoe-Jorgensen, A.L.; Juul-Madsen, H.R.; Stagsted, J. *J. Mass. Spectrom*. **2009**, 44, 338-345.

Wu, C., Ifa, D.R., Manicke, N.E., Cooks, R.G., *Anal. Chem*. **2009**, 81, 7618-7624.

Yamashita, M.; Fenn, J. *J. Phys. Chem*., **1984**, 88 (20), 4451-4459.

Yinon, J. *Trends Anal. Chem*. **2002**, 21(4), 292-301.

Yip, T.T.; Van de Water, J.; Gershwin, M.E.; Coppel, R.L.; Hutchens, T.W. *J.Biol. Chem*. **1996**, 271, 32825-32833.

Yu, L-P; Sun, Y-Z; Z, Z-X. *Current Pharmaceutical Analysis* **2009**, 5(2), 112-119.

Zacharisa, C.K.; Tzanavaras, P.D.; Themelisa, D.G. *J. of Pharm.Biomed. Anal.* **2009**, 50 384–391.

Zenobi, R.; Knochenmuss, R. *Mass Spectrom. Rev*. **1998**, 17, 337-366.

Zhou, H.; Ranish, J.A.; Watts, J.D.; Aebersold, R. N*ature Biotech* **2002**, 19, 512-515.

Vita

Joseph E. Chipuk, Jr. was born on January 19, 1972 in Parma, OH to Joseph E. Chipuk, Sr. and Ruth Kummerlen. After graduating from North Royalton High School in North Royalton, OH in 1990, he enrolled at Texas A&M University and was a student in the department of chemical engineering. In 1995, he transferred to the University of Texas at Austin and received his B.S. degree in chemistry in December of 1996. Afterwards, he worked as an analytical chemist for Radian Corporation in Austin, TX. In 2002 he returned to the University of Texas at Austin to pursue a Masters degree in chemistry, which he was awarded in December of 2006. He began pursuit of a doctoral degree in the Department of Chemistry and Biochemistry at the University of Texas at Austin, immediately thereafter.

Permanent address: 1720 Giles Street, Austin, TX 78722

This dissertation was typed by the author.